h. 1426

UR-3490-1878

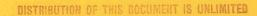
DOE RESEARCH AND DEVELOPMENT REPORT



ANNUAL REPORT UNIVERSITY OF ROCHESTER DEPARTMENT OF RADIATION BIOLOGY AND BIOPHYSICS

BRIEF DESCRIPTION OF RESEARCH PAPERS ACCEPTED FOR PUBLICATION DURING 1979

UNIVERSITY OF ROCHESTER DEPARTMENT OF RADIATION BIOLOGY AND BIOPHYSICS ROCHESTER, NEW YORK





6

3490-1878

DISCLAIMER

This report was prepared as an account of work sponsored by an agency of the United States Government. Neither the United States Government nor any agency Thereof, nor any of their employees, makes any warranty, express or implied, or assumes any legal liability or responsibility for the accuracy, completeness, or usefulness of any information, apparatus, product, or process disclosed, or represents that its use would not infringe privately owned rights. Reference herein to any specific commercial product, process, or service by trade name, trademark, manufacturer, or otherwise does not necessarily constitute or imply its endorsement, recommendation, or favoring by the United States Government or any agency thereof. The views and opinions of authors expressed herein do not necessarily state or reflect those of the United States Government or any agency thereof.

DISCLAIMER

Portions of this document may be illegible in electronic image products. Images are produced from the best available original document.

This report was prepared as an account of work sponsored by the United States Government. Neither the United States nor the United States Department of Energy, nor any of their employees, nor any of their contractors, subcontractors, or their employees, makes any warranty, express or implied, or assumes any legal liability or responsibility for the accuracy, completeness or usefulness of any information, apparatus, product or process disclosed, or represents that its use would not infringe privately owned rights.

Printed in the United States of America

Available from

National Technical Information Service U.S. Department of Commerce 5285 Port Royal Road Springfield, Virginia 22161

Price: Printed Copy \$6.50; Microfiche \$3.00

UNCLASSIFIED

UR-3490-1878

UC-48 **Biology and Medicine** TID-4500-R68

UNIVERSITY OF ROCHESTER

Department of Radiation Biology and Biophysics 400 Elmwood Avenue Rochester, New York 14642

Contract DE-AC02-76EVO3490 between the U.S. Department of Energy and the University of Rochester administered by the Department of Radiation Biology and Biophysics of the School of Medicine and Dentistry

ANNUAL REPORT UNIVERSITY OF ROCHESTER DEPARTMENT OF RADIATION BIOLOGY AND BIOPHYSICS **BRIEF DESCRIPTION OF RESEARCH PAPERS** ACCEPTED FOR PUBLICATION DURING

1979 . #

Prepared by: Dorris B. Nash, Editorial Assistant

Submitted by: Paul L. La Celle, Director

iot necessarily co

Date of Issue: June 16, 1980

litute or imply lt\$ States Government or any agency thereof. The views a nenessarily state or retlect mose of the United States Co

UNCLASSIFIED

makes any

DISTRIBUTION OF THIS DOCUMENT IS UNLIMITED

Abboud, C. N.; Brennan, J. K.; Lichtman, M. A. and Nusbacher, J.: Quantification of erythroid and granulocytic precursor cells in plateletpheresis residues. Transfusion, (in press) (UR-3490-1594)

Mononuclear cell fractions of human blood and plateletpheresis residues were compared for their content of hemopoietic precursor cells. Erythroid burst-forming units (BFU-E) averaged 560 ± 130 per ml of blood and granulocyte-monocyte colony forming units (CFU-C) averaged 240 ± 90 per ml blood. Estimates based on a blood volume of 7% of body weight indicate that the total blood pools of BFU-E and CFU-C are about $3.5 \ge 10^6$ and $1.5 \ge 10^6$ cells respectively.

Plateletpheresis residues prepared after a mean of 3.4 liters of blood had been processed contained $1.3 \pm 0.22 \ge 10^6$ BFU-E and $0.50 \pm 0.13 \ge 10^6$ CFU-C. These values represent a 68% and 63% recovery respectively of BFU-E and CFU-C from the processed 3.4 liters of blood.

Sequential studies were performed over three days following one plateletpheresis in four donors. CFU-C and BFU-E approximately doubled between 48 and 72 hours after a plateletpheresis. During this time there was no significant alteration in the percent of null, T or B lymphocytes in blood. Thus, plateletpheresis appears to lead to a mobilization of precursor cells which results in a transient increase in their concentration in blood. Therefore, pheresis 48 to 72 hours after an initial short-term procedure could harvest much larger numbers of precursor cells. Moreover, such techniques would put blood precursor cell content of plateletpheresis residues within reach of the precursor cell content in the volume of human marrow used for transplantation.

Abramson, J. J. and Shamoo, A. E.: Anionic detergents as divalent cation ionophores across black lipid membranes. J. Memb. Biol., (in press) (UR-3490-1513)

Three ionic detergents commonly used in membrane-bound protein isolation and reconstitution experiments: SDS, cholate, and DOC, are shown to act as divalent cation ionophores when incorporated into black lipid membranes made from either oxidized cholesterol or a mixture of phosphatidylcholine and cholesterol (PC:cholesterol = 5 mg : 1 mg). At a concentration greater than or equal to 1 μ M, SDS shows large selectivity differences between cations and anions and between the different cations tested (Ba²⁺, Ca²⁺, Sr²⁺, Mg²⁺, and Mn²⁺). Deoxycholate and cholate at concentrations greater than 4 x 10⁻⁴ M and 10⁻³ M, respectively, also act as divalent cation ionophores. The selectivity sequence measured for these two detergents is evidence for a strong ionic interaction between the divalent cation and the anionic charged groups on the detergent. In the case of cholate, the conductance depends on the third or fourth power of the cholate concentration and shows a linear dependence on CaCl₂ concentration. The conductance for deoxycholate depends on the sixth or seventh power of the DOC concentration and is also

6.

-1-

linearly dependent on the CaCl₂ concentration. In an oxidized cholesterol black lipid membrane in the presence of 5 mM CaCl₂, small concentrations of LaCl₃ ($\langle 1 \mu M \rangle$) inhibit the ionophoric activity of each of the detergents tested. Evidence is presented to show that this inhibitory effect is a nonspecific effect on oxidized cholesterol BLMs and is not due to a direct effect of La³⁺ on detergent-mediated transport.

Bean, B. P.: Modification of sodium and potassium channel kinetics by diethyl ether and studies on sodium channel inactivation in the crayfish giant axon membrane. Ph.D. Thesis, University of Rochester School of Medicine and Dentistry (Supervised by Dr. D. A. Goldstein and Dr. P. Shrager) (1979) (UR-3490-1787)

The effects of ether and halothane on membrane currents in the voltage clamped crayfish giant axon membrane were investigated. Concentrations of ether up to 300 mM and of halothane up to 32 mM had no effect on resting potential or leakage conductance. Ether and halothane reduced the size of sodium currents without changing the voltage dependence of the peak currents or their reversal potential. Ether and halothane also produced a reversible, dose-dependent speeding of sodium current decay at all membrane potentials. Ether reduced the time constants for inactivation measured with the double pulse technique and also shifted the midpoint of the steady-state inactivation curve in the hyperpolarizing direction. Large concentrations of ether or halothane resulted in an irreversible shift, in the depolarizing direction, of the voltage-dependence of other sodium channel parameters. Potassium currents were smaller with ether present, with no change in the voltage dependence of steady-state currents. The activation of potassium channels was faster with ether present; the time to half maximum potassium current was decreased at all membrane potentials. There was no apparent change in the capacitance of the crayfish giant axon membrane with ether concentrations of up to 100 mM.

Experiments on sodium channel inactivation kinetics were performed using 4-aminopyridine to block potassium currents. The spatial uniformity of voltage clamp currents was checked by the method of Cole and Moore (J. Gen. Physiol. 44, 123) using a closely spaced pair of electrodes to measure relatively localized current density. Sodium currents decayed with a time course generally fit well by a single exponential. The time constant of decay was a steep function of voltage, especially in the negative resistance region of the peak current vs voltage relation. The time course of inactivation measured with the double-pulse procedure was very similar to that of the decay of the current at the same potential. The measurement of steady-state inactivation curves with different test pulses showed no shifts along the voltage axis of the type described in other

- 2 -

axons and predicted by some sodium channel models. Measurements of the voltage-dependence of the integral of sodium conductance were made in order to test models of sodium channel inactivation in which channels must open before inactivating; the results appear inconsistent with some of the simplest cases of such models.

Berg, G. G. and Miles, E. F.: Mechanisms of inhibition of active transport ATPases by mercurials. Chem.-Biol. Interactions, 27: 199-219 (1979) (UR-3490-1454)

Inhibition by methylmercury and mercuric chloride of Mg,Ca ATPase and Na,K ATPase activities in human erythrocyte ghosts was correlated with the binding capacity of ghosts for the mercurial. Full inhibition was always reached below saturation of binding capacity, and halfinhibition at levels as low as 10% saturation. Under such conditions, concentrations of free inhibitor were negligibly low, and existing mathematical models of inhibition were not applicable. New inhibitor partition equations were introduced to model the mechanisms of action of mercurials. Up to seven methylmercury groups were calculated to bind to one Na,K ATPase molecule at noninhibitory sites while only one reacted with the inhibitory site. Mg,Ca ATPase showed simple one-hit inhibition (one mercurial per enzyme); further washing of ghosts, however, unmasked a second binding site (cooperative two-hit inhibition). Affinities of mercurials to sites of inhibition were calculated relative to other ligands in erythrocyte membranes: the ratios ranged from 3 : 1 to 50 : 1. The results demonstrated the use of binding capacity assays and inhibitor partition equations to measure and compare the susceptibilities of membrane-bound enzymes to poisoning by mercurials.

Bidlack, J. M.: Molecular mechanism by which cyclic AMP regulates myocardial contractility. Ph.D. Thesis, University of Rochester School of Medicine and Dentistry (Supervised by Dr. A. E. Shamoo) (1979) (UR-3490-1692)

The addition of cyclic AMP-dependent protein kinase and cyclic AMP to canine cardiac sarcoplasmic reticulum is known to increase Ca^{2+} transport into the sarcoplasmic reticulum. The mechanism of this enhanced transport is investigated here. Cyclic AMP-dependent protein kinase phosphorylates a 6,000 and a 22,000 dalton protein as determined by SDS-polyacrylamide slab gel electrophoresis and autoradiography. Maximal phosphorylation occurs when protein kinase and cyclic ADP are incubated with the microsomes. However, the isolated sarcoplasmic reticulum does contain endogenous adenylate cyclase and protein kinase, which phosphorylate both proteins. Phosphodiesterase completely inhibits phosphorylation. In the presence of a phosphatase inhibitor, the time course of the phosphorylation of the two proteins differs. The 22,000 dalton protein is phosphorylated more rapidly than the 6,000 dalton protein. Once phosphorylated the 22,000 dalton protein is soluble in acidified chloroform:methanol while the 6,000 dalton protein is not. Prior to phosphorylation, both proteins can be digested by trypsin and cannot be phosphorylated later. When phosphorylated first, both proteins are resistant to digestion by trypsin. Prior to phosphorylation, both proteins are soluble in a low concentration of the detergent, deoxycholate (DOC). After phosphorylation, neither protein can be solubilized by DOC. Phosphorylation appears to cause the proteins to become buried in the membrane.

By employing very low concentrations of DOC (less than $1 \mu g$ DOC/mg microsomal protein), purification of the 22,000 dalton protein and the Ca²⁺ + Mg²⁺-ATPase has been accomplished. After solubilizing the extrinsic membrane proteins including the 22,000 dalton protein by a low concentration of DOC, passage of these proteins through a Sephadex G - 75 column results in the purification of the 22,000 dalton protein. The protein is still specifically phosphorylated by cyclic AMP-dependent protein kinase, incorporating approximately 0.15 moles of phosphate/mole of protein. Approximately 5 moles of phospholipid are bound to 1 mole of purified protein.

The Ca²⁺ + Mg²⁺-ATPase is purified by first solubilizing the extrinsic proteins with DOC. Then the addition of an increasing amount of DOC to the pellet from the first solubilization results in the solubilization and purification of the Ca²⁺ + Mg²⁺-ATPase to at least 95% purity. The Ca²⁺ concentration required for half maximal activity of the ATPase is approximately 5.2 μ M. The purified ATPase hydrolyzes ATP at the rate of 2.47 μ moles Pi/mg/min.

When the purified $Ca^{2+} + Mg^{2+}$ -ATPase is reconstituted into asolectin vesicles, the ATPase actively transports Ca^{2+} into the vesicles with the transport dependent on the presence of ATP. When the 22,000 dalton protein is reconstituted with the ATPase, no change in the transport of Ca^{2+} is observed during a short time course. However, when phosphate is included inside the vesicles to precipitate entering Ca^{2+} , maximal transport is observed when the ATPase and the phosphorylated 22,000 dalton protein are reconstituted together. The reconstituted ATPase and the nonphosphorylated 22,000 dalton protein do not transport Ca^{2+} at a greater rate than that observed by the ATPase alone. The phosphorylated 22,000 dalton protein reconstituted without the ATPase facilitates the transport of Ca^{2+} . The enhanced transport seen when the phosphorylated 22,000 dalton protein and the ATPase are reconstituted together is an additive effect of the two individual processes. The phosphorylated 22,000 dalton protein does not regulate the ATPase's ability to transport Ca^{2+} but instead is capable of transporting Ca^{2+} itself. In vesicles without phosphate inside, the initial rate of Ca^{2+} uptake for the reconstituted 22,000 dalton protein is approximately eight times greater for the phosphorylated protein than the

- 4 -

nonphosphorylated one. Including phosphatases in the uptake medium reduces the uptake of the originally phosphorylated 22,000 dalton protein to that of the nonphosphorylated protein. Ba²⁺, Sr²⁺, and Mn²⁺ have virtually no effect on the transport of Ca²⁺ into the vesicles. Zn²⁺ inhibits transport by approximately 30% and Hg²⁺ and ruthinum red inhibit Ca²⁺ transport almost completely.

As a result of these experiments, it appears that the phosphorylated 22,000 dalton protein does not regulate the transport properties of the ATPase. Instead phosphorylation of the 22,000 dalton protein causes it to become buried in the membrane, transporting Ca^{2+} into the sarcoplasmic reticulum and thereby elevating the Ca^{2+} concentration in the sarcoplasmic reticulum available for release to the myofibrils.

Brand, J. S.; Cushing, J. and Hefley, T.: Potassium, sodium, and the intracellular fluid space of cells from bone. Calc. Tiss. Intern., 29: 119-125 (1979) (UR-3490-1619)

Cells enzymatically dispersed from fetal rat calvaria were analyzed for sodium and potassium content and intracellular fluid space (ICF). Even when obtained in comparatively high yield, the cells are damaged by the isolation procedure as evidenced by high sodium and low potassium content immediately after isolation. During a postincubation period, potassium is accumulated and sodium extruded to steady-state levels. Although electrolyte content of cells after recovery did not vary as a function of cell yield, ICF was increased in cells obtained in lower yield, suggesting cell swelling as a result of membrane damage.

The weighted mean values obtained by the best cell preparations were 117 mM K⁺ and 27 mM Na⁺. Based on DNA assay of isolated cells and the whole tissue, 20- to 21-day calvaria were found to have an average of 8.1×10^6 cells/calvarium. Combining cell data with analysis of total tissue sodium, potassium, and water, it was concluded that the tissue extracellular sodium is in equilibrium with blood but that the potassium concentration is approximately 5-fold higher than blood levels.

Brennan, J. K.; DiPersio, J. F.; Abboud, C. N. and Lichtman, M. A.: The exceptional responsiveness of certain human myeloid leukemia cells to colony-stimulating activity. Blood, 54: 1230-1239 (1979) (UR-3490-1630)

We have studied the marrow cells from a patient with acute myeloid leukemia (AML) for their responsiveness to colony-stimulating activity (CSA) in vitro. The ADL cells were stimulated by CSA to rapid and extended growth in liquid culture. In the absence of CSA, the majority of cells died. CSA also stimulated the clonal growth of AML cells and the minimum requirement for CSA was one-tenth to one-fiftieth that required to stimulate the growth of normal marrow CFU-C. CSA for AML cells was eluted from Sephacryl S-200 columns in fractions that represented an apparent molecular weight of 45,000 daltons. This fraction also produced optimal stimulation of normal human marrow. During remission, the patient's marrow cells did not grow in liquid culture and produced normal numbers of granulocytic and erythroid colonies in response to CSA and erythropoietin. Extended culture of the AML cells resulted in cell differentiation evidenced by decreasing proliferative capacity and by morphological and histochemical changes. These studies indicate that certain AML cells are extraordinarily responsive to CSA, an *in vitro* mediator of normal granulopoiesis.

Brennan, J. K.; Lichtman, M. A.; Di Persio, J. F. and Abboud, C. N.: Modulators of granulopoiesis: a review. Exptl. Hematol., (in press) (UR-3490-1535)

The marrow is a diffuse organ distributed within the cortex of central bones making it extremely difficult to delineate the biochemical environment of hemopoietic cell growth. Moreover, very early, undifferentiated precursors compose only a small percentage of mitotic cells thereby rendering the study of stem cells and their immediate descendents *in situ* extremely difficult. The ability to grow animal marrow in viscous culture and the adaptation of this technique to the study of human marrow has provided a powerful tool with which to explore the regulation of hemopoiesis. Although marrow culture cannot reproduce the unique stromal-parenchymal relationships of marrow, it surmounts the principal obstacle to studying the physiology of primitive marrow cells, inaccessability. The viscous culture system has provided a means whereby stimulators and inhibitors of primitive hemopoietic cells can be studied. The purpose of this review is to discuss chemicals that influence granulopoiesis, emphasizing those that function in viscous culture.

Brommage, R. and Neuman, W. F.: Bone mineral solubility and its alteration by 1,25-dihydroxyvitamin D₃. In <u>Vitamin D Basic Research and its Olinical Application</u>, Ed. by A. W. Norman, K. Schaefer, D. v. Herrath, H.-G. Grigoleit, J. W. Coburn, H. F. DeLuca, E. B. Mawer and T. Suda. Walter de Gruyter and Co., Berlin, New York, pp. 369-372 (1979) (UR-3490-1531)

In vitro incubations of neonatal mouse calvaria were performed in a buffer designed to prohibit cellular metabolism and thereby permit the estimation of the solubility of bone mineral. Bone mineral solubility decreased through four days of incubation and this decrease, together with an increasing mineral Ca/P ratio, strongly suggests that a mineral phase transition occurs upon the cessation of bone cell activity. Since the estimates of the *in vivo* bone mineral solubility were found to be close to the calculated free Ca X P_i product in the plasma of these mice, plasma may not be normally supersaturated with respect to bone mineral.

- 6 -

Injection of 20 ng of 1,25-(OH)₂D₃, an active metabolite of vitamin D₃, into the mice 24 hours before the start of the incubation increased bone mineral solubility. This increased solubility is proposed to: (a) result from a solubilizing agent(s) secreted by bone cells in response to 1,25-(OH)₂D₃, and (b) play a role in the mechanism by which 1,25-(OH)₂D₃ promotes the mobilization of bone mineral.

Camner, P.; Clarkson, T. W. and Nordberg, G. F.: Routes of exposure, dose and metabolism of metals. Chapt. 5 in <u>Handbook on the Toxicology of Metals</u>, Ed. by L. Frieberg et al. Elsevier/ North-Holland and Biomedical Press, Amsterdam, pp. 65-97 (1979) (UR-3490-1678)

When evaluating the potential adverse effects of metal exposure it is important to understand the mechanisms by which the metal is delivered from the source to the site of action in the human body. Where such mechanisms are a result of events taking place in the ecosystem, they will be dealt with mainly in Chapter 4. This chapter will focus on mechanisms and factors of importance for the uptake and distribution of metals when they contact the human organism. Since airborne metals occur most frequently as aerosols, a considerable part of the chapter will deal with factors of importance for aerosol deposition and absorption in the human lung. As regards the absorption of aerosols of metals, some general knowledge is available which is applicable for prediction of absorption mechanisms. Such knowledge is not available to the same extent either for other absorption routes or for factors governing distribution and excretion of metals. These aspects will therefore be dealt with more briefly.

In parts of this chapter dealing in detail with particular questions (e.g., aerosols, metabolic models), original publications are referred to. In other parts, original references are not given since other chapters give further details.

Some details on how the dose rate may influence mathematical models for dose-effect and dose-response relationships are discussed in Chapter 7. Such influence of dose rate may be sometimes explained by the rates for absorption, transport, biotransformation and excretion which control the dose reaching the site of effect. These factors will be dealt with in this chapter.

Campbell, K. P. and Shamoo, A. E.: Chloride-induced release of actively loaded calcium from light and heavy sarcoplasmic reticulum vesicles. J. Memb. Biol., (in press) (UR-3490-1639)

Light and heavy sarcoplasmic reticulum vesicles isolated from rabbit leg muscle have been used in a study of chloride-induced calcium release. The biochemical and morphological data indicate that light sarcoplasmic reticulum vesicles are derived from the longitudinal reticulum and heavy sarcoplasmic reticulum vesicles are derived from the terminal cisternae of the sarcoplasmic reticulum.

The light and heavy sarcoplasmic reticulum vesicles were both able to accumulate calcium in the presence of ATP to amounts greater than 100 nmoles calcium per mg of protein in less than one minute. Light and heavy sarcoplasmic reticulum vesicles each had a biphasic time course of calcium uptake. The initial uptake was followed by a rapid release after approximately one minute, of 30% to 40% of the accumulated calcium, which was then followed by a slower phase of calcium accumulation.

Calcium taken up by the SR vesicles could be released from both the light and heavy SR vesicles by changing the anion outside the vesicles from methanesulfonate to chloride. Due to the difference in permeability between methanesulfonate and chloride, this change should result in a decreased positivity inside the vesicles with respect to the exterior. It could also result in a swelling of the vesicles. Changing the ionic medium from chloride to methanesulfonate caused no release of calcium. The percentage of accumulated calcium released in 6 seconds by changing the anion outside the vesicles from methanesulfonate to chloride was approximately 40% and 20% for light and heavy SR, respectively.

Sucrose (200 mM) caused a slight inhibition of chloride-induced calcium release from the heavy SR vesicles but it greatly reduced the release of calcium from the light SR vesicles. The specificity of calcium release was measured using SR vesicles which had been passively loaded with $10 \text{ mM } ^{22}\text{Na}^+$ or 14C sucrose. The amount of $^{22}\text{Na}^+$ or 14C sucrose released during a chloride-induced release of cold calcium was then measured. The light SR vesicles released three to five times more $^{22}\text{Na}^+$ than the heavy SR vesicles. There was a significant difference in the amount of ^{14}C sucrose released from light vs heavy SR.

Sodium dantrolene (20 μ M) had no effect on the release of calcium from the light SR vesicles but it inhibited the release of calcium from the heavy SR vesicles.

Our results indicate that the chloride-induced release of calcium may be acting by two mechanisms, osmotic swelling and depolarization. The release of calcium from the light SR vesicles is probably due to swelling and the release of calcium from the heavy SR vesicles is probably due to depolarization.

Cardillo, T. S.; Landry, E. F. and Wiberg, J. S.: *regA* protein of bacteriophage T4D: identification, schedule of synthesis and autogenous regulation. J. Virol., 32: 905-916 (1979) (UR-3490-1597)

Proteins labeled with ¹⁴C-amino acids after infection of *Escherichia coli* B by T4 phage were examined by electrophoresis in the presence of sodium dodecyl sulfate. Four *regA* mutants (*regA*1, *regA*8, *regA*11, and *regA*15) failed to make a protein having a molecular weight of about 12,000,

- 8 -

whereas mutant regA9 did make such a protein; regA15 produced a new, apparently smaller protein that was presumably a nonsense fragment, whereas regA11 produced a new, apparently larger protein. We conclude that the 12,000-dalton protein was the product of the regA gene. The molecular weight assignment rested primarily on our finding that the regA protein had the same mobility as the T4 gene 33 protein, which we identified by electrophoresis of whole-cell extracts of *E. coli* B infected with a gene 33 mutant, amE1120. Synthesis of wild-type regA protein occurred from about 3 to 11 minutes after infection at 37° C in the DNA⁺ state and extended to about 20 minutes in the DNA⁻ state. However, synthesis of the altered regA proteins of regA9, regA11, and regA15occurred at a higher rate and for a much longer period in both the DNA⁺ and DNA⁻ states; thus, the regA gene is autogenously regulated. At 30° C, both regA9 and regA11 exhibited partial regAfunction by eventually shutting off the synthesis of many T4 early proteins; the specificity of this shutoff differed between these two mutants. We also obtained evidence that the regA protein is not Stevens's "polypeptide 3." As a technical point, we found that, when quantitating acid-precipitable radioactivity in protein samples containing sodium dodecyl sulfate, it was necessary to use 15% to 20% trichloroacetic acid; use of 5% acid, e.g., resulted in loss of over half of the labeled protein.

Carstensen, E. L.; Child, S. Z.; Law, W. K.; Horowitz, D. R. and Miller, M. W.: Cavitation as a mechanism for the biological effects of ultrasound on plant roots. J. Acoust. Soc. Am., 66: 1285-1291 (1979) (UR-3490-1577)

The growth rate of roots is reduced by exposure to ultrasound at 10 W/cm^2 for 1 minute. The reduction is somewhat greater at 1 MHz than at 5 MHz. A hydrostatic pressure of 30 atm reduced, but did not eliminate, the effect of ultrasound on growth. The frequency and pressure dependence taken together with earlier observations support the postulate that a cavitationlike mechanism is at least partly responsible for the action of ultrasound on the growth of these developing plant tissues.

Carter Su, C. and Kimmich, G. A.: Effect of membrane potential on Na⁺-dependent sugar transport by ATP-depleted intestinal cells. Am. J. Physiol., (in press) (UR-3490-1552)

The role of the membrane potential as a thermodynamic driving force and as a determinant of kinetic parameters of Na⁺-dependent sugar transport was investigated using ATP-depleted isolated chicken intestinal cells. Inside-negative membrane potentials were established by incubating K⁺-loaded rotenone-inhibited cells with valinomycin in a low K⁺ medium. Oversitoots of 3-0-methyl-glucose (3-OMG) accumulation as high as ten-fold were observed in the presence of valinomycin even in the absence of a Na⁺-chemical gradient.

- 9 -

The magnitude of overshoot was diminished by decreasing the magnitude of the imposed $[K^+]$ gradient and abolished altogether when nigericin was also included. An Eadie-Hofstee plot of initial flux data showed that the imposed membrane potential increases the V_{max} of transport in the absence of a chemical gradient for Na⁺ from 3 to 12 nmoles 3-OMG/mg protein/min. The K_T is not significantly altered. Similar kinetic results were obtained when a membrane potential as well as a $[Na^+]$ gradient were imposed. These results suggest that the membrane potential is a more important contributor to alterations in the kinetics of transport than the Na⁺ chemical potential. These findings are discussed in terms of their usefulness for predicting the charge of a bound or unbound carrier protein based on the kinetic model of Geck and Heinz.

Carter-Su, C. and Kimmich, G. A.: Membrane potentials and sugar transport by ATP-depleted intestinal cells: effect of anion gradients. Am. J. Physiol., 237: C67-C74 (1979) (UR-3490-1450)

Rotenonc or dinitrophenol treatment was used to decrease cellular ATP levels in isolated chicken intestinal epithelial cells by over 90% and to produce a cell population in which no steady state accumulation of 3-0-methylglucose (3-OMG) against a concentration gradient is observed. In the presence of imposed inward-directed Na-anion gradients, these cells accumulate 3-OMG against a concentration gradient. The degree of maximal 3-OMG accumulation and initial influx stimulation in the presence of a given anion or combined Na-anion, gradient can be correlated with the magnitude of the diffusion potential as determined by the membrane permeability of the given anion $(SCN^{-}) Cl^{-}$ Isethionate $> SO_{4}^{-}$). 3-OMG influx in the presence of a large NaCl gradient is comparable in ATP-depleted and normally energized cells. The slight difference in influx (energized > ATP-depleted) is diminished by ouabain, suggesting that energized cells maintain a larger membrane potential (diffusion potential or rheogenic Na⁺-K⁺ ATPase ion pump-generated potential) than the ATP-depleted cells. Although initial rates of 3-OMG uptake into Na⁺-depleted normally energized cells also varies with the anion gradient, these differences disappear with time of incubation in Na⁺ or when cells are preincubated in Na⁺. In this situation, function of a rheogenic Na⁺ pump can establish a membrane potential in contrast to the case with ATP-depleted cells which have a potential only as long as imposed ion gradients are maintained. All of these experiments point to an important role for the electrical membrane potential as a driving force for Na⁺-dependent solute transport systems in both ATP-depleted and normally energized cells.

Casarett, G. W.: Radiogenic cancer risk estimation. In <u>Archives of the President's Commission on</u> the Accident at Three Mile Island (in press) (UR-3490-1760)

This paper contains general discussions of various aspects of radiogenic cancer, including mechanisms, nonspecificity, latency in relation to age, temporal advancement and absolute excess, dose threshold versus lack thereof, relative biological effectiveness (RBE) and dose-effect relationships for low- and high-LET (linear energy transfer) radiations, influence of dose size and dose rate on dose-effect relationships, problems of extrapolation from observed data at high doses and/or dose rates to low radiation levels, means and assumptions for such extrapolation or interpolation for pragmatic reasons and purposes of prudent radioprotection, scientific validity of such means and assumptions, sources and limitations of human data, pertinent principles from animal experimentation and radiobiologic theory, and absolute versus relative risk estimation models. Following this background discussion, radiogenic cancer risk estimation models and values which have been developed by various national and international bodies are presented and discussed.

Casarett, G. W. (Leader); Abrahamson, S.; Bair, W. J.; Bender, M. A.; Bloom, A. D.; Bond, V. P. and Fabrikant, J. I.: Report on radiation health effects. In <u>Staff Reports to the President's</u> <u>Commission on the Accident at Three Mile Island. Reports of the Public Health and Safety</u> <u>Task Force. Washington, D. C., pp. 195-255 (1979) (UR-3490-1850)</u>

This report presents assessments of the potential health impact on the approximately two million offsite residents within 50 miles of the Three Mile Island (TMI) Nuclear Station and on workers onsite from collective and individual ionizing radiation exposure doses received as a consequence of the nuclear plant accident on March 28, 1979.

Chattoo, B. B.; Palmer, E.; Ono, B. and Sherman, F.: Patterns of genetic and phenotypic suppression of *lys2* mutations in the yeast *Saccharomyces cerevisiae*. Genetics, (in press) (UR-3490-1613)

A total of 358 lys2 mutants of the yeast Saccharomyces cerevisiae have been characterized for suppressibility by the following suppressors: UAA and UAG suppressors that insert tyrosine, serine or leucine; a putative UGA suppressor; an omnipotent suppressor SUP46; and a frameshift suppressor SUF1-1. In addition, the lys2 mutants were examined for phenotypic suppression by an aminoglycoside antibiotic paromomycin, for osmotic remediability and for temperature sensitivity. The mutants exhibited over 50 different patterns of suppression and most of the nonsense mutants appeared similar to nonsense mutants previously described. A total of 24% were suppressible by one or more of the UAA suppressors, 4% were suppressible by one or more of the UAG suppressors while only one was suppressible by the UGA suppressor and only one was weakly suppressible by the frameshift suppressor. One mutant responded to both UAA and UAG suppressors, indicating that UAA or UAG mutations at certain rare sites can be exceptions to the specific action of UAA and UAG suppressors. Some of the mutants appear to require certain types of amino acid replacements at the mutant sites in order to produce a functional gene product while others appeared to require suppressors that were expressed at high levels. Many of the mutants suppressible by the SUP46 suppressor and by paromomycin were not suppressible by any of the UAA, UAG or UGA suppressors, indicating that omnipotent suppression and phenotypic suppression need not be restricted to nonsense mutations. All of the mutants suppressible by SUP46 were also suppressible by paromomycin, suggesting a common mode of action of omnipotent suppression and phenotypic misreading.

Chattoo, B. B.; Sherman, F.; Azubalis, D. A.; Fjellstedt, T. A.; Mehnert, D. and Ogur, M.: Selection of *lys2* mutants of the yeast *Saccharomyces cerevisiae*. Genetics, (in press) (UR-3490-1609)

Normal strains of the yeast Saccharomyces cerevisiae do not use α -aminoadipate as a principal nitrogen source. However α -aminoadipate was utilized as a nitrogen source by lys2 and lys5 strains having complete or partial deficiencies of α -aminoadipate reductase or to a limited extent by heterozygous lys2/+strains. Lys2 mutants were conveniently selected on media containing α -amino-adipate as a nitrogen source, lysine, and other supplements to furnish other possible auxotrophic requirements. The lys2 mutations were obtained in a variety of laboratory strains containing other markers, including other lysine mutations. In addition to the predominant class of lys2 mutants, low frequencies of lys5 mutants and mutants not having any obvious lysine requirement were recovered on α -aminoadipate medium. The mutants not requiring lysine appeared to have mutations at the lys2 locus that caused partial deficiencies of α -aminoadipate reductase. Such partial deficiencies are believed to be sufficiently permissive to allow lysine biosynthesis but sufficiently restrictive to allow for the utilization of α -aminoadipate. Although it is unknown why partial or complete deficiencies of α -aminoadipate reductase causes utilization of α -aminoadipate as a principal nitrogen source, the use of α -aminoadipate medium has considerable utility as a selective medium for lys2 and lys5 mutants.

Clark, R. W.; Wever, G. H. and Wiberg, J. S.: High-molecular-weight DNA and the sedimentation coefficient: a new perspective based on DNA from T7 bacteriophage and two novel forms of T4 bacteriophage. J. Virol., (in press) (UR-3490-1466)

The DNA molecules from T7 bacteriophage and a recently obtained mutant form of T4D were studied. The DNA of this T4 mutant contains cytosine in place of all of the glucosylated hydroxy-

- 12 -

methylcytosines normally present in T4. Molecular weights were measured with an electron microscope technique, and sedimentation coefficients were determined in isokinetic sucrose gradients. T7 DNA was found to have an M_r of 26.5 X 10⁶. The T4 mutant, which we have termed T4c, produces two distinct phage head and DNA size classes. DNA from the standard heads (T4c DNA) has an M_r of 114.9 X 10⁶, and DNA from the petite heads (T4cp DNA) has an M_r of 82.9 X 10⁶. This enabled the derivation of an equation of sedimentation coefficient at zero concentration corrected to water at 20° C versus M_r for the molecular weight range of 25 X 10⁶ to 115 X 10⁶ that is based solely on cytosine-containing DNA standards, thereby avoiding possible anomalies introduced by the glucosylation and hydroxymethylation of cytosine. The theory of Gray et al. provided the best description of the sedimentation coefficient versus M_r relationship, based on the sedimentation coefficients and the molecular weights of the three DNA standards and other evidence.

Clarkson, T. W.: Effects — general principles underlying the toxic action of metals. Chapt. 6 in <u>Handbook on the Toxicology of Metals</u>, Ed. by L. Friberg et al. Elsevier/North-Holland Biomedical Press, Amsterdam, pp. 99-117 (1979) (UR-3490-1253)

Metals produce a wide range of effects in man resulting from their action at molecular, cellular, tissue and organ levels. Depending upon the particular metal involved, the metal action may manifest itself as a local effect on the skin, pulmonary membranes or gastrointestinal tract or it may manifest itself as a systemic effect that could potentially involve any tissue or organ in the body. Furthermore, metals may act as allergens, mutagens, teratogens or carcinogens. No group or class of effects is unique to the metals. Indeed it is the diversity of effects that, if anything, is characteristic of the metals.

A comprehensive, all-inclusive description of the biological effects of metals would amount to a textbook of general pathology. Instead, this chapter will attempt to discuss the general principles underlying the toxic action of metals. Effects associated with a particular metal are described in those chapters of this book dealing with the specific metals.

Cokelet, G. R.: Rheology and hemodynamics. Ann. Rev. Physiol., (in press) (UR-3490-1634)

This is a brief review of the recent literature on two topics: (1) studies of the viscoelastic and time-dependent viscous properties of blood, and (2) studies which investigate the fluid mechanics of blood flow in microvascular-size vessels and its relationship to macroscopic rheological data for blood. Both sections not only review reported findings, but point out some conflicts between reported data, possible experimental artifacts, limitations of data analysis, and areas needing further investigation.

Cokelet, G. R.; Meiselman, H. J. and Goldsmith, H. L.: Some potential blood flow experiments for space. Proc. Fluids Experiment System Workshop, July 1979, Huntsville, Alabama. University of Alabama, Huntsville, (in press) (UR-3490-1729)

Blood is a colloidal suspension of cells, predominantly erythrocytes (red cells), in an aqueous solution called plasma. Because the red cells are more dense than the plasma, and because they tend to aggregate, erythrocyte sedimentation can be significant when the shear stresses in flowing blood are small. This behavior, coupled with equipment restrictions, has prevented certain definitive fluid mechanical studies from being performed with blood in ground-based experiments. Among such experiments, which could be satisfactorily performed in a microgravity environment, are the following: (a) studies of blood flow in small tubes, to obtain pressure-flow rate relationships, to determine whether increased red cell aggregation can be an aid to blood circulation, and to determine vessel entrance lengths, and (b) studies of blood flow through vessel junctions (bifurcations), to obtain information on cell distribution in downstream vessels of (arterial) bifurcations, and to test flow models of stratified convergent blood flows downstream from (venous) bifurcations.

Coleman, J. R. and Young, L. B.: Metal binding by intestinal mucus. Proc. Scanning Electron Microscopy Meeting, April 1979, Washington, D. C. (SEM/1979), pp. 801-806 (1979) (UR-3490-1539)

The study of mucus has been hampered by the fact that it is heterogeneous, consisting of a protein core associated with highly variable branched chain sugar residues. This heterogeneity introduces ambiguities that have made isolation of mucus difficult. Electron probe microanalysis offers distinct advantages for the study of intestinal mucus. This technique permits analysis of metal binding *in situ*, requires only a small amount of tissue, allows several experiments to be performed with one animal, and can resolve variations in binding that may occur in different portions of the intestine.

We have used electron probe microanalysis to examine the metal binding capacity of intestinal mucus *in situ*. We have exposed portions of excised intestine to various concentrations of several metals, rapidly frozen the tissue and freeze-dried it. After anhydrous embedding, thick sections were cut and analyzed on silicon discs. Qualitative analysis shows three distinctive patterns of distribution. The results of this work show clearly that several metals are bound by mucus, the influence of mucus must be considered in short-term measurements of metal uptake, that mucus exhibits different affinities for different metals, and the binding of metals is not uniform throughout mucus.

Cory-Slechta, D. A.; Garman, R. H. and Seidman, D. S.: Lead-induced crop dysfunction in the pigeon. Toxicol. Appl. Pharmacol., (in press) (UR-3490-1536)

Pigeons consuming or treated with lead acetate (12, 36, or 72 mg Pb/kg/day and 1000 or 3000 ppm lead acetate solution) displayed crop dilatation and stasis and motor incoordination, regurgitated crop fluid, and suffered severe wasting of breast muscle. Ball bearings inserted in the crop failed to pass to the stomach. Such retardation of motility reliably preceded signs of overt toxicity. The etiology of the crop stasis could not be determined by histopathologic examination, suggesting a subcellular mechanism. These results suggest that behavioral changes induced by lead in pigeons cannot be attributed to CNS dysfunction alone but, more likely, arise from starvation or, at best, from combined CNS damage and starvation.

Dahle, D.; Griffiths, T. D. and Carpenter, J. G.: Subchromosomal DNA synthesis in X-irradiated V-79 cells. Radiation Res., 78: 542-549 (1979) (UR-3490-1383)

The effect of X radiation on DNA replication in Chinese hamster V-79 cells has been investigated by DNA fiber autoradiography. The only effect observed at the replicon level is a reduction in the frequency of initiation events. The dose-response for this reduction is multiphasic indicating that some initiation events are much more radioresistant than others. When the data obtained from DNA fiber autoradiography are compared to kinetic data for thymidine incorporation, it is evident that at least for V-79 cells, the effects of X radiation on thymidine uptake into acidprecipitable material can be entirely accounted for by alterations in the frequency of initiation of replicon clusters.

DeTraglia, M. C.: I. The use of m- and p-azidobenzamidine, 4-fluoro-3-nitro-phenylazide, and 3-azido-1,2,4-triazole as photoaffinity probes of tryptic binding site conformation. II. Analysis of tryptophan in proteins by an acidic reaction of 3-diazonium-1,2,4-triazole. Ph.D. Thesis, University of Rochester School of Medicine and Dentistry (Supervised by Dr. J. S. Brand) (1979) (UR-3490-1689)

Meta- and para-azidobenzamidine have been prepared and evaluated as photoaffinity labels. The compounds inhibit trypsin reversibly in the dark and are competitive with substrate binding. Upon photolysis, irreversible noncompetitive inhibition is observed and is dependent upon concentration, photolysis time, and pH. Specificity of the probes is indicated by experiments in which p-tosyl-L-arginine methyl ester, a trypsin substrate, is used to protect against photoinactivation.

Evaluation of the pH dependence of photoaffinity labeling reveals that the probes are capable of producing varying degress of irreversible inactivation of trypsin depending upon the pH maintained during photolysis. This phenomenon is caused by the ability of the reagents to

- 15 -

(x)

translate the affinity of complement binding sites at any pH to a proportionate level of photoinactivation upon photolysis. That the degree of photoinactivation observed with these inhibitors represents a measure of specific binding affinity versus pH is corroborated by 1) the enzyme's activity profile, 2) ORD spectra, and 3) affinity versus pH data obtained for m-ABA by UV spectral titration. In contrast, photolytic inhibition by 4-fluoro-3-nitrophenylazide shows maxima at pH 3 and 9 with little inhibition at pH 6 to 7. This demonstrates 1) that hydrophobic sites are revealed at pH extremes (enzyme denaturation) and 2) that pH extremes alone are not deterrent to covalent nitrene attachment. These results demonstrate that under controlled conditions photoaffinity techniques may be used to probe changes in target site affinity as a function of pH.

Unlike conventional aryl diazonium reagents which are reactive at alkaline pH, 3-diazonium-1, 2,3-triazole (3-DT) has been found to react with a variety of proteins at acid pH. The rate of 3-DT coupling to the indole nucleus has been shown to increase exponentially from $\langle 200 \text{ M}^{-1} \text{ min. at} \text{ pH 6 to} \rangle 2400 \text{ M}^{-1} \text{ min.}^{-1}$ at pH 2.5. In experiments using trypsin, 3-DT was found to cause loss in enzymatic activity at acidic as well as alkaline pH. Furthermore, amino acid analysis has demonstrated that the acidic reaction with trypsin resulted in the modification only of tryptophan. A scintillation method for determining the tryptophan content of proteins has been developed using 1.4C-3-DT.

DeTraglia, M. C.; Brand, J. S. and Tometsko, A. M.: Application of light-sensitive chemicals to probe protein structure and function. Ann. N. Y. Acad. Sci., (in press) (UR-3490-1629)

Certain photoaffinity labelling reagents such as 4-fluoro-3-nitrophenylazide (FNPA), m- and p-azidobenzamidine (m- and p-ABA), and 3-azido-1,2,4-triazole (3-AT) are capable of producing varying degrees of irreversible inactivation of trypsin depending upon the pH maintained during photolysis. This phenomenon is caused by the ability of the reagents to translate the affinity of complement binding sites at any pH to a proportionate level of photoinactivation upon photolysis. The results cannot be attributed to rates of azide photolysis (nitrene generation), as these bear no pH dependence.

Maximum tryptic inhibition by m- and p-ABA and 3-AT occurs in the range of pH 6 to 7 and is prevented in the presence of the protecting substrate TAME. That the degree of photoinactivation observed with these inhibitors represents a measure of specific binding affinity vs pH is corroborated by comparison with 1) the enzyme's activity profile, 2) ORD spectra, and 3) affinity vs pH data obtained for p-ABA by UV spectral titrations.

In contrast, photolytic inhibition by FNPA shows maxima at pH 3 and 9 with little inhibition

- 16 -

at pH 6 to 7. This demonstrates 1) that hydrophobic sites are revealed at pH extremes (enzyme denaturation) and 2) *most importantly* that pH extremes are not deterrent to nitrene insertion.

These results demonstrate that under controlled conditions photoaffinity techniques may be used to probe target site conformation and enzyme function.

DeTraglia, M. C.; Brand, J. S. and Tometsko, A. M.: The reaction of 3-diazonium-1,2,4-triazole with tryptophan at acid pH: a scintillation method for tryptophan determination in proteins. Anal. Biochem., 99: 464-473 (1979) (UR-3490-1541)

Unlike conventional aryl diazonium reagents which are usually reactive at alkaline pH, 3-diazonium-1,2,4-triazole (3-DT) has been found to react with a variety of proteins at acid pH. Using indole, phenol, and imidazole as models of aromatic amino acid side chains, the rate of 3-DT coupling to the indole nucleus has been shown to increase exponentially from $\langle 200 \text{ M}^{-1}$ at pH 6 to $\rangle 2400 \text{ M}^{-1}\text{min}^{-1}$ at pH 2.5. Coupling rates with phenol and imidazole show the conventional alkaline reactivity, with no evidence of reaction at acid pH. In parallel experiments using trypsin, 3-DT was found to cause loss in enzymatic activity at acidic as well as alkaline pH. Furthermore, amino acid analysis has demonstrated that the acidic reaction with trypsin resulted in the modification only of tryptophan. Based on the acidic specificity of 3-DT seen in these studies, a scintillation method for determining the tryptophan content of proteins has been developed. Using 3-diazonium-1,2,4[5-¹⁴C] triazole, accurate tryptophan contents for trypsin, chymotrypsin, lysozyme, pepsin, insulin, and fibrinogen have been measured.

Douthwright-Fasse, J. A.: Studies of DNA repair in Saccharomyces cerevisiae. I. Characterization of a new allele of RAD6. II. Investigation of events in the first cell cycle after DNA damage. Ph.D. Thesis, University of Rochester School of Medicine and Dentistry. (Supervised by Dr. C. W. Lawrence) (1979) (UR-3490-1790)

Studies in two independent, but related, areas of DNA repair have been carried out in the eucaryotic yeast, Saccharomyces cerevisiae. The first is the characterization of a new allele in the RAD6 gene suggesting that the gene is multifunctional. The second is the utilization of photoreactivation as a probe of events occurring during the first cell cycle after DNA damage.

Strains carrying the new allele, designated rad6-4, of the RAD6 locus are about as sensitive to UV and ionizing radiation as those carrying rad6-1 or rad6-3 but, unlike them, are capable of induced mutagenesis and sporulation. Diploids homozygous for rad6-4 or heteroallelic for rad6-4 and either rad6-1 or rad6-3 allow UV-induced reversion of the ochre alleles arg4-17 and cyc1-9, of the proline missense allele cyc1-115, and of the frameshift allele cyc1-239. They also permit EMS-induced reversion of cyc1-115. The frequency of reversion is greater than wild-type in each case.

Homozygous rad6-4 diploids sporulate as well as wild-type. Although rad6-4 may well be a missense mutation, our evidence shows that it is unlikely that this phenotype is due to leakiness. Instead, the data suggest that the RAD6 gene is multifunctional. One function is necessary to recover from DNA damage in an error-free manner and the other is concerned with mutagenic processes and sporulation. Rad6-1 and rad6-3 strains are deficient in both of these functions, while rad6-4 strains are deficient only in the error-free function.

The loss of photoreversibility (LOP) of ultraviolet-induced mutations to arginine independence in an excision-defective strain carrying *arg4-17* examines the events occurring in the first cell cycle after DNA damage. LOP is dependent upon *de novo* protoin synthesis. The post UV protein synthesis causes pyrimidine dimers to become inaccessible to the photoreactivating enzyme in some unknown manner. LOP begins immediately after UV irradiation, before semiconservative DNA synthesis takes place, and is complete after four hours in growth medium. There is no evidence indicating whether the normal function of the protein is involved in excision repair or in one of the two repair processes believed to be inducible; induced mutagenesis or recombinational repair.

Dunn, J. D. and Clarkson, T. W.: Does mercury exhalation signal demethylation of methylmercury? Health Phys., Note, (in press) (UR-3490-1685)

Expiration of mercury after administration of MeHg was tested in intact CBA/J mice injected with purified 203 Hg-labeled MeHg at 0.5 mg Hg/kg. At various times up to day 7 after MeHg, mice were assayed for Hg exhalation rates with or without ethanol. The chemical form of mercury eliminated, as well as the change in the mercury volitalization rate with time after mercury administration, and the effect of ethanol on this route of elimination, was investigated over this period of time. Increase in the percent of body burden exhaled, in addition to the increased inorganic fraction of mercury in several tissues, indicate that mercury is subject to exhalation *in vivo* only after the carbon-mercury bond is broken.

Evans, I. M.; Forrest, N.; Lawrence, A. and Eberle, H.: Effect of blocking protein synthesis at nonpermissive temperatures on temperature-sensitive deoxyribonucleic acid mutants of *Escherichia coli*. J. Bacteriol., 140: 445-451 (1979) (UR-3490-1424)

When protein synthesis was blocked in temperature-sensitive deoxyribonucleic acid synthesis mutants of *Escherichia coli* at nonpermissive temperatures, it reduced the amount of apparent subsequent chain elongation to approximately half that observed in the mutants either at nonpermissive temperatures alone or when protein synthesis was blocked at the permissive temperature. Blocking protein synthesis at the nonpermissive temperatures for periods of 40 minutes caused the loss of ability to reinitiate deoxyribonucleic acid synthesis at the permissive temperature.

Ferin, J. and Leach, L. J.: Horizontal air flow inhalation exposure chamber. Chapt. 25 in <u>Generation of Aerosols</u>, Ed. by K. Willeke. (Proc. Symp. on Aerosol Generation and Exposure Facilities, April 1979, Honolulu, Hawaii.) Ann Arbor Science Publishers, Inc., Ann Arbor, Mich., (in press) (UR-3490-1471)

Many investigators have described inhalation exposure chambers of various forms commonly utilizing vertical (in the direction of gravity) air flow patterns. In this type of exposure unit, experimental animals are usually housed in vertically stacked cages thus allowing those at lower levels to be in direct contact with excreta expelled from above. Unless the location of the animals is changed systematically, there is a good possibility of varied exposure to the test material, microorganisms, animal dander, products of excretion and temperature and humidity. For these reasons, we have attempted to design and build a new exposure apparatus which utilizes horizontal airflow. This allows the use of excreta-collecting trays between each level of cages and since the air passes horizontally through a single layer of cages, the probability of transmitting airborne disease is lowered.

Finkelstein, J. N. and Mavis, R. D.: Biochemical evidence for internal proteolytic damage during isolation of type II alveolar epithelial cells. Lung, 156: 243-254 (1979) (UR-3490-1378)

The metabolic integrity of cells isolated from tissues by proteolytic dissociation is a question of vital importance in the interpretation of studies in such cells. The integrity of cells isolated from protease-treated lung was investigated by preparing subcellular fractions from isolated cells, proteasetreated lung, or alveolar macrophages. Activities and distribution of marker enzymes and enzymes of phosphatidylcholine synthesis in these fractions were compared with similar fractions from untreated whole lung and macrophages. Although the isolated cells appeared viable by virtue of trypan blue exclusion, the specific activity of the endoplasmic reticulum marker enzyme NADPH cytochrome c reductase was reduced four-fold in fractions from cells and tissues treated with protease. In addition, 38% of the enzyme activity was released into the 150,000 X g supernatant. CDP choline: 1,2 diacylglycerol cholinephosphotransferase activity in similar fractions was reduced by a factor of two to seventeen, depending on the amount of trypsin used in the incubation mixture, with little apparent effect on its subcellular distribution. Phosphatidate phosphohydrolase activity in these fractions was not reduced by protease treatment and was, in fact, increased by elastase digestion. Direct protease treatment of microsomes isolated from normal lung showed that both trypsin and elastase were capable of releasing NADPH cytochrome c reductase from the membrane. Under similar conditions, trypsin virtually eliminated choline phosphotransferase activity while elastase was without effect. These results suggest that during isolation of cells from lung by proteolytic dissociation, the isolated cells are damaged by intracellular uptake of protease and that the analysis of microsomal enzyme activities of cells provides a sensitive method for assessing their functional integrity after isolation. The use of this approach may aid in the development of less harsh methods of tissue dispersion and cell isolation and may yield more native cell populations in general and undamaged type II epithelial cells in particular.

Forbes, G. B. and Drenick, E. J.: Loss of body nitrogen on fasting. Am. J. Clin. Nutrit., 32: 1570-1574 (1979) (UR-3490-1771)

An analysis of the change in total body nitrogen during fasting shows that it declines exponentially, a small fraction being lost rapidly ($t_{1/2}$ of a few days), and the remainder being lost slowly ($t_{1/2}$ of many months). The obese faster loses N, and weight, at a slower relative rate than the nonobese; and the ratio of N loss to weight loss during an extended fast is inversely related to body fat content, being about 20 g/kg in the nonobses and about 10 g/kg in those with body fat burdens of 50 kg or more. The loss of body N on a low protein-calorie adequate diet can also be described in exponential terms, and this function allows an estimate to be made of the N requirement.

Fu, Y-K.; Kaufman, G. E.; Miller, M. W.; Griffiths, T. D. and Lange, C. S.: Modification by cysteamine of ultrasound lethality to Chinese hamster V-79 cells. Radiation Res., 80: 575-580 (1979) (UR-3490-1544)

Exposure of Chinese hamster V-79 cells to 1.1-MHz continuous wave (CW) ultrasound at intensities of 10, 20, and 30 W/cm² resulted in cell lysis and the loss of reproductive integrity (i.e., a decrease in plating efficiency) in the remaining intact cells. Sonication in the presence of 8 mM cysteamine, a free-radical scavenger, did not alter the amount of cell lysis, but did result in a smaller decrease in plating efficiency at 20 and 30 W/cm². Hence, while free radicals do not appear responsible for ultrasonically induced cell lysis, free radicals do appear to be at least partially responsible for loss of reproductive integrity in the remaining intact cells.

Fu, Y-K.; Miller, M. W.; Kaufman, G. E.; Lange, C. S. and Griffiths, T. D.: Ultrasound lethality to synchronous and asynchronous Chinese hamster V-79 cells. Ultrasound Med. Biol., (in press) (UR-3490-1665)

Chinese hamster V-79 cells were exposed in suspensions for 1 to 15 minutes to 1.1 MHz continuous wave (CW) ultrasound at axial intensities from 0.25 to 30 W/cm^2 . Cell lysis was evidenced by a decrease in the number of intact cells, and loss of reproductive integrity was evidenced by a decrease in the plating efficiency of the remaining intact cells. The magnitude of these effects was a function of both intensity and exposure duration. Mitotically synchronized cells displayed a differential sensitivity depending upon cell cycle position. The M and S phases of the cell cycle were more resistant with respect to cell lysis and loss of reproductive integrity than were the G_1 and G_2 phases.

Gentry, G. D. and Marr, M. J.: Choice and delay of reinforcement. J. Exptl. Anal. Behav., (in press) (UR-3490-1551)

Previous studies of choice between two delayed reinforcers have indicated that the relative immediacy of the reinforcer is a major determinant of the relative frequency of responding. Parallel studies of choice between two interresponse times (IRTs) have found exceptions to this generality. The present study looked at the choice of pigeons between two delays, one of which was always four times longer than the other, but the absolute durations were varied across conditions. The results indicated that choice is not uniquely determined by the relative immediacy of reinforcement, but that absolute delays are also involved. Models for concurrent chained schedules appear to be more applicable to the present data than the matching relation; however, these too failed to predict choice for long delays.

Griffiths, T. D.: X-ray response of Chinese hamster ovary cells during the latter part of G₂. Biophys. J., 28: 497-501 (1979) Brief Communication (UR-3490-1672)

The ability of Chinese hamster ovary (CHO) cells to repair X-radiation damage during the transit from the late G_2 to early M cell cycle stages was investigated by conventional dose-fractionation techniques. Despite their relatively high radiation sensitivity, CHO cells positioned in late G_2 exhibit increased survival when a given dose of ionizing radiation is administered as two fractions (separated by 40 to 50 minutes) instead of as a single fraction. This increased survival apparently respresents repair since neither cell cycle progression nor changes in the number of "effective targets" can account for the observed dose-sparing effect.

Griffiths, T. D. and Carpenter, J. G.: Premature chromosome condensation following X-irradiation of mammalian cells: expression time and dose-response. Radiation Res., 79: 187-202 (1979) (UR-3490-1489)

Premature chromosome condensation (PCC) in Chinese hamster ovary (CHO) cells following exposure to 300 kVp X-rays was first detected in the mitosis that followed the second postirradia-

74

tion S phase. Thus, cells irradiated in G1 first expressed PCC at the second postirradiation mitosis while cells irradiated in G2 did not express PCC until the third postirradiation mitosis. Cells irradiated in the S phase expressed PCC at the second postirradiation mitosis with a frequency that was related to the position of the cells in the S phase at the time of exposure, cells in the first half of the S phase (at the time of exposure) showing a higher frequency than cells positioned in the second half. Thus, DNA replication during the first postirradiation S phase may be involved in the processing of lesions that eventually give rise to PCC. For cells in G1 at the time of exposure, the D_o for PCC expression at the second postirradiation mitosis was around 825 rad, indicating that PCC may play only a minor role in X-ray-induced cell killing. Autoradiographic analysis indicated approximatoly 50% of the PCC patches scored were replicating DNA at the time condensation was attempted. Daughter cells derived from such cells would suffer loss of genetic material.

Goldstein, D. A.: Calculation of the concentrations of free cations and cation-ligand complexes in solutions containing multiple divalent cations and ligands. Biophys. J., 26: 235-242 (1979) (UR-3490-1271)

The method described permits the computation of the concentrations of free ions and ionligand complexes in a solution containing arbitrary numbers of divalent cations and ligands. It is required that the pH be known, along with appropriate sets of ligand-hydrogen and ligand-divalent cation concentration binding constants. It is assumed that these sets of constants are chosen to be consistent with the ionic strength of the complete solution which contains the divalent cations and ligands. The technique is an iterative one which provides upper and lower bounds for the values of the unknowns. The method does not require initial guesses at the values of the unknowns, and it gives correct answers even when the concentrations involved are many orders of magnitude apart. The present formulation of the problem is restricted to the case where only one cation can bind to a given ligand at any one time. The method is applicable to large molecules with multiple "sub-ligands" provided these sub-ligands are independent in their function as ion-binding sites. These sub-ligands need not all have the same properties. It is also shown that a simple modification of the method permits the determination of the subset of total ion concentrations that are required in order to produce a specified subset of free ion concentrations. The modifications required to include monovalent cation binding are presented in outline form.

Guillet, R.; Saffran, M. and Michaelson, S. M.: Pituitary-adrenal response in neonatal rats. Endocrinol., (in press) (UR-3490-1520)

Neonatal rats were, until recently, believed to be relatively nonresponsive to stress. With improved methods now available, rat pups as young as 1 to 2 days of age have been found to have basal and stimulated plasma corticosterone (B) values approaching those of adults but have very low values at 4 to 11 days which increase thereafter and reach adult values at about 21 days of age. We examined the responsiveness of neonatal rats to the administration of a crude preparation of corticotropinreleasing factor (CRF) and ACTH to determine the locus of the variation with age of the response. Plasma B increased in 1-day-old rats after ACTH or CRF. In 7-day-old rats, neither caused increases in plasma B. Some response after these stimuli was elicited in 14-day-old rats, and the responses of 21-day-old rats approached those in adults. Adrenal tissue from rats of the same ages showed a pattern of sensitivity to ACTH *in vitro* similar to that *in vivo*, except that the response of adrenals from 21-day-old rats was still feeble. Pretreatment of rat pups for the first 6 postnatal days with ACTH or corticosterone resulted in a moderate increase in plasma B after CRF or ACTH on day 7. The postnatal fall in sensitivity is partially explained by a decreased adrenal sensitivity to ACTH.

Harwell, O. D.; Sweeney, M. L. and Kirkpatrick, F. H.: Conformation changes of actin during formation of filaments and paracrystals and upon interaction with DNase I, cytochalasin B, and phalloidin. J. Biol. Chem., (in press) (UR-3490-1455)

Spin labels attached to rabbit muscle actin became more immobilized upon conversion of actin from the G state to the F state with 50 mM KCl. Titration of G-actin with MgCl₂ produced F-actinlike EPR spectra between 2 and 5 mM, and F-actin filaments by electron microscopy. Higher concentrations of MgCl₂ produced bundles of actin and eventually paracrystals, accompanied by further immobilization of spin labels. The effects of MgCl₂ and KCl were competitive: addition of MgCl₂ to 50 mM could convert F-actin (50 mM KCl) to paracrystalline (P) actin; the reverse titration (0 to 200 mM KCl in the presence of 20 mM MgCl₂) was less complete.

Addition of DNase I to G- or F-actin gave the expected amorphous electron micrographic pattern, and the actin was not sedimentable at $(400,000 \times g \times h)$. EPR showed that the actin was in the G conformation. Addition of DNase I to paracrystalline actin gave the F conformation (EPR) but the actin was "G" by electron microscopy. Phalloidin converted G-actin to F-actin, had no effect on F-actin, and converted P-actin to the F state by electron microscopy but maintained the P conformation by EPR. Cytochalasin B produced no effects observable by EPR or centrifugation but "untwisted" paracrystals into nets. Since actin retained its P conformation by EPR in two states which were morphologically not P, we conclude that the P state is a distinct conformation of the actin molecule and that actin filaments aggregate to form bundles (and eventually paracrystals) when actin monomers are able to enter the P conformation.

Hefley, T. J.: The enzymatic isolation of cells from bone: a critical evaluation. Ph.D. Thesis, University of Rochester School of Medicine and Dentistry (Supervised by Dr. J. S. Brand) (1979) (UR/3490/LCP-16)

Crude bacterial collagenase is essential to the enzymatic isolation of the cells from fetal rat calvaria. However, bacterial collagenase is the cause of the extensive damage and destruction observed in the isolated cells. In an attempt to standardize the digestion of fetal rat calvaria, bacterial collagenase was fractioned into its component enzymes and the participation of each of those enzymes in the digestion process was examined.

Several lots of bacterial collagenase were screened on the basis of the cell yield per digestion. The total cell yield per calvarium was found to be dependent upon the lot of collagenase used in the digestion. It was also found that a lot of collagenase that initially gave a very high yield of cells per calvarium deteriorated with time.

Crude collagenase can be fractioned by molecular sieving on Sephacryl S-200 into its component enzymes: aminopeptidase, collagenase, clostripain, and neutral protease. These enzymes can be recombined after fractionation and still retain the ability to digest fetal rat calvaria. It was also shown that digestion of the tissue with these recombined enzymes resulted in extensively damaged cells.

Crude collagenase was fractioned on a preparatory scale and the component enzymes were further purified by ion exchange chromatography. It was found that only three of the component enzymes were required for the digestion of fetal rat calvaria: collagenase, clostripain, and neutral protease. The amounts of each of these enzymes that are required to completely digest the tissue are given in terms of their enzymatic activity and the conditions of the digestion are described.

Izzo, J. L.; Roncone, A. M.; Helton, D. L. and Izzo, M. J.: Subcellular distribution of intraportally injected 125I-labeled insulin in rat liver. Arch. Biochem. Biophys., 198: 97-109 (1979) (UR-3490-1431)

Time course studies revealed that at 30 s after intraportal injection of $200 \ \mu\text{U}$ of 125I-labeled insulin per 100 g rat 47.9 $\pm 2.8\%$ of the injected radioactivity was recovered from the liver homogenate by precipitation with trichloroacetic acid. Trichloroacetic acid precipitable radioactivity declined to very low levels during the next 30 minutes whereas trichloroacetic acid soluble radioactivity reached a peak value of 9.56 $\pm 1.9\%$ at 5 minutes and declined gradually thereafter. At 30 s mean peak accumulations ± SE of 6.83 ± 0.42, 5.06 ± 0.27, 14.90 ± 1.85, and 3.58 ± 0.58% of injected radioactivity were recovered in trichloroacetic acid precipitates from the 700g (nuclei + debris), 10,000g (mitochondria + lysosome), 105,000g (microsomes), and supernatant (cytosol) subfractions, respectively. Mean peak values of 0.72 ± 0.08 , 0.12 ± 0.02 , and $1.11 \pm 0.16\%$ of injected radioactivity were recovered in the partially purified mitochondrial fraction, purified nuclei, and plasma membranes, respectively, as trichloroacetic acid precipitable material. Most of the trichloroacetic acid precipitable activities in the subfractions were immunoprecipitable. Trichloroacetic acid soluble radioactivity was found mainly in the cytosol and microsomal fractions. Peak specific activity (percentage of injected dose/mg protein X 10^{-3}) was highest in the microsomes, intermediate in the plasma membranes, and very low in the purified nuclei and partially purified mitochondrial fraction. The specific activity of the microsomes remained at or near peak levels for 5 minutes after 125I-labeled insulin injection and then declined, whereas specific activity of the plasma membranes dropped precipitously to 25% of peak values at 5 minutes. Sephadex gel filtration of the radioactivity in the deoxycholate soluble fraction of microsomes at 5 minutes after 125I-labeled insulin injection resulted in the elution of a major peak (Peak I) in the region of 125Ilabeled insulin and a minor peak (Peak II) in the region of the labeled A and B chains. Incubation of the fraction for 30 minutes at 37° C with 3 mM reduced glutathione and 15 mM EDTA resulted in a reciprocal fall in Peak I and rise in Peak II. The data suggest that intraportally injected 125_{I-1} labeled insulin is rapidly internalized and concentrated in the rat liver microsomes. The time courses of appearance and disappearance of trichloroacetic acid precipitable radioactivity in plasma membrane and microsomes further suggest, although do not prove, that insulin binds to plasma membranes before it is internalized. They also provide presumptive evidence suggesting that the sequential degradative pathway is operative in vivo.

Jain, S. C.; Bhandary, K. K. and Sobell, H. M.: Visualization of drug-nucleic acid interactions at atomic resolution. VI. Structure of two drug-dinucleoside monophosphate crystalline complexes, ellipticine-5-iodocytidylyl (3'-5') guanosine and 3,5,6,8-tetramethyl-N-methyl phenanthrolinium-5-iodocytidylyl (3'-5') guanosine. J. Mol. Biol., 135: 813-840 (1979) (UR-3490-1595)

Ellipticine and 3,5,6,8-tetramethyl-N-methyl phenanthrolinium form complexes with the dinucleoside monophosphate, 5-iodocytidylyl(3'-5')guanosine. These crystals are isomorphous: ellipticine-iodoCpG⁺ crystals are monoclinic, space group P2₁, with a = 13.88 Å, b = 19.11 Å,

† Abbreviations used: iodoCpG, 5-iodocytidylyl(3'-5')guanosine; TMP, 3,5,6,8-tetramethyl-Nmethyl phenanthrolinium.

- 25 -

c = 21.42 Å, $\beta = 105.4$; TMP—iodoCpG crystals are monoclinic, space group $P2_1$, with a = 13.99 Å, b = 19.12 Å, c = 21.31 Å, $\beta = 104.9^{\circ}$. Both structures have been solved to atomic resolution by Patterson and Fourier methods, and refined by full matrix least-squares.

The asymmetric unit in the ellipticine—iodoCpG structure contains two ellipticine molecules, two iodoCpG molecules, 20 water molecules and 2 methanol molecules, a total of 144 atoms, whereas, in the tetramethyl-N-methyl phenanthrolinium—iodoCpG complex, the asymmetric unit contains two TMP molecules, two iodoCpG molecules, 17 water molecules and 2 methanol molecules, a total of 141 atoms. In both structures, the two iodoCpG molecules are hydrogen-bonded together by guanine—cytosine Watson—Crick base-pairing. Adjacent base-pairs within this paired iodoCpG structure are separated by about 6.7 Å; this separation results from intercalative binding by one ellipticine (or TMP) molecule and stacking by the other ellipticine (or TMP) molecule above or below the basepairs. Base-pairs within the paired nucleotide units are related by a twist of 10 to 12° . The magnitude of this angular twist is related to conformational changes in the sugar—phosphate chains that accompany drug intercalation. These changes partly reflect the mixed sugar puckering pattern observed: C3' endo (3'-5') C2' endo (i.e., both iodocytidine residues have C3' endo conformations, whereas both guanosine residues have C2' endo conformations), and additional small but systematic changes in torsional angles that involve the phosphodiester linkages and the C4'-C5' bond.

The stereochemistry observed in these model drug-nucleic acid intercalative complexes is almost identical to that observed in the ethidium—iodoUpA and —iodoCpG complexes determined previously This stereochemistry is also very similar to that observed in the 9-aminoacridine—iodoCpG and acridine orange—iodoCpG complexes described in the preceding papers. We have already proposed this stereochemistry to provide a unified understanding of a large number of intercalative drug—DNA (and RNA) interactions and discuss this aspect of our work further in this paper.

Jeng, A. Y.: Isolation and characterization of a Ca^{2+} carrier candidate from calf heart inner mitochondrial membrane. Ph.D. Thesis, University of Rochester School of Medicine and Dentistry (Supervised by Dr. A. E. Shamoo) (1979) (UR-3490 1586)

A protein was isolated from calf heart inner mitochondrial membrane with the aid of an electron paramagnetic resonance assay based on the relative binding properties of Ca^{2+} , Mn^{2+} , and Mg^{2+} to the protein. The molecular weight of this protein was estimated to be about 3000 by urea/sodium dodecyl sulfate gel electrophoresis and amino acid analysis. The protein had two classes of binding sites for Ca^{2+} by flow dialysis studies. The dissociation constants of the high- and low affinity binding sites for Ca^{2+} were 9.5 and 33 μ M, respectively. This protein could extract Ca^{2+} into an organic phase. The selectivity sequence of this protein determined from the organic solvent extraction experiments showed that it favored divalent cations over monovalent cations. Also, the relative selectivity sequence for divalent cations was Ca^{2+} , $Sr^{2+}
ightarrow Mn^{2+}
ightarrow Mg^{2+}$. Ruthenium red and La^{3+} were shown to inhibit the protein-mediated extraction of Ca^{2+} into the organic solvent. The calcium translocation in a Pressman cell mediated by this protein was selectively driven by a hydrogen ion gradient, with a higher pH on the donor aqueous phase. When the pH gradient was reversed, no Ca^{2+} translocation occurred. Also, no Ca^{2+} translocation was observed when a gradient of Na⁺, K⁺, or Ca^{2+} was substituted for the H⁺ gradient.

The isolated protein was found to be contaminated with a large amount of phospholipids, which was consistent with the fact that no extra lipophilic anions were required to extract Ca^{2+} into the organic phase. It was found that there were 150 moles of phospholipids associated with each mole of the protein. Partial delipidation of the protein was performed by using either the organic solvent extraction procedure or the silicic acid column chromatography. Control experiments indicated that the Ca^{2+} transport properties of the isolated protein were not due to the contaminating phospholipids.

A complete delipidation procedure was developed by using Sephadex LH-20 column chromatography. The mole ratio of phospholipids to the delipidated protein could be reduced to 0.1 mole of phospholipids per mole of protein. There were no free fatty acids, hexosamines, or sialic acids associated with the delipidated protein. The extraction of Ca^{2+} into an organic phase mediated by the delipidated protein required the presence of a lipophilic anion, picrate. Picrate also enhanced the rate of the delipidated protein-mediated Ca^{2+} translocation through a bulk organic phase.

Further characterization of the physical and chemical properties of the delipidated protein were investigated. It would found that the delipidated protein becomes more hydrophobic in the presence of Ca^{2+} and alkaline pH in the organic solvent extraction of experiments. The pH profile of the mole ratio of Ca^{2+} to protein exhibited a typical titration curve, showing a pK_a of 8.0 to 8.1. The relative cation selectivity of the delipidated protein determined from the organic solvent extraction experiments was Zn^{2+} > Ca^{2+} , Sr^{2+} > Rb^{2+} , Na^+ > Mn^{2+} . Ruthenium red and La^{3+} were again shown to inhibit the protein-mediated Ca^{2+} extraction into the organic phase. Respiratory inhibitors, oligomycin, and an uncoupling agent had no effect on the Ca^{2+} extraction. Phosphate did not stimulate the protein-mediated Ca^{2+} extraction.

The Ca²⁺-protein complex appears to have two positive charges. The delipidated protein only had one class of Ca²⁺-binding sites as revealed from the flow dialysis studies. These Ca²⁺-binding sites had a dissociation constant of $5.2 \ \mu$ M and bound 1 mole of Ca²⁺ per mole of calciphorin.

Evidence suggests that this <u>calcium</u> iono<u>phore</u> prote<u>in</u> (named "calciphorin") may be a strong candidate for the Ca²⁺ carrier responsible for the influx mechanism in mitochondrial Ca²⁺ transport system. Two possible models for calciphorin-mediated Ca²⁺ transport in mitochondria are proposed.

Jeng, A. Y. and Shamoo, A. E.: Isloation and characterization of a Ca^{2+} carrier from calf heart inner mitochondrial membrane. I. Physical properties. J. Biol. Chem., (in press) (UR-3490-1583)

A protein was isolated from calf heart inner mitochondrial membrane with the aid of an electron paramagnetic resonance (EPR) assay based on the relative binding properties of Ca^{2+} , Mn^{2+} , and Mg^{2+} to the protein. The molecular weight of this protein has been estimated to be about 3000 by urea/sodium dodecyl sulfate gel electrophoresis and amino acid analysis. The isolated protein was found to be contaminated with a large amount of phospholipids. There were 150 moles of phospholipids associated with each mole of the protein. Partial delipidation of the protein was performed by using either the organic solvent extraction procedure or the silicic acid column chromatography. The bulk phase transport experiments with the partially delipidated protein strongly suggested that the ionophorous properties reported were associated with the protein and not the contaminating phospholipids. The majority of the phospholipids associated with the protein could be digested by phospholipase C. While digested phosphatidylethanolamine (PE) decreased its ability in translocating Ca^{2+} through a bulk organic phase, the phospholipase C digestion left the proteinmediated Ca^{2+} translocation unchanged.

Jeng, A. Y. and Shamoo, A. E.: Isolation and characterization of a Ca^{2+} carrier from calf heart inner mitochondrial membrane. II. Electrophoretic properties. J. Biol. Chem., (in press) (UR-3490-1584)

The isolated calcium ionophore protein (named calciphorin) was delipidated using Sephadex LH-20 column chromatography. The mole ratio of phospholipids to calciphorin could be reduced to 0.1 mole of phospholipids per mole of calciphorin. There were no free fatty acids, hexosamines, or sialic acids associated with the delipidated calciphorin. The extraction of Ca^{2+} into an organic phase mediated by the delipidated calciphorin required the presence of a lipophilic anion, picrate. Picrate also enhanced the rate of calciphorin-mediated Ca^{2+} translocation through a bulk organic phase. Thus, calciphorin seems to be an electrogenic Ca^{2+} ionophore. The relative cation selectivity of calciphorin determined from the organic solvent extraction experiments was $Zn^{2+}
angle Ca^{2+}$, $Sr^{2+}
angle Rb^+$, $Na^+
angle Mn^{2+}$. Kaufman, G. E. and Miller, M. W.: Lack of effect of electric field exposure on rats: a data re-evaluation. Radiation Environ. Biophys., (in press) (UR-3490-1538)

Three recent investigations of the possible effects of 60 Hz electric fields on rats have yielded apparently contradictory results. While one group of investigators reported that chronic exposure to a 15 kV/m field caused several biological effects, the other two groups did not find these effects at 25 kV/m and 100 kV/m, respectively. A re-examination of the data from the 15 kV/m experiments indicates that the reported effects were probably artifacts due to improper statistical analysis and to a cage design which resulted in transient electric shocks (spark discharges) to the exposed rats. Hence, the results of all three investigations are consistent with a lack of biological effects from chronic exposure to 15 to 100 kV/m electric fields.

Keller, C. A. and Doherty, R. A.: Correlation between lead retention and intestinal pinocytosis in the suckling mouse. Am. J. Physiol., (in press) (UR-3490-1663)

Young animals absorb and retain a greater fraction of an oral dose of lead than do adult animals. It has been proposed that pinocytotic activity in young animals is responsible for the increased lead retention and absorption. Radiolabeled lead (5 mg/kg) and polyvinylpyrrolidone (PVP, 50 mg/kg) were administered orally to 12-day-old suckling mice and to adult mice, and the uptake of lead and PVP was determined periodically during a six-day interval. Small intestines were removed, flushed clear of intraluminal contents, then divided into 24 segments of equal length for analysis. Intestinal tissue from the distal jejunum and ileum were found to contain the greatest quantities of both lead and PVP. Pretreatment of suckling mice with cortisone acetate resulted in decreased content of lead and PVP within tissue of the intestine, and decreased whole body lead retention. Cortisone pretreatment produced lower lead concentrations in blood, brain, kidney and liver. Pretreatment with cortisone was also found to reduce lead absorption following intraluminal injection of lead into the ileum. Lead and PVP uptake into intestinal tissue of adult mice was much less than uptake in suckling pups. Cortisone pretreatment of adult mice had no effect on whole body lead retention or intestinal tissue content of lead or PVP. The correlation between pinocytotic activity and lead retention supports the hypothesis that pinocytosis is involved in lead absorption in suckling mice.

Keller, C. A. and Doherty, R. A.: Distribution and excretion of lead in young adult female mice. Environ. Res., (in press) (UR-3490-1579)

The kinetics of whole-body lead elimination and organ distribution were studied in ten-day-old and adult female mice following a single dose of lead. Necropsies were performed periodically during the 50-day experiment to assess organ lead distributions and lead elimination. Between days 15 and 50 excretion of lead was found to occur nearly equally through urinary and fecal routes. Whole-body lead retention during the terminal elimination phase was observed to have a half-time similar to that of lead retained in femur. Rates of lead elimination from femur and from whole body of young mice were apparently less rapid than comparable elimination rates in adult mice. Lead fluxes from the brains of young and adult mice were closely approximated by single component exponential equations. The results suggest that a three-compartment model for lead distribution and clearance does not adequately account for the pharmacokinetics of lead in mouse brain.

Keller, C. A. and Doherty, R. A.: Effect of dose on lead retention and distribution in suckling and adult mice. Toxicol. Appl. Pharmacol., (in press) (UR-3490-1588)

Single doses of lead (trace to 445 mg/kg) were administered *per os* to suckling and adult mice. Developmental differences were found in the Fraction of Initial Dose (FID) retained for all doses. In the dose range between 4 and 445 mg/kg of lead there were no differences in FID retained among the dose groups of suckling mice or among the dose groups of adult mice. A much larger FID was retained in both age groups following administration of carrier-free ²⁰³Pb. The results are consistent with a mechanism of gastrointestinal lead absorption comprising two or more processes. Ontogenetic differences were also observed in organ lead concentration relative to whole body concentration for kidneys, skull, and brain six days following lead administration. Lead retention (relative to wholebody retention) in brain and in bone was linearly related to dose of lead administered in both suckling and adult age groups. Though uptake of lead into brain and femur was observed to be directly related to dose over a wide range, relative blood lead concentrations were not linearly correlated with dose administered. The relationships between organ and blood lead concentrations were also shown to be nonlinear relative to dose. However, blood lead concentration was found to be a reliable indicator of renal and hepatic lead concentrations following an acute lead exposure.

Keller, C. A. and Doherty, R. A.: Lead and calcium distribution in blood, plasma, and milk of the lactating mouse. J. Lab. Clin. Med., (in press) (UR-3490-1640)

Though it has been established that lead is transferred in milk from other to suckling offspring, the physiological processes and parameters involved are not well understood. Single i.v. or p.o. doses of radiolabeled lead were administered to lactating and nonlactating female mice, and lead concentrations in blood, plasma and milk were determined during a period of 21 days. Large differences in lead elimination were observed between lactating and nonlactating mice. A significant fraction (25%) of the initial maternal dose was transferred to the suckling pups. The ratio of lead concentration in milk to lead concentration in plasma was found to be nearly constant over time. However, the milk to blood concentration ratios decreased during the same period. Furthermore, the concentration of lead in milk exceeded the plasma concentration by a factor of 30 indicating that there is a physiological process(es) which establishes a large milk to plasma concentration gradient. It is concluded that plasma lead concentration is a more accurate index for the estimation of milk lead concentration than is whole blood lead concentration.

Keng, P. C.; Li, C. K. N. and Wheeler, K. T.: Synchronization of 9L rat brain tumor cells by centrifugal elutriation. Cell Biophys., (in press) (UR-3490-1625)

Asynchronous 9L cells were separated into relatively homogeneously-sized populations using the Beckman JE-6 elutriator with both the conventional collection method and a modification of the long collection method. A substantial increase in the homogeneity of the volume distributions and in the degree of synchrony of the separated fractions was obtained using this long collection method. Autoradiographic data indicated that fractions containing 297% G₁ cells, 80% S cells, and 70 to 75% G₂ cells could be routinely recovered with this procedure. Recovery in these fractions varied from 5 to 8% of the total number of cells elutriated. The colony forming efficiency (CFE) of cells from fractions representing each phase of the cell cycle was a constant 60 to 70% which was comparable to the 60 to 80% usually found for asynchronous 9L cells. The percentage of cells in G₁, S, and G₂ in the elutriated fractions was more accurately determined from the volume distributions than from computer fits of the DNA histograms obtained from flow cytometry. In general, the degree of synchrony was related to the coefficient of variation (CV) of the volume distributions of the elutriated fractions. The CV was about 14% for all elutriated fractions. When the \geq 97% G₁ population was allowed to progress to S and G₂, the CVs were about 17% and 20%, respectively. Thus, the best nonperturbing method for obtaining synchronous 9L cells was direct elutriation of S and G2 cells with the modified long collection method.

Kimmich, G. A.: Intestinal transport: studies with isolated epithelial cells. J. Environ. Health Sci., (in press) (UR-3490-1643)

Isolated intestinal epithelial cells have been extremely useful for characterizing the nature of intestinal absorption processes and for providing insight into the energetics of Na⁺-dependent transport systems. This report describes a number of experimental approaches which have been used for investigating the specific epithelial transport systems involved in sugar absorption, but provides information which ultimately should prove useful for characterizing a number of different intestinal transport events. Similar experiments should also prove useful for exploring the effect of environmental agents on the function of intestinal tissue.

In the case of sugars, net absorption is accomplished via a mucosal, Na⁺-dependent concentrative transport system acting in sequence with a passive serosal system which does not require Na⁺. The serosal system limits the full gradient-forming capability of the mucosal system. Agents such as phloretin or cytochalasin B which inhibit serosal transport allow the cells to establish sugar gradients as high as 70-fold in contrast to 10- to 15-fold gradients observed for control cells. Seventy-fold sugar gradients cannot be explained in terms of the energy available in the electrochemical potential for Na⁺ if the Na⁺:sugar coupling stoichiometry is 1:1 as commonly assumed. New information indicates that the true Na⁺:sugar stoichiometry is in fact 2:1. Flow of two Na⁺ ions per sugar molecule down the transmembrane electrochemical potential for Na⁺ provides more than sufficient energy to account for observed 70-fold sugar gradients. If flow of sugar by other routes could be completely inhibited, theoretical sugar gradients as high as 400 could be achieved assuming that the cells maintain a membrane potential of -36 mv as measured for intact tissue.

Kimmich, G. A. and Randles, J.: Energetics of sugar transport by isolated intestinal epithelial cells: effects of cytochalasin B. Am. J. Physiol., 237: C56-C63 (1979) (UR-3490-1402)

Concentrative capability of isolated intestinal cells for sugars via the Na⁺-dependent transport system is diminished by function of a Na-independent facilitated diffusion system. Cytochalasin B is a potent inhibitor of the passive system, and allows the cells to establish a sugar gradient much higher than normal. When extracellular [3-OMG] is 1 mM,cytochalasin induces cellular sugar accumulation ratios of 30-fold ($^{\pm}$ phlorizin). At a lower sugar concentration (100μ M), cytochalasin (100μ M) becomes fully effective and induces 40-fold accumulation ratios. When changes in extracellular sugar concentration are taken into account, maximal concentration gradients achieved are 70-fold. Gradients of this magnitude represent the approximate maximum expected for a transport system driven exclusively by the transmembrane electrochemical potential for Na⁺. The conditions described here may represent those necessary for the Na⁺-dependent sugar carrier to bring the transmembrane difference in chemical potential for sugars into equilibrium with the difference in Na⁺-electrochemical potential. If so, the data indicate that phlorizin may be a one-way inhibitor of the concentrative system. On the other hand, if cytochalasin and phlorizin insensitive sugar "leaks" exist in the membrane of concentrative cells, then it is necessary to invoke the participation of an energy input beyond that due to the Na⁺ potential.

- 32 -

Kimmich, G. A. and Randles, J.: Evidence for an intestinal Na⁺:sugar transport coupling stoichiometry of 2.0. Biochim. Biophys. Acta, (in press) (UR-3490-1662)

Membrane potentials maintained by normally-energized intestinal epithelium interfere with an accurate determination of the Na⁺:sugar coupling stoichiometry associated with Na⁺-dependent transport systems. The interference is due to the fact that basal Na⁺ influx is itself a potentialdependent event, and sugar transport induces a membrane depolarization which therefore modifies basal Na⁺ entry. New information obtained under circumstances in which the membrane potential is maintained near 0 indicates that the true coupling stoichiometry is 2:1 rather than the commonlyaccepted value of 1:1. A 2:1 stoichiometry means that cellular electrochemical Na⁺ gradients are adequate to account for recently observed 70-fold sugar gradients maintained by these cells under certain conditions.

Kimmich, G. A. and Randles, J.: Regulation of Na⁺-dependent sugar transport in intestinal epithelial cells by exogenous ATP. Am. J. Physiol., (in press) (UR-3490-1589)

Exogenous ATP (1 mM) exerts a dramatic biphasic effect on the accumulation of 100 μ M 3-O-methylglucose (3-OMG) by isolated intestinal epithelial cells. The initial effect ensues approximately 15 seconds after exposure and inhibits 80% of the unidirectional sugar influx. Cellular phosphatases totally degrade the added ATP within a period of 20 minutes leading to a reactivation of transport capability. The cells exposed to ATP ultimately establish a concentration gradient of sugar about twice as high as that observed for control cells. Pyrophosphate (10 mM) delays the degradation of added ATP and prolongs the interval of transport inhibition. The late effect of gradient enhancement is still observed. No other nucleoside triphosphate induces the early inhibition of transport but ADP is approximately two-thirds as effective as ATP.

AMP and other molecules containing the adenine ring system can cause the late effect of gradient enhancement without causing an early transport inhibition. Because rotenone-treated, ATP-depleted cells also show an ATP-induced inhibition of sugar influx, it seems likely that the early effect represents a direct modification of carrier capability rather than an effect mediated via an alteration of cellular energetics.

King, M. A.; Weber, D. A.; Casarett, G. W.; Burgener, F. A. and Corriveau, O.: A study of irradiated bone. Part II: Changes in Tc-99m pyrophosphate bone imaging. J. Nucl. Med., (in press) (UR-3490-1486)

Quantitative Tc-99m pyrophosphate hone imaging was carried out in locally irradiated and control areas of New Zealand albino rabbits to determine the potential role of bone imaging in assessing the time course of radiation effects in bone and surrounding tissues. In vitro Tc-99m tissue assays and serial radiographs from the irradiated and contralateral limbs were obtained at regular intervals over the first 12 months following irradiation for comparison with quantitative results from the camera studies. The autoradiographic localization of TcPPi was also studied in the X-irradiated and contralateral bones of the rabbits. The results show that TcPPi bone imaging is a sensitive in vivo indicator of early radiation effects upon vasculature and bone remodeling. The findings suggest that the quantitative bone-imaging technique may be useful in the evaluation of the effects of treatment modalities on the skeleton.

King, M. A.; Casarett, G. W.; Weber, D. A.; Burgener, F. A.; O'Mara, R. E. and Wilson, G. R.: A study of irradiated bone. III: Scintigraphic and radiographic detection of radiogenic osteosarcomas. J. Nucl. Med., (in press) (UR-3490-1638)

Within one year after localized irradiation of a hind limb with single (1756 rads) or fractionated (4650 rads in 3 weeks) X-ray doses, radiation-induced osteosarcomas were observed in 4 of 9 single-dose rabbits and 2 of 11 fractionated-dose rabbits. The tumors arose in the proximal tibia in five cases and the distal femur in one case. In terms of production of osteoid or osseous tissue, three tumors were well differentiated, one slightly differentiated, and two (spindle-cell tumors) undifferentiated. This report summarizes the 99mTc-pyrophosphate (99mTc-PPi) imaging and autoradiographic, radiographic, and histologic studies of these osteosarcomas. The four differentiated osteosarcomas were detected one month earlier (2 cases) or 2½ months earlier (2 cases) by 99mTcPPi imaging than by radiography, whereas the two nondifferentiated tumors were suspected two weeks or 3½ months earlier radiographically. Autoradiographs showed 99mTcPPi localization in bone produced by differentiated osteosarcomas, and in reactive bone resorption and formation regions peripheral to tumors. The results support a recommendation for combined radiographic and isotopic imaging techniques for early detection of osteosarcomas.

Kirkpatrick F. H.; Muhs, A. G.; Kostuk, R. K. and Gabel, C. W.: Dense (aged) circulating red cells contain normal concentrations of adenosine triphosphate (ATP). Blood, 54: 946-950 (1979) (UR-3490-1543) Concise Report

The densest 0.1% to 1% of circulating red cells were separated from fresh blood and the ATP content of a representative sample of such cells was determined. The dense ("old") cells had decreased amounts of ATP relative to unfractionated cells. However, the dense cells were also smaller and the concentration of ATP in these cells was the same as in controls. Therefore, it seems unlikely that loss of cellular ATP is a causative factor in removal of senescent red cells from the circulation.

Kornbrust, D. J.: Microsomal lipid peroxidation as a mechanism of cellular damage. Ph.D. Thesis, University of Rochester School of Medicine and Dentistry (Supervised by Dr. R. D. Mavis) (1979) (UR-3490-1765)

The NADPH/iron-dependent peroxidation of lipids in rat liver microsomes was found to depend on the presence of free ferrous iron. High concentrations of Fe^{2+} initiated microsomal lipid peroxidation at an initial rate which was independent of NADPH. With Fe^{3+} , lower Fe^{2+} concentrations, or longer incubation times, NADPH stimulated microsomal lipid peroxidation and this stimulation was blocked by cytochrome c which is capable of accepting electrons from the microsomal NADPHcytochrome P-450 reductase. NADPH did not induce peroxidation in the absence of iron, nor did ferric iron in the absence of NADPH. Thus the role of NADPH appears to be maintenance of iron in the reduced Fe^{2+} state. The presence of superoxide dismutase, catalase, or the hydroxyl radical scanvengers ethanol or thiourea had little or no effect on the iron-initiated peroxidation, ruling out dependence on reduced states of oxygen. Complete chelation of iron by EDTA completely inhibited peroxidation and no stimulation by either EDTA or ADP was observed over the peroxidation produced by free iron alone. Preincubation of microsomes in the absence of iron did not enhance the rate of peroxidation upon subsequent addition of iron, suggesting that iron acts by initiating peroxidative decomposition of membrane lipids rather than by catalyzing the breakdown of pre-formed hydroperoxides.

Liposomes of extracted microsomal lipid also underwent peroxidation in the presence of ferrous iron at a rate comparable to intact microsomes. Ascorbate stimulated iron-induced liposomal peroxidation but had no effect in the absence of iron. Hydrogen peroxide did not enhance iron-induced liposomal peroxidation and inhibited at high concentrations, ruling out a role for hydroxyl radicals produced by reduction of H_2O_2 by Fe^{2+} .

Carbon tetrachloride initiated lipid peroxidation in isolated rat liver microsomes in the absence of free metal ions. In contrast to the nonenzymatic process stimulated by ferrous iron, CCl_4 -induced peroxidation showed an absolute requirement for NADPH and appeared dependent on the integrity of cytochrome P-450 as reflected by measurement of aminopyrine demethylase and aniline hydroxylase activities. The peroxidation subsided after only 10% of the total peroxidizable polyunsaturated fatty acids had reacted, at which point the cytochrome P-450 activities were 85 to 95% inhibited, whereas NADPH-cytochrome P-450 reductase activity was not significantly affected. Ferrous iron, in contrast, caused peroxidation of 100% of the available polyunsaturated fatty acids and produced decreases in cytochrome P-450 activities as well as loss of susceptibility to CCl_4 -induced peroxidation that approximately paralleled the extent of peroxidation. Thus, CCl_4 -induced peroxidation appeared to be ten times more potent in inhibiting cytochrome P-450 activities than the peroxidation caused by iron. Boiled liver microsomes or liposomes prepared from extracted liver lipid underwent extensive peroxidation in the presence of untreated microsomes when ferrous iron was the initiating species. In contrast, the CCl₄-induced peroxidative response was not affected by addition of these exogenous forms of lipid substrate and thus the initiating species appeared to be confined to the active microsomes. No detectable peroxidation was induced by CCl₄ in microsomes from brain, kidney, or lung, and microsomal aminopyrine demethylase and aniline hydroxylase activities were more than ten-fold lower in these tissues compared to liver. These results are consistent with activation of CCl₄ by cytochrome P-450 to a reactive short-lived radical which initiates peroxidation in the immediate vicinity of the cytochrome and thereby inhibits enzyme activity either by destruction of essential lipids or by direct attack on the enzyme by reactive intermediates of the peroxidative process. Loss of cytochrome P-450 activity then results in cessation of the CCl₄induced peroxidative response prior to more extensive reactions of membrane polyunsaturated lipids.

Rates of *in vitro* lipid peroxidation of microsomes and homogenates were found to vary widely between different tissues and species. In rats and rabbits, lung microsomes peroxidized at a 25- to 50-fold lower rate than liver, kidney, testes, and brain microsomes. Heart microsomes peroxidized at a rate slightly greater than, but most similar to, lung microsomes. Comparison of tissue homogenates also revealed the unique resistance of lung and heart to lipid peroxidation. Vitamin E levels in lung and heart microsomes were several-fold higher than in microsomes from the other tissues studied, which accounted for the relative resistance of lung and heart to lipid peroxidation. Liposomes of extracted rat lung microsomal lipid were also resistant to peroxidation and the amount of vitamin E contained in the lung lipid extract was sufficient to confer the same degree of resistance when incorporated into an equivalent amount of rat liver lipid. Higher rates of peroxidation in mouse lung microsomes relative to rabbit, rat, and human lung microsomes was similarly correlated with a lower concentration of vitamin E in mouse lung microsomes. These data provide strong support for the role of vitamin E as the major cellular antioxidant, with respect to lipid peroxidation, and demonstrate the utility of the microsomal system in characterizing tissue differences in susceptibility to peroxidative membrane decomposition.

Rat lung and liver microsomes did not undergo lipid peroxidation in the absence of iron when incubated with NADPH and widely varying concentrations of paraquat. Paraquat also did not stimulate rat liver and lung microsomal peroxidation induced by added iron and NADPH, and was inhibitory at concentrations above 10 μ M. Similarly, no stimulation of peroxidation was produced

- 36 -

by paraquat in rabbit or human lung microsomes; however, under similar conditions, paraquat enhanced NADPH/iron-dependent peroxidation in mouse lung and liver microsomes, apparently by facilitating reduction of iron by the mouse microsomes. In lung microsomes obtained from rats sacrificed at 12, 18, and 24 hours following a lethal dose of paraquat (50 mg/kg, i.p.), there was no loss of vitamin E or increase in peroxidizability which would be expected if lipid peroxidation had occurred *in vivo*, although extensive lung damage developed during this time period. In addition, no decrease in peroxidizable polyunsaturated fatty acids was observed in lung homogenate or microsomes obtained from the paraquat-treated rats although there was a significant reduction in the palmitate content of these fractions at 24 hours postinjection. These results indicate that paraquat does not cause pulmonary toxicity by initiating peroxidation of lung lipids and the decrease of palmitate in paraquat-damaged lungs is consistent with inhibition of fatty acid synthesis as an early event in the pathogenesis of paraquat toxicity.

Kornbrust, D. J. and Mavis, R. D.: The effect of paraquat on microsomal lipid peroxidation in vitro and in vivo. Toxicol. Appl. Pharmacol., (in press) (UR-3490-1693)

Rat lung and liver microsomes did not undergo lipid peroxidation in the absence of iron when incubated with NADPH and widely varying concentrations of paraquat. Paraquat also did not stimulate rat liver and lung microsomal peroxidation induced by added iron and NADPH and was inhibitory at concentrations above 10 μ M. Similarly, no stimulation of peroxidation was produced by paraquat in rabbit or human lung microsomes; however, under similar conditions, paraquat enhanced NADPH/iron-dependent peroxidation in mouse lung and liver microsomes apparently by facilitating reduction of iron by the mouse microsomes. In lung microsomes obtained from rats sacrificed at 12, 18, and 24 hours following a lethal dose of paraquat (50 mg/kg, i.p.), there was no loss of vitamin E or increase in peroxidizability which would be expected if lipid peroxidation had occurred in vivo although extensive lung damage developed during this time period. In addition, no decrease in peroxidizable polyunsaturated fatty acids was observed in lung homogenate or microsomes obtained from the paraquat-treated rats although there was a significant reduction in the palmitate content of these fractions at 24 hours postinjection. These results indicate that paraquat does not cause pulmonary toxicity by initiating peroxidation of lung lipids and the decrease of palmitate in paraquat-damaged lungs is consistent with inhibition of fatty acid synthesis as an early event in the pathogenesis of paraguat toxicity.

- 37 -

Kornbrust, D. J. and Mavis, R. D.: Microsomal lipid peroxidation. I. Characterization of the role. of iron and NADPH. Mol. Pharmacol., (in press) (UR-3490-1523)

The NADPH/iron-dependent peroxidation of lipids in rat liver microsomes was found to depend on the presence of free ferrous iron. High concentrations of Fe^{2+} initiated microsomal lipid peroxidation at an initial rate which was independent of NADPH. With Fe^{3+} , lower Fe^{2+} concentrations, or longer incubation times, NADPH stimulated microsomal lipid peroxidation and this stimulation was blocked by cytochrome c which is capable of accepting electrons from the microsomal NADPHcytochrome P-450 reductase. NADPH did not induce peroxidation in the absence of iron, nor did ferric iron in the absence of NADPH. Thus the role of NADPH appears to be maintenance of iron in the reduced Fe^{2+} state. The presence of superoxide dismutase, catalase, or the hydroxyl radical scavengers ethanol or thiourea had little or no effect on the iron-initiated peroxidation, ruling out dependence on reduced states of oxygen. Complete chelation of iron by EDTA completely inhibited peroxidation and no stimulation by either EDTA or ADP was observed over the peroxidation produced by free iron alone. Preincubation of microsomes in the absence of iron did not enhance the rate of peroxidation upon subsequent addition of iron suggesting that iron acts by initiating peroxidative decomposition of membrane lipids rather than by catalyzing the breakdown of pre-formed hydroperoxides.

Liposomes of extracted microsomal lipid also underwent peroxidation in the presence of ferrous iron at a rate comparable to intact microsomes. Ascorbate stimulated iron-induced liposomal peroxidation but had no effect in the absence of iron. Hydrogen peroxide did not enhance iron-induced liposomal peroxidation and inhibited at high concentration, ruling out a role for hydroxyl radicals produced by reduction of H_2O_2 by Fe^{2+} .

Kornbrust, D. J. and Mavis, R. D.: Microsomal lipid peroxidation. II. Stimulation by carbon tetrachloride. Mol. Pharmacol., (in press) (UR-3490-1545)

Carbon tetrachloride initiated lipid peroxidation in isolated rat liver microsomes in the absence of free metal ions. In contrast to the nonenzymatic process stimulated by ferrous iron, CCl_4 -induced peroxidation showed an absolute requirement for NADPH and appeared dependent on the integrity of cytochrome P-450 as reflected by measurement of aminopyrine demethylase and aniline hydroxylase activities. The peroxidation subsided after only 10% of the total peroxidizable polyunsaturated fatty acids had reacted, at which point the cytochrome P-450 activities were 85 to 95% inhibited, whereas NADPH-cytochrome P-450 reductase activity was not significantly affected. Ferrous iron, in contrast, caused peroxidation of 100% of the available polyunsaturated fatty acids, and produced decreases in cytochrome P-450 activities as well as loss of susceptibility to CCl_4 -induced peroxidation

- 38 -

that approximately paralleled the extent of peroxidation. Thus, CCl_4 -induced peroxidation appeared to be ten times more potent in inhibiting cytochrome P-450 activities than the peroxidation caused by iron. Boiled liver microsomes or liposomes prepared from extracted liver lipid underwent extensive peroxidation in the presence of untreated microsomes when ferrous iron was the initiating species. In contrast, the CCl_4 -induced peroxidative response was not affected by addition of these exogenous forms of lipid substrate and thus the initiating species appeared to be confined to the active microsomes. No detectable peroxidation was induced by CCl_4 in microsomes from brain, kidney, or lung, and microsomal aminopyrine demethylase and anailine hydroxylase activities were more than ten-fold lower in these tissues compared to liver. These results are consistent with activation of CCl_4 by cytochrome P-450 to a reactive short-lived radical which initiates peroxidation in the immediate vicinity of the cytochrome and thereby inhibits enzyme activity either by destruction of essential lipids or by direct attack on the enzyme by reactive intermediates of the peroxidative process. Loss of cytochrome P-450 activity then results in cessation of the CCl_4 -induced peroxidative response prior to more extensive reactions of membrane polyunsaturated lipids.

Kostuk, R. K.; Muhs, A. G.; Kirkpatrick, F. H. and Gabel, C. W.: Measurement of adenosine triphosphate content in single red blood cells using the firefly bioluminescent reaction. Applied Optics, 18: 1527-1532 (1979) (UR-3490-1480)

A unique optical instrument is described which uses the firefly bioluminescent reaction to measure adenosine triphosphate (ATP) levels in single red blood cells. The method allows chemical content level to be associated with individual cell features. The optical instrument consists of a phase contrast microscope to view cells, a pulsed argon-ion laser to rupture the cell membrane, and a photon counting system to measure the bioluminescent yield. The technique has been calibrated against a standard ATP measurement using bulk analysis methods. The ATP loss mechanism for blood cells in a controlled depletion experiment was also investigated.

Laties, V. G.: I.V. Zavadskii and the beginnings of behavioral pharmacology: an historical note and translation. J. Exptl. Anal. Behav., 32: 463-472 (1979) (UR-3490-1623)

I. V. Zavadskii, who worked in Pavlov's laboratory between 1907 and 1909, performed a study that has many of the characteristics of modern behavioral pharmacology. He studied the effects of alcohol, morphine, cocaine and caffeine on the conditioned salivary reflex. A translation of his paper and some brief comments on his life are presented.

Laties, V. G. and Cory-Slechta, D. A.: Some problems in interpreting the behavioral effects of lead and methylmercury. Neurobehav. Toxicol., 1: Suppl. 1, 129-135 (1979) (UR-3490-1611)

Two sets of observations are reported as illustrations of problems encountered in behavioral toxicology. First, in an attempt to determine the contribution of methylmercury-induced ataxia to behavioral changes observed on the fixed-consecutive-number schedule, some ancillary control experiments were undertaken. Neither pharmacologically-produced incoordination (ethanol) nor mechanically-produced incoordination (foot taping) led to behavioral changes similar to those seen after exposure to methylmercury. Second, total crop impaction in a pigeon that died during a behavioral experiment on lead suggested some further work. Lead-induced crop stasis in pigeons was measured by X-raying the passage of force-fed stainless steel ball bearings through the crop. This retardation of motility reliably preceded signs of overt toxicity. These results suggest that the behavioral changes in the pigeon noted by us and reported by other investigators cannot be attributed to CNS dysfunction alone but more likely arise from starvation or from combined CNS damage and starvation. In addition, these results demonstrate that the appearance of behavioral effects prior to overt toxicity does not necessarily reflect CNS damage.

Lawrence, C. W. and Christensen, R. B.: Absence of relationship between UV-induced reversion frequency and nucleotide sequence at the CYC1 locus of yeast. Mol. gen. Genet., 177: 31-38 (1979) (UR 3490-1612)

The UV-induced mutation frequency of a given base pair located at different sites within the *CYC1* gene of *Saccharomyces cerevisiae* was found to vary by more than fifty-fold, indicating the existence of hotspots and coldspots typical of those found in other organisms. We were unable, however, to find any feature of the nucleotide sequence at or near the sites of mutation that explains this variability. These and other data suggest that hotspots are not located within regions particularly susceptible to the formation of premutational lesions. More probably the variation in mutability depends on differences in the activity of enzymes responsible for producing mutations though the reasons for these differences are not understood and may depend on factors not directly related to nucleotide sequence.

Lawrence, C. W. and Christensen, R. B.: Metabolic suppressors of trimethoprim and ultraviolet light sensitivities of *Saccharomyces cerevisiae rad6* mutants. J. Bacteriol., 139: 866-876 (1979) (UR-3490-1659)

Dominant mutations at two newly identified loci, designated SRS1 and SRS2, that metabolically suppress the trimethoprim sensitivity of rad6 and rad18 strains, have been isolated from trimethoprim-resistant mutants arising spontaneously in rad6-1 rad18-2 strains of the yeast Saccharomyces cerevisiae. The SRS2 mutations also efficiently suppress the ultraviolet light sensitivity of the parent strains. They do not, however, suppress their sensitivity to ionizing radiation or their deficiency with respect to induced mutagenesis and sporulation. Such observations support the hypothesis that RAD6-dependent activities can be separated into two functionally distinct groups: a group of error-free repair activities that are responsible for a large amount of the radiation resistance of wild-type strains and also for their resistance to trimethoprim and a group of error-prone activities that are responsible for induced mutagenesis and are also important in sporulation but which account at best for only a very small amount of wild-type recovery.

Liao, H. H. and Sherman, F.: Yeast cytochrome c-specific protein-lysine methyltransferase: corrdinate regulation with cytochrome c and activities in cyc mutants. J. Bacteriol., 138: 853-860 (1979) (UR-3490-1496)

The cytochromes c of fungi and higher plants contain one or two residues of ϵ -N-trimethyllysine, whose biological role in unknown. A cytochrome c-specific S-adenosylmethionine:protein-lysine methyltransferase (methylase) activity was shown to be present in extracts of the bakers' yeast Saccharomyces cerevisiae, and basic kinetic properties of this enzyme are described. The specific activity of the methylase was lower in extracts of cells grown under conditions of catabolite (glucose) repression or anaerobiosis where cytochrome c levels were low compared with cells grown under derepressed conditions where cytochrome c levels were high. During anaerobic-to-aerobic adaptation, the methylase was induced in parallel with cytochrome c, thus suggesting that the syntheses of cytochrome c and cytochrome c methylase are coordinately regulated. None of the cyc strains surveyed (cyc1, cyc2, cyc3, cyc4, cyc5, and cyc6) had diminished levels of methylase, although some of them were completely or almost completely deficient in cytochrome c.

Lichtman, M. A.: An invited commentary on "Enzyme release and morphological changes in leukocytes induced by mechanical trauma". Blood Cells, 5: 511-512 (1979) (UR-3490-1823)

This represents a commentary on an article on the effects of mechanical trauma on leukocytes.

Lichtman, A., Segel, C. B. and Lichtman, M. A.: Total and exchangeable calcium in mitogen-treated lymphocytes. Proc. 13th Intern. Leukocyte Culture Conf., May 1979, Ottawa, Canada, (in press) (UR-3490-1645)

In summary, these data indicate that mitogenic concentrations of PHA result in a very early increase in the exchangeable cell Ca, but not the total cell Ca. In contrast, at mitogenic concentrations A23187 increased total and exchangeable lymphocyte Ca. It is likely that mitochondria sequester most of the extra Ca brought into the cell by A23187. Since an increase in the exchangeable frac-

- 41 -

tion of cell Ca was consistently observed with either A23187 or PHA, the increase may be significant in the initiation of mitosis; however, an early increase in total cell Ca does not appear to be required for mitosis.

Lichtman, A. H.; Segel, G. B. and Lichtman, M. A.: An ultrasensitive method for the measurement of human leukocyte calcium: lymphocytes. Clin. Chim. Acta, 97: 107-121 (1979) (UR-3490-1462)

Studies of the transport and distribution of calcium in leukocytes have been severely hampered by the inability to measure accurately and reproducibly the concentration of calcium in small numbers of cells. We have applied a recent development in analytical chemistry, the graphite furnace atomic absorption spectrophotometer, to this problem. The calcium content of human blood lymphocytes was determined by both graphite furnace and conventional flame atomic absorption spectrophotometry. The linearity, sensitivity and detection limits of the two techniques were compared. For measurement of calcium, the graphite furnace sensitivity was 55 times higher in aqueous samples and 60 times higher in cell samples than the flame technique. The detection limit of the graphite furnace was 800 times lower in aqueous samples and 1500 times lower in cell samples. The enhanced sensitivity of this technique allowed us to prepare samples with 20 times fewer blood cells. We have employed this graphite furnace technique to measure lymphocyte calcium content and its relationship to the calcium concentration and proportion of serum in the suspending medium. In the absence of serum, the lymphocyte calcium content approximately doubled as the medium calcium concentration was increased from $1 \mu mol/l$ to 0.5 mmol/l. At medium calcium concentrations of 0.5 mmol/l and above, the lymphocyte calcium content was 1.0 mmol/l cells. In medium adjusted to 2 mmol/l calcium, the lymphocyte calcium content approximately doubled as the medium serum concentration was increased from 0 to 2%. At medium serum concentrations of 2% and above, lymphocyte calcium content was 2 mmol/l cells. The exchangeable cell calcium, measured with 45 Ca in the same samples, did not increase as serum was added to the medium.

Liebman, S. W. and Sherman, F.: Extrachromosomal ψ^+ determinant suppresses nonsense mutations in yeast. J. Bacteriol., 139: 1068-1071 (1979) (UR-3490-1642)

The extrachromosomal ψ^+ determinant in the yeast Saccharomyces cerevisiae enhanced the expression of Mendelian UAA suppressors by 6- to 10-fold. The ψ^+ determinant by itself is a weak UAA suppressor that caused the production of approximately 1% of the normal level of iso-1-cytochrome c in a strain containing the UAA mutation cyc1-72.

Lotz, W. G. and Michaelson, S. M.: Effects of hypophysectomy and dexamethasone on rat adrenal response to microwaves. J. Appl. Physiol.: Respirat. Environ. Exercise Physiol., 47: 1284-1288 (1979) (UR-3490-1296)

Circulating corticosterone levels were measured to compare the adrenocortical response to acute microwave exposure of normal, hypophysectomized, or sham-hypophysectomized rats. Plasma corticosterone levels in acutely hypophysectomized rats exposed to 60 mW/cm^2 for 60 minutes were below control levels indicating that the microwave-induced corticosterone response observed in normal, intact rats is dependent on ACTH secretion by the pituitary. In other groups of rats pretreated with dexamethasone before being exposed to microwaves for 60 minutes, the corticosterone response to a 50-mW/cm^2 exposure was completely suppressed by doses equal to or greater than $3.2 \,\mu$ g dexamethasone/100 g body weight. However, the corticosterone response to a 70 -mW/ cm² exposure was only partially suppressed by prior administration of $3.2 \text{ or } 5.6 \,\mu$ g dexamethasone/100 g BW. The evidence obtained in these experiments, in conjunction with the results of other experiments previously reported, is consistent with the hypothesis that the stimulation of the adrenal axis in the microwave-exposed rat is a systemic, integrative process due to a general hyperthermia.

Lozansky, E. D.; Sobell, H. M. and Lessen, M.: Does DNA have two structures in solution that coexist at equilibrium? In <u>Stereodynamics of Molecular Systems</u>, Ed. by R. H. Sarma. Pergamon Press, Inc., Oxford, New York, Frankfurt, Paris, pp. 265-270 (1979) (UR-3490-1569)

In this paper, we postulate the existence of two discrete structures for different regions of DNA at equilibrium in solution. These structures correspond to B DNA and to an inelastically deformed DNA structure, denoted β kinked DNA. β kinked DNA corresponds to a second order phase transition in the polymer, different regions of DNA undergoing this transition at different temperatures, and arises from a specific normal mode oscillation in DNA structure that is excited by Brownian motion of solvent molecules. It is possible that these multiply-kinked premelted regions play an important role in RNA polymerase-promoter recognition.

Lu, S-T., Lotz, W. G. and Michaelson, S. M.: Advances in microwave-induced neuroendocrine effects: the concept of stress. Proc. IEEE, (in press) (UR-3490-1694)

Recent evidence indicates that neuroendocrine effects are induced by microwave exposure with a threshold intensity required for the onset of the response. The level of that threshold is dependent upon intensity and duration of exposure. The threshold can vary with the given endocrine parameter studied. The level of that threshold is yet unclear due to conflicting reports of effect in chronic or repeatedly exposed populations of man or experimental animals. The response of the endocrine systems appears to be a nonspecific stress reaction in the case of adrenocortical and growth hormone changes, but it is apparently a metabolically specific response to increased energy input in the case of pituitary-thyroid changes.

Madden, K. P.: ESR-ENDOR study of X-irradiated single crystals of α -D-glucopyranose and α -methyl-D-glucopyranoside; environmental effects upon radiation and free radical chemistry in carbohydrate model systems. Ph.D. Thesis, University of Rochester School of Medicine and Dentistry (Supervised by Dr. W. A. Bernhard) (1979) (UR/3490/LCP-18)

Single crystals of X-irradiated α -D-glucopyranose (α Glu) and α -methyl-D-glucopyranoside (α MeGlu) were studied using electron spin resonance and electron nuclear double resonance spectroscopy, to determine products and reaction mechanisms in carbohydrate radiation and free-radical chemistry.

Four free-radical products were identified in α MeGlu single crystals irradiated and studied at 77K; a reoriented 06 primary alkoxy radical (06RPA), and 02 secondary alkoxy radical (02SA), a deprotonated C6 primary hydroxyalkyl radical (C6DPH), and a C5 secondary oxyalkyl radical (C5SO). Irradiation and observation at 12K produced yet another species, an unreoriented 06 primary alkoxy radical (06PA).

Four free radicals were identified in α Glu single crystals irradiated and observed at 12K and 77K; two different 02 secondary alkoxy radicals (02SA and 02SA'), a C6 primary hydroxyalkyl radical (C6PH), and a C3 secondary hydroxyalkyl radical (C3SH).

Study of the free radical environment about 06 in α Glu and α MeGlu using X-ray and neutron diffraction data indicated that the 06-H(06) bond in α MeGlu has considerably more ionic character than its counterpart in α Glu. This ionic character was used to explain the deprotonated state of the C6DPH radical, and the change in [C6DPH]/[06PA] with deuteration of labile protons in the α MeGlu system. The presence of an additional hydrogen bond to 06 in α MeGlu was used to explain the reorientation of the 06PA radical, and the stability of this species in the α MeGlu host crystal.

Free radical reactions in α Glu and α MeGlu were induced by slowly warming crystals irradiated at 77K until conversion occurred. In α MeGlu, the major reaction sequence was C6DPH \rightarrow C58O \rightarrow C2 primary hydroxyalkyl radical (C2PH) \rightarrow room temperature allylic radical. The C6DPH \rightarrow C5SO conversion is a net 1,2 hydrogen shift; an experiment with isotopically labelled material was performed to verify this reaction mechanism.

In α MeGlu, the major pathway is C6PH \rightarrow C2PH \rightarrow C2 secondary hydroxylkyl radical (C2SH). Environmental influences upon these free-radical reaction mechanisms are discussed. In α DeGlu, the proposed mechanism from magnetic resonance evidence is compared to one postulated from end product analysis of irradiated polycrystalline α Glu. The results from previous work on irradiated aqueous glasses of α Glu is briefly reviewed and compared to those obtained from the single crystal system.

Madden, K. P. and Bernhard, W. A.: ESR-ENDOR study of α -D-glucopyranose single crystals X irradiated at 12 and 77K. J. Phys. Chem., 83: 2643-2649 (1979) (UR-3490-1603)

Single crystals of anhydrous α -D-glucopyranose X irradiated at 12 and 77K contain four freeradical species: two secondary alkoxy radicals centered at O-2, a primary hydroxyalkyl radical centered at C-6, and a secondary hydroxyalkyl radical centered at C-3. Structural considerations are discussed, and the radicals compared with four radicals found in single crystals of α -D-glucopyranoside X irradiated under similar conditions.

Madden, K. P. and Bernhard, W. A.: ESR-ENDOR study of X-irradiated α -methyl-D-glucopyranoside single crystals at 12K: influence of hydrogen bonding on primary alcohol group radiation chemistry. J. Chem. Phys., (in press) (UR-3490-1641)

Single crystals of α -methyl-D-glucopyranoside X-irradiated at 12K contain a primary alkoxy radical. In contrast to the previously characterized primary alkoxy radical found at 77K, the C–O bond does not significantly reorient. This result, as well as deprotonation of an accompanying primary hydroxyalkyl radical, is explained by the presence of three, instead of the usual two, hydrogen bonds about the O₆ atom.

Mahler, P.: A study on the induction of thyroid tumors in rats using X-irradiation in conjunction with a goitrogen. Ph.D. Thesis, University of Rochester School of Medicine and Dentistry (Supervised by Dr. G. W. Casarett) (1979) (UR-3490-1607)

This research was designed to examine the influence of acute localized thyroid X-irradiation and chronic goitrogen administration, separately or combined, on thyroid tumor formation in mature female Rochester ex-Wistar rats.

In the first experiment, the radiation doses were 0; 80; 160; 320; or 640 rads, and the dosages of goitrogen were 0, 4, or 40 parts per million (ppm) of 1 methyl-2 mercaptoimidazole (methimazole, or MMI) in the drinking water. From the third month, serum thyroxine (T_4) levels were determined monthly. The surviving rats were sacrificed 13 months after the start of the experiment. The thyroids were examined and classified on the basis of: 1) presence or absence of tumor, 2) tumor type, and 3) tumor extent. Nontumorous thyroid tissue was quantified in terms of relative areas of histologic sections occupied by: 1) vasculature, 2) follicular epithelium, 3) colloid, and 4) connective tissue.

As evaluated by the χ^2 lest statistic, the incidence of rats with thyroid tumors in any treated group receiving 0 or 4 ppm MMI (0 to 30%) was not significantly greater than the incidence in the

nontreated control group (6%). However, the incidence in any of the 40 ppm MMI groups (65-100%) was significantly greater than that in the nontreated control group. At all the radiation doses other than 80 rads, the incidence was significantly greater than that in the nonirradiated group (χ^2 , p (.05). The 87% incidence in the 80 rad group was not significantly greater statistically than the 65% incidence in the nonirradiated group. The χ^2 test did not reveal any statistically significant difference in the incidence of rats with thyroid tumors on the basis of radiation dose size, although an increase in incidence with increasing radiation dose was seen in the 40 ppm MMI group. The incidence was so high at the low dose of 80 rads (87%) that there was little margin for further increase with further increase in radiation dose.

The incidence of naturally occurring thyroid medullary tumors did not change with any of the treatment used. Except for one rat, at 640 rads and no MMI, all twelve rats with thyroid carcinomas were in the 40 ppm MMI groups and the incidence appeared to increase with increasing radiation dose (5% at 0 rads to 20% at 640 rads) but not significantly.

Quantitative histology revealed significant MMI dosage dependent increase in mean relative area of follicular epithelium and decrease in mean relative area of colloid. The mean relative area of connective tissue increased with increasing radiation dose.

The mean serum thyroxine levels at 40 ppm MMI, 4 ppm MMI, and 0 ppm MMI were 1.9, 3.5, and $3.7 \mu g/100$ ml, respectively. No marked effect of thyroid irradiation on mean serum thyroxine levels was seen.

In the second experiment, rats receiving 200 ppm MMI in the drinking water and localized thyroid irradiation were sacrificed at 7½ months after onset of treatment. Nearly all (93%) rats in the 0 and 80 rad groups and all in the 160, the 320, and the 640 rad groups had thyroid tumors. As in Experiment I, thyroid carcinoma incidence tended to increase with increasing radiation dose.

In the third experiment, serum T_4 levels were measured for 12 weeks in rats receiving methimazole or thyroid irradiation, or both treatments. Rats receiving 640 rads + 0 ppm MMI showed a slight decrease in serum T_4 as compared to nontreated controls, while no change in serum T_4 levels was seen in rats receiving 0 rads + 4 ppm MMI or 640 rads + 4 ppm MMI. All rats receiving 40 ppm MMI, regardless of radiation dose, showed decreased serum T_4 levels by one to three weeks after onset of treatment. Maniloff, J.; Putzrath, R. M. and Nowak, J. A.: Mycoplasma and spiroplasma viruses: molecular biology. Chapt. 15 in <u>The Mycoplasmas</u>, Vol. 1, Ed. by M. Barile and S. Razin. Academic Press, New York, pp. 411-430 (1979) (UR-3490-1430)

Although the first mycoplasmavirus was not isolated until 1970, since then they have been reported in species of *Mycoplasma*, *Acholeplasma* and *Spiroplasma* (described in this chapter). The apparent ubiquity of the mycoplasma- and spiroplasmaviruses may reflect the spread of viruses and/or infectious DNA in the normal ecological situation.

The further development of mycoplasma and spiroplasma virology should allow the evaluation of these viruses as pathogenic determinants. Both the ubiquity of the viruses and considerations of comparative pathology indicate that a viral role in mycoplasma and spiroplasma associated disease states needs clarification. In addition, further studies promise to contribute to an understanding of viral replication and virus-cell interactions in systems of plasma membrane bounded viruses and cells.

Finally, these viruses allow new approaches to studies of the molecular biology of mycoplasmas and spiroplasmas.

Mann, A. J. and Auer, H. E.: Partial inactivation of cytochrome c oxidase by nonpolar mercurial agents. J. Biol. Chem., (in press) (UR-3490-1223)

Purified beef heart cytochrome c oxidase is inactivated to the extent of 35 to 50% by the nonpolar mercurial reagents mercuric chloride and ethylmercuric chloride. The inactivation is complete within 5 minutes. In titrations of activity, the plateau level of inactivation is attained at added ethylmercuric chloride:heme a ratios of about 1:1. Up to 3 mercury atoms/heme a are bound to the oxidase, although only the first of these affects its enzymatic activity. Incubation of the ethylmercury-modified oxidase with sulfhydryl compounds reverses the inactivation, with 2,3-dimercaptopropanol being most effective of the reagents tested. Spectrophotometric and polarographic assays of enzymatic activity show that K_m values for the native and the ethylmercury-modified enzymes are practically indistinguishable, and that the partial inactivation observed for the latter is reflected exclusively in a lower value of V_{max} compared to that of the native enzyme. Based on these results, we propose that ethylmercuric chloride reacts with a single crucial —SH group per heme a, and that electron transfer processes in the modified product are partially inhibited.

Martin, P. S.: The characterization of an MMS sensitive mutant of *Saccharomyces cerevisiae*. Ph.D. Thesis, University of Rochester School of Medicine and Dentistry (Supervised by Dr. L. Prakash) (1979) (UR/3490)LCP-19)

We have characterized a methyl methanesulfonate sensitive mutant of the yeast Saccharomyces cerevisiae in order to learn more about DNA repair and mutagenesis in this organism. The mutation,

designated mms3-1, also confers sensitivity to ultraviolet light and to ethyl methanesulfonate in both haploids and homozygous diploids. Its effect on γ -ray sensitivity, however, is a function of the ploidy of the cell and its effect on induced mutation is a function of both the ploidy of the cell and the nature of the inducing agent. Our major findings are as follows. 1) UV induced mutation of the ochre suppressible alleles arg4-17 and lys2-1 and the missense allele his1-7 is decreased in and only in diploids which are both homozygous for mms3-1 and heterozygous for mating type. mms3-1 haploids and homozygous mating type mms3-1/mms3-1 diploids exhibit wild type reversion frequencies for these alleles. On the other hand, EMS induced mutation of the alleles his1-7 and his1-315 is decreased in both mms3-1 haploids and diploids. γ -ray induced mutation of the his1-315 allele is decreased in mms3-1/mms3-1 diploids but not haploids but reversion of other alleles, such as his1-1, lys_{2-1} and arg_{4-17} is not altered by either cell ploidy or the absence of the MMS3 gene product. 2) Although mms3-1/mms3-1 a/α diploids are moderately sensitive to the lethal effects of ionizing radiation when compared to wild type a/α diploids, mms3-1 haploids are less sensitive than the corresponding wild type haploids. mms3-1/mms3-1 diploids which are homozygous for mating type are also less sensitive to γ -rays than wild type diploids which are homozygous for mating type. 3) MMS3 lies in the same epistatic group as RAD6, RAD9, RAD18 and RAD52 for the reapir of EMS induced lethal damage in haploids but MMS3 is epistatic only to RAD6 and RAD18 but not to RAD9 and RAD52 for the repair of MMS induced lethal damage. 4) Both UV and MMS but not EMS induced intragenic mitotic recombination are moderately decreased in mms3-1/mms3-1 diploids heterozygous as the his1 site.

Our data indicate that: 1) Saccharomyces cerevisiae has an error prone pathway for the repair of UV damage controlled by the MMS3 gene product operating in and only in, and possibly induced by conditions present only in, a/α diploids. 2) In diploids, at least, there exists at least one step in the error prone repair of UV induced damage which is different from a step in the error prone repair of EMS induced damage. 3) a/α mms3-1/mms3-1 diploids may be defective in a step common to the repair of mutagenic lesions following UV irradiation and lethal lesions following γ irradiation. 4) There are steps in the repair of MMS induced lethal damage that are different from steps in the re-

pair of EMS induced lethal damage.

;

Maurissen, J. P. J.: Development of a model for the assessment of somesthetic sensitivity impairment in human and nonhuman primates: normative data and applications to the study of drugs and toxic chemicals. Ph.D. Thesis, University of Rochester School of Medicine and Dentistry (Supervised by Dr. B. Weiss) (1979) (UR-3490-1845)

Numerous physical, chemical and biological agents are known to produce cutaneous sensory

- 48 -

symptoms usually associated with peripheral nerve disorders. Biochemical, morphological, electrophysiological and clinical studies have attempted to define the exact nature of these neurotoxic effects. The approach I chose can be referred to as a psychophysical approach. It consists of the scientific study of the relations between stimuli and resulting sensations and can be used with human as well as nonhuman primates.

Cutaneous sensations are heterogeneous and cannot be described adequately in terms of a single cutaneous sensory quality. However, I chose vibration sensitivity, which presented several advantages. Vibration sensitivity involves at least two different sets of end organs and nerve fibers. Deep receptors, and, supposedly, more superficial ones, are excited by vibration. Furthermore, several chemicals, such as acrylamide and methylmercury, can selectively cause partial loss of or damage to large myelinated fibers. Since vibratory information travels through such fibers, an insult of this nature could result in decreased vibratory sensitivity. A computerized system for an accurate and automated study of vibration sensitivity was therefore designed and developed. It has been employed with both monkeys and humans.

Sensitivity is assessed in the following manner. The monkey sits in a restraining chair in front of a small table. The left hand is immobilized in a plasticene mold. The tip of the middle finger is placed on a vibrating probe that protrudes through a hole. The right hand is free and has access to a telegraph key. A spout next to the monkey's mouth delivers fruit juice when an electromagnetic valve is activated.

Similarly, the human subject sits on a chair facing a table. Instruction is given to keep the left hand in a relaxed position with the tip of the middle finger on the vibrating contactor. The right hand has access to a telegraph key. Verbal instructions are given to the subject about the task requested.

The testing session is divided into discrete trials. A tone is turned on. The subject presses the key, holds it down, and, after a variable interval, vibration is delivered to the finger. A key release during vibration is rewarded either by fruit juice (monkeys) or by the addition of a point to a counter (humans). Catch trials are randomly introduced in the testing session in order to get a quantitative estimate of guessing bias. Normative data have been obtained in monkeys and humans.

One human subject received, in a blind experiment, several doses of the local anesthetic carbocaine. The time course of the effects of the drug on vibration sensitivity was studied and a doseeffect curve obtained.

Two monkeys received the drug misonidazole and showed a decreased vibration sensitivity. Patients receiving the same drug also displayed elevated thresholds after receiving high neurotoxic doses. Two other monkeys received methylmercury chronically. A decrease in vibration sensitivity occurred without any other detectable signs of intoxication such as weight loss or motor incoordination. Changes in vibration sensitivity seem to be an early sign of poisoning.

In conclusion, vibration sensitivity, as assessed by the technique described here, presents several advantages and can be used as a model for the study of somesthetic dysfunction induced by neuro-toxic chemicals. Data collected under control conditions show a remarkable consistency over time in humans as well as in monkeys. Furthermore, since monkeys share many functional and anatomical characteristics with humans, and their sensitivity is indistinguishable from that of humans, monkeys studied with this technique represent an excellent model of human vibration sensitivity. Application of this model to toxicity studies is likely to provide meaningful data directly applicable to the human situation.

Maurissen, J. P. J.: Effects of toxicants on the somatosensory system. Neurobehav. Toxicol., 1: Suppl. 1, 23031 (1979) (UR-3490-1600)

A computerized system for an objective and accurate study of vibration sensitivity has been designed. Sensitivity can be assessed in human as well as nonhuman primates. Its usefulness in the study of peripheral nerve disorders induced by chemical exposure is emphasized.

Maurissen, J. P. J. and van der Heide, A.: AXIS: a routine to plot logarithmic axes. DECUS Program Library Catalog (1979) (UR-3490-1479)

This program is a modified version of DEC's routine AXIS.FS. It has been developed on a PDP-12 computer. This subroutine has one new argument which allows use of full logarithmic or reverse logarithmic cycles. Labeling of tic marks has been changed so that on both X and Y axes, labels are written at a 0 degree angle.

Mercer, T. T.: Book review of "Radiation Protection in Uranium and Other Mines", by D. J. Beninson, Chairman, A. J. Breslin, D. A. Holaday, J. Pradel, R. Rock, S. D. Simpson and J.-O. Snihs. Annals of the ICRP, Vol. 1, 28 pp., 1977. Health Phys., 36: 94 (1979) (UR 3490-1809)

The protective measures described in ICRP Publication 24 and the monitoring systems necessary for adequate surveillance of these measures are briefly summarized; the success of the authors in describing the principles underlying both protective measures and monitoring methods is assessed; and the usefulness of this publication for health physicists in general is evaluated. Merigan, W. H.: Effects of toxicants on visual systems. Neurobehav. Toxicol., 1: Suppl. 1, 15-22 (1979) (UR-3490-1602)

The analysis of visual toxicity is complicated by the heterogeneity of visual capacities in different regions of the visual field. Since various toxicants may impair different functions allied to localized portions of the visual field, it is important to explore the relationship of field defects to residual visual abilities. We have begun this exploration by studying methylmercury poisoning in macaque monkeys. Extended exposure to this toxicant produces a marked concentric constriction of visual fields, a result similar to that found in human victims. In addition, visual sensitivity is greatly reduced on those tests in which the periphery of the visual field is more sensitive than the center. Our findings suggest simple but reliable clinical tests for screening suspected victims of substances impairing peripheral vision.

Michaelson, S. M.: Analyses of studies related to biologic effects and health implications of exposure to power frequencies. The Environmental Professional, (in press) (UR-3490-1788)

A careful review of the scientific literature provides a basis upon which to make an accurate judgment concerning the health, safety, and general biological environmental effects of high voltage transmission lines. Analysis of the results of field and laboratory studies in man as well as laboratory studies in animals and plants indicate that there are no demonstrable biological effects which may be hazardous to health or safety or to the general biological environment as a result of the presence of electric and magnetic fields from high voltage transmission lines.

Electric fields of up to 20 kV/m and magnetic fields up to 240 A/m, individually or in combination, do not present any threat to health. There is no evidence of specific symptoms in humans due to exposure to electric fields. Consistent with this, no mechanism of action is known by which electric fields produce direct effects on living organisms.

It is imperative that the public recognize the fact that practical decisions must be made on the basis of <u>what is known</u> rather than what is postulated or assumed without any rational basis. In North America, there are currently more than 200,000 circuit miles of overhead transmission lines rated 138 kV or higher of which 14,000 miles constitute 500 kV and several thousands of miles of 765 kV lines have been operating since 1969. Typical values of maximum vertical EF at 4 feet above ground level under EHV transmission lines range from 5 to 9 kV/m. Although the research data in humans is rather limited, one can take comfort in the fact that there is no evidence of harm to humans or animals from high voltage transmission lines.

· : .

- 51 -

Michaelson, S. M.: Health aspects of exposure to microwave radiofrequency energies. In <u>World</u> <u>Health Organization Manual on Nonionizing Radiation Protection</u>. European Regional Office, Who, Copenhagen, (in press) (UR-3490-1697)

The purpose of this document is to provide practical information on health aspects of exposure to microwave (MW) and radiofrequency (RF) radiant energies. Descriptions are given of the physical characteristics, biophysical principles, as well as the biological effects of exposure to these energies. Public and occupational health implications and protective measures against the hazards of exposure to microwave and radiofrequency radiation are also described.

Existing standards for general public and occupational exposure have been tabulated and described to inform the reader about the presently-accepted maximum permissible exposure levels in various countries.

The frequency ranges considered in this document are 300 kHz to 300 MHz (radiofrequency) and 300 MHz to 300 GHz (microwaves). These ranges represent one of several conventions used in defining this part of the electromagnetic spectrum. By another widely accepted convention, RF describes all frequencies below 300 GHz, with the microwave domain as part of the whole RF spectrum.

It should be pointed out that most of the current health effects information has been reported in the microwave region. However, inferences about effects at lower frequencies can be made in certain instances.

An attempt has been made to delineate areas of uncertainty with respect to biological effects and gaps in the state of knowledge. There are many problems requiring solution. For example, there is considerably less knowledge on offcots from partial than for whole-body exposure. Present exposure standards generally refer to plane wave exposure in the far field and do not relate to the more complex situation which exists in the near field.

A continuing problem has been the difficulty of communication between people of different disciplines working in the microwave/RF field. These problems could be readily solved through the encouragement of multidisciplinary approaches to research or the expansion of training programs to include information from other disciplines.

Michaelson, S. M.: Behavioral effects. Section 11 of Chapt. 2, Bioeffects of electromagnetic waves, in <u>URSI Review of Radio Science 1975-1977</u>, Ed. by S. A. Bowhill. Intern. Union of Radio Science, pp. 15-25 (1978) (UR-3490-1277)

In the area of behavioral effects of microwave exposure, we have seen improved dosimetry, differentiation between CW and pulsed microwaves, greater appreciation of absorbed dose and scaling factors. It has become apparent that many endogenous and exogenous influences can change the rate or probability of some behavior, depending on the details of the test situation. Baseline behavior may drift, particularly in long-term studies with repeated measurement. This baseline drift can complicate the interpretation of behavioral results. Change in sensitivity to the stimulus may result from repeated or extended exposure. Several factors, such as diurnal rhythms, degree of schedule control, discriminative stimuli, and stimulus complexity may enter into and modulate behavioral response studies. The reported responses in laboratory animals are a function of regulation against thermal inputs to maintain homeostasis. Species scaling is critical in the area of microwave bioeffects, more so than in many other disciplines. From the results of theoretical analysis of a simple physical model and considerations of comparative aspects of size, metabolism, and thermal tolerance, some general conclusions can be made on the validity of scaling results from one species of animal to another, particularly man. It is of practical importance to realize that experiments on biological effects at 2450 MHz on small animals like mice and rats do not scale to man at 2450 MHz but rather more to effects on man at VHF frequencies (approximately 100 MHz).

Michaelson, S. M.: Microwave biological effects: an overview. Proc. IEEE, (in press) (UR-3490-1722)

Although most investigators accept the fact that "high power density" of microwaves can result in pathophysiological manifestations of a thermal nature, some reports have suggested that "low power density" microwave energy can affect neural and immunologic function in animals and man. Most of these reports have emanated from the USSR and other Eastern European countries. Since most reported "low level" effects relate to behavioral and central nervous system changes, studies are needed to determine the nature and mechanism(s) of the nervous system's reactions, if any, to electromagnetic fields and to investigate the degree to which the individual's performance capabilities may be affected. Because of their important integrative regulatory functions, the neuroendocrine and central nervous system should receive attention as possible sensitive areas. Neurochemical assays and immunological reactivity could indicate basic mechanisms of interaction.

A critical review of studies into the biological effects of microwaves indicates that many of the investigations suffer from inadequacies of either technical facilities and energy measurement skills or insufficient control of the biological specimens and the criteria for biological change. There is a great need for systematic and quantitative comparative investigations using well-controlled experiments. This should be done by using sound biomedical and biophysical approaches at the various organizational levels from the whole animal to the subcellular level on an integrated basis with full recognition of the multiple associated and interdependent variables.

Above all there is a need for scientific competence and integrity. It is important to maintain

- 53 -

a proper perspective and assess realistically the biomedical effects of microwave exposure so that the worker or general public will not be unduly exposed nor will research, development, and beneficial utilization of this energy be hampered or unnecessarily restricted.

Miller, M. W.: Increased G₂ duration in sonicated root meristem cells of *Pisum sativum*. Environ. Exptl. Botany, 19: 357-364 (1979) (UR-3490-1278)

Roots were exposed to 2.3 MHz ultrasound at intensity levels of 7 and 11 W/cm². The meristematic cells yielded an intensity dependent delay in their transit through $G_2 + 1/2$ M.

Miller, M. W.: The micronucleus test applied to Vicia faba root meristem cells exposed to X-rays or ultrasound. Serie Biol. Exptl., (in press) (UR-3490-1525)

X-irradiation (200 R) but not ultrasound (1.1 MHz, 8 W)cm² spatial peak intensity, 1 min. continuous wave exposure) induced a statistically significant increase in the frequency of a micronuclei in root meristem cells of *Vicia faba* 6 to 36 hours postexposure. The distribution of autoradiographic ³H-label among cells with nuclei <u>and</u> micronuclei for control and X-irradiated cells was comparable.

Moore, C. W. and Schmick, A.: Genetic effects of impure and pure saccharin in yeast. Science, 205: 1007-1010 (1979) (UR-3490-1591)

Yeast cells were grown in media containing impure or purified saccharin preparations. Dosedependent increases in frequencies of cells possessing aberrant cell morphologies were revealed by light microscopy. At each test dose, cells grown in impure saccharin exhibited up to sevenfold higher frequencies of mitotic crossing-over or gene conversion in three of four assays for genetic recombination than cells grown in purified saccharin from the same lot. With one exception, the sweetener produced by the Maumee process caused larger increases in recombination and gene reversion than the sweetener produced by the Remsen-Fahlberg process. The several test markers did not respond equally to any test saccharin. Cells grown in liquid media containing no saccharin or two of three test concentrations of saccharin produced cell titers that were approximately equivalent.

Moore, C. W. and Schmick, A.: Recombinogenicity and mutagenicity of saccharin in Saccharomyces cerevisiae. Mutation Res., 67: 215-219 (1979) (UR-3490-1563)

Diploid yeast grown in the presence of a commercial lot of saccharin exhibited reproducible, dose-dependent increases in intergenic and intragenic recombination and mutation. Cells grew to nearly the same titer in media without saccharin and containing 2 or 20 mg saccharin/ml although cell viability was somewhat reduced in saccharin-containing media. At the high test dose of 100 mg/ml, titers and cell viability were more markedly lowered. Differences between this study and previous (negative) tests of saccharin in yeast are described.

Morken, D. A.: The biological and health effects of radon: a review. Special Publication by National Bureau of Standards of Roundtable Discussion of Radon in Buildings, June 1979, Gaithersburg, Md., (in press) (UR-3490-1673)

The history of radon in health and disease is reviewed. Biological effects of irradiation are presented, as are health effects, good and bad.

The current problem of the association of bronchial cancer in uranium miners, thought due to radon, with elevated levels of radon in buildings, especially homes, is introduced. Current concepts of dosimetry which involve deposition in, and clearance from, the respiratory tract of the radioactive aerosol produced by the decay products of radon, and the location of specific target volumes, are discussed.

A review of animal experiments suggests that these have not unequivocally demonstrated that lung cancer results from radon inhalation and for human exposure recourse to epidemiological information is necessary. The limitations of epidemiology are discussed, especially with regard to the presence of synergistic agents.

Morris, J. B.: The absorption, distribution and excretion of inhaled hydrogen fluoride in the rat. Ph.D. Thesis, University of Rochester School of Medicine and Dentistry (Supervised by Dr. F. A. Smith) (1979) (UR-3490-1658)

The experiments described in this thesis were performed to obtain quantitative information on the absorption, distribution and excretion of inhaled hydrogen fluoride. Male Long Evans rats were subjected to whole-body HF exposure for 6 hours or to nose-only HF exposure for 1 hour. Total (ashed samples) and/or ionic (unashed samples) fluoride concentrations in lung, plasma, kidney, trachea, femur, urine and feces were determined at various times following exposure. Both total and ionic lung, plasma and kidney concentrations were determined, the difference, referred to as the Δ F fraction, being attributed to the presence of a fluoride specie(s) which did not respond to the fluoride ion sensitive electrode.

In rats sacrificed 6 hours after whole-body exposure to 11 to 179 mg F/m³ HF dose-dependent increases in lung, plasma and kidney total and ionic fluoride concentration occurred. Plasma ionic fluoride ranged from 0.6 μ g/ml after exposure to 11 mg F/m³ to 5.7 μ g/ml after exposure to 116 mg

 F/m^3 (control 0.03 µg/ml). In addition, a dose-dependent increase in plasma ΔF concentration was evident. Plasma ΔF concentration averaged 7 to 18% of the plasma total fluoride concentration and was strongly correlated with the log of the plasma total fluoride concentration. The source of this ΔF is unknown. Rats excreted many times more fluoride in the urine after whole-body exposure to HF than could be explained by the amount of HF inhaled. The results of these experiments provide considerable evidence that airborne HF deposits on fur and is then ingested due to preening activity.

Urinary fluoride excretion was increased by nose-only exposure to $63 \text{ mg F/m}^3 \text{ HF}$. Approximately 90% of the excess fluoride excreted as a result of exposure was eliminated with 24 hours of the start of 1-hour exposure, the remainder was excreted the following day. The urinary fluoride excretion accounted for approximately twice the fluoride estimated to be inhaled during exposure. The amount of fluoride present on the fur covering the nose was of sufficient magnitude to account for the difference.

Tissue fluoride concentrations were elevated immediately after nose-only exposure. Fluoride concentrations in lung and kidney returned to control levels within 12 hours. Plasma fluoride concentration was slightly elevated 24 hours after the start of the 1-hour exposure but was at control levels at 96 hours.

Immediately following nose-only exposure lung ionic fluoride concentrations were less than plasma ionic fluoride concentrations suggesting that the fluoride in the lung had reached that site via plasma transport rather than by inhalation. In a separate experiment HF laden air was drawn through the upper respiratory tract of the rat while room air was respired through an endotracheal tube. Analysis of the fluoride concentration in air drawn into and leaving the upper respiratory tract indicated that greater than 99.9% of airborne HF was removed during passage through that site. A dose-dependent increase in plasma ionic fluoride concentration occurred after upper respiratory tract HF exposure providing strong evidence that fluoride is absorbed systemically from that site. The plasma ionic fluoride concentration after upper respiratory tract exposure was of sufficient magnitude to account for the plasma fluoride concentrations observed intact nose-only exposed rats.

In summary, inhaled HF is near completely deposited in the upper respiratory tract and is absorbed systemically from that site. Two forms of fluoride are present in the plasma of HF exposed rats, one ionic in nature, the other a fluoride specie(s) which does not respond to the fluoride ion sensitive electrode.

- 56 -

Morrow, P. E.: Physics of airborne particles and their deposition in the lung. Ann. N. Y. Acad. Sci., (in press) (UR-3490-1723)

The use of aerosol physics for predicting or retrospectively analyzing the degree and pattern of particulate matter deposition in the conducting airways and alveolar spaces is reviewed briefly. The principal deposition processes, namely, sedimentation, inertial impaction, and diffusion are considered in relation to sites of respiratory deposition and to particle size ranges. The concept of aerodynamic particle size is also examined. Emphasis is placed on those aspects of particulate behavior which may serve as a model for viral rickettsial, bacterial and fungal penetration into and deposition within the human respiratory system. An attempt is made, albeit incomplete, to relate pertinent information on airborne transmission of infection with the general principles governing aerosol deposition.

Morrow, P. E.; Beiter, H.; Amato, F. and Gibb, F. R.: Pulmonary retention of lead: an experimental study in man. Environ. Res., (in press) (UR-3490-1724)

This human investigation of lead absorption from the lungs utilized two forms of lead, lead chloride and lead hydroxide; the former was used in picogram amounts and the latter at microgram levels. These two species of lead were selected in an attempt to simulate the range of physicochemical properties found in atmospheric lead (urban air). Aerosols labeled with lead-203 were made of comparable aerodynamic size (MMAD $0.25 \,\mu \text{m}^{\pm} 0.1$) by using sodium chloride as the deposition-determining aerosol. After brief, mouth-piece exposures, seventeen subjects were followed by serial counting with a thoracic array of 12-2" scintillation detectors and 2-2" leg counters, all coupled to single channel analyzers. Serial blood samples were also taken. The two exposure groups showed similar total deposition values (23 vs 26 percent) and the same biological retention half-times, viz., 22.6 hours. When the retention data were "corrected" for blood borne 203Pb, the biological half-times for lung lead retention averaged 13.1 and 14.2 hours, respectively, and were insignificantly different. Blood build-up data were also indistinguishable in the two groups. The authors discuss these findings in relation to other inhalation studies and conclude the collective evidence supports the view that atmospheric lead is rapidly and completely absorbed from the human lungs.

Morrow, P. E.; Utell, M. J.; Gibb, F. R. and Hyde, R. W.: Studies of pollutant aerosol simulants in normal and susceptible human subjects. Proc. Gesellschaft für Aerosolforschung (GAF), October 1979, Düsseldorf, Germany, (in press) (UR-3490-1700)

The human studies described in this presentation utilized relatively high concentrations of either particulate nitrate ($\sim 7 \text{ mg m}^{-3}$) or sulfate ($\sim 1 \text{ mg m}^{-3}$) for brief exposure period (16 min.).

Sodium chloride aerosols of the same MMAD (0.5 to $1.0 \,\mu$ m) and mass concentration were used as a control. Dry, electrically-neutralized aerosols were administered in a double-blind manner to each subject through a respiratory mouthpiece during (normal) tidal volume breathing. Less than $300 \,\mu g$ of aerosol were deposited in the average subject. Immediately after exposure, each subject's pulmonary function was evaluated and compared to pre-exposure values, post-sodium chloride exposure values, and values obtained after a standardized parasympathomimetic (PNS) challenge with carbachol; the latter comparison examined possible potentiation of the bronchoconstrictor response. Functional assessments were made in an air-conditioned, flow-integrated, pressure-corrected body plethysmograph. The first study of the series was performed with a NaNO₃ aerosol in seven normal subjects and 11 asymptomatic asthmatic volunteers, all nonsmokers. The findings were essentially negative; that is, no significant changes were found between postexposure NaCl and NaNO3 values nor between either aerosol and pre-exposure values. The second study was designed identically, but utilized 11 volunteers with naturally-acquired influenza A (H_1N_1) which included two cigarette smokers. Unlike the normals and asthmatics in the first study, subjects with acute respiratory disease developed airway constriction following nitrate exposure. Significant decreases in specific airway conductance (P < 0.005) and in partial expiratory flow rates (PEFR) at 40% of total lung capacity (TLC) (P $\langle 0.05 \rangle$, were found in infected subjects following NaNO₃ when compared to NaCl. The third study examined the possibly adverse effects of sodium bisulfate, ammonium sulfate, ammonium bisulfate and sulfuric acid aerosols in 15 nonsmoking, normal subjects. All subjects were briefly exposed to each acidic sulfate aerosol and the sodium chloride aerosol in a random order over a two-day period. Normal subjects exhibited small but significant reduction ($P \langle 0.05$) in maximum expiratory flow rates at 60% (TLC) and in PEFR's at 40% and 60% TLC with all sulfate aerosols compared to NaCl. In addition, the bronchoconstrictor action of carbachol was potentiated by exposure to the more acidic sulfates. The results of these studies (a) stress the importance of investigating susceptible subpopulations, (b) indicate the value of a standardized challenge procedure, and (c) strongly infer that the airway response elicited by certain aerosols cannot be explained in terms of nonspecific irritation.

Morrow, P. E.; Leach, L. J.; Smith, F. A.; Gelein, R. M.; Scott, J. B.; Beiter, H. D. and Yuile, C. L.: UF₆/UO₂F₂ studies in experimental animals. NUREG Rept. No. CR-1045, (in press) (UR-3490-1780)

This report described the biological studies completed during the first year of the University of Rochester UO_2F_2/UF_6 study in rodents and dogs. Although the project was initiated in 1977, due to inordinate delays in receiving the uranium compounds, the effective period of the report is June

- 58 -

1978 to July 1979. The second year of the study was approved for an October 1, 1979 starting date and accordingly, a second report will be issued to cover July 1979 to Ocotber 1980 studies and provide an overall summary.

The material described in the present report was reviewed in part at a meeting July 18, 1979 between the investigators and representatives of NRC in Silver Spring, Maryland. Peer-reviewed publication of portions of this material is also contemplated in the near future.

Neuman, M. W. and Neuman, W. F.: On the measurement of water compartments, pH and gradients in calvaria. Calc. Tiss. Intern., (in press) (UR-3490-1753)

The concept of fluid compartmentalization in bone has emphasized the need for and lack of suitable methodology for the quantitation of water "spaces" in bone, in particular intracellular water, ICF, and extracellular water, BECF. Over a dozen commonly used marker substances were studied intensively. Small columns of hydroxyapatite crystals were employed to reveal physiochemical interactions with the mineral phase and isotope distributions in live and dead calvariae (rat pup, and adult mice) were employed to evaluate interactions with the combined organic-inorganic matrix of bone itself. The results were most discouraging. For example, for total water space, only water itself (either by direct weight or ³H₂O exchange) is a reliable measure in all instances. All markers studied were passively concentrated or excluded to varying degrees. In the end, it was necessary to measure intracellular space "by difference". An extracellular marker, polyethylene glycol (14 C-, mol. wt. 4000) was incubated with viable calvariae and also with comparable calvariae having lysed cells (0.1% Triton X-100). The intracellular space thus determined by differences agreed well with correlative data obtained on mixed cell-isolates from similar specimens. In neonatal calvariae, the intracellular space was 30% of the total water present; that of adult mouse tibia, 18%; and of adult moust calvariae, 14.5%. Measurements of DMO distribution in live and lysed calvaria revealed an overall pH differential (inside bone vs medium) of 0.1 unit or less. Using the best available data for ICF, BECF, and the passive concentrating effects of matrix-K⁺ interactions, there still remained an unexplained excess of K^+ in the BECF. The implications of these findings are discussed.

Neuman, M. W.; Neman, W. F. and Lane, K.: Formation and serum disappearance of fragments of parathyroid hormone in the infused dog. Calc. Tiss. Intern., 28: 79-81 (1979) (UR-3490-1511)

Radioiodinated parathyroid hormone [125I-PTH(1-84)] was infused into intact dogs. At various times venous samples were chromatographed to determine the levels of intact hormone (1-84) and large fragments in the circulation. Both bioactive (electrolytically iodinated) and inactive

- 59 -

(chloramine-T-labeled) preparations were used. In both instances, plateau concentrations of intact hormone and of large metabolite(s) were quickly reached. After cessation of infusion the levels of intact hormone and metabolite(s) quickly declined. Clearly, in the dog, the peripheral formation and disappearance of large fragments of exogenous PTH occur at rates comparable to the clearance of the intact hormone itself.

Neuman, W. F.: RIA: the only way to go? Calc. Tiss. Intern., 27: 195-197 (1979) Editorial (UR-3490-1532)

It is established that, in the field of parathyroid hormonc (PTH) metabolism, major laboratories cite literature references dealing only with results derived from radioimmunoassay (RIA). Reference to any work based on traditional radioisotopic labeling is studiously avoided. The possible reasons for this remarkable exclusion of data are explored. It is surmised that workers generally are of the opinion that labeled PTH is not bioactive. Therefore, published data on the biological activity of iodinated PTH are reviewed. It can be shown that iodination does not perceptibly reduce the biological response in six different bioassays ranging from cell-free systems to intact animals. Included is an assay of intensely labeled (1300 Ci/nmole) 125I PTH. Thus, there is no scientific justification for the exclusive consideration of RIA results.

Neuman, W. F. and Schneider, N.: The parathyroid hormone-sensitive adenyl cyclase system in plasma membranes of rat liver. Endocrinol., (in press) (UR-3490-1628)

Purified plasma membranes were prepared from normal rat livers. These membranes were unable to degrade parathyroid hormone, bPTH(1-84) or bPTH(1-34). The entire molecule bPTH(1-84) caused a marked activation of adenyl cyclase (cAMP production increased over fivefold) with half-maximal stimulation at 6.9×10^{-8} M. The amino terminal fragment bPTH(1-34) was equipotent but gave a smaller maximal cAMP production. The human amino acid sequence, hPTH(1-34) was only weakly effective at a concentration of 10^{-5} M. A similar species-specificity was shown with crude rat renal cortical membranes. Of a variety of ligands, only glucagon and 10^{-3} M F⁻ were cyclase activators in these liver plasma membranes. Binding of 125 bPTH by these membranes was fairly extensive but showed a saturation of binding only at high hormone concentrations (over 10^{-6} M). The possible significance of these findings are discussed.

Norton, G. E.: Fluorescence quenching studies of the effects of magnesium ion, glucose, viscosity and pH on the structure of yeast hexokinase isozymes. Ph.D. Thesis, University of Rochester School of Medicine and Dentistry (Supervised by Dr. I. Feldman) (1979) (UR/3490/LCP-17)

Titrations of the tryptophan fluorescence of yeast hexokinase isozymes A and B (HkA and HkB) were performed with Mg^{2+} , Li⁺, Na⁺ and K⁺ ions as titrant in the absence and in the presence of glucose and vice versa, at pH 8.3 and 5.5 at 20° C. Mg^{2+} quenches the fluorescence of surface tryptophan primarily and does so by producing a conformational change which alters the microenvironment of the tryptophan. In the presence of glucose Mg^{2+} seems to quench much more strongly but, actually, the Mg^{2+} enhances the glucose quenching by causing a conformation change which increases the glucose-binding constant. At pH 8.3 Na⁺, but not K⁺ or Li⁺, has a small enhancing effect. Regardless of ionic strength, glucose binding by HkB is noncooperative at pH 8.3 in the presence of any of these four cations and at pH 5.5 in the presence of Mg^{2+} or K⁺. However, concavity exhibited by Scatchard plots of glucose titrations of HkB at pH 5.5 demonstrated apparent negative cooperativity for glucose binding by this isozyme in the presence of 30 mM Na⁺ or Li⁺.

Scatchard-type plots of the fluorescence-quenching titrations demonstrated that glucose binding to HkA in 0.02 M buffer exhibits positive cooperativity at pH 8.3 and 5.5, with Hill coefficients equal to 1.56 and 1.42, respectively. At pH 5.5 the degree of cooperativity is unchanged by any of these four cations at 0.03 ionic strength, i.e., 10 mM MgCl₂ and 30 mM alkali chlorides, while at pH 8.3 all four cations at these concentration decrease the degree of cooperativity the same amount, as evidenced by a lowering of the Hill coefficient by each cation to about 1.3. Nevertheless, each cation enhances the glucose-binding strength of HkA at both pH's, but to a greater extent at the higher pH. Mg^{2+} has the largest effect, indicating that, at least for this cation, the action is partly a specific ion effect rather than merely an ionic strength effect.

Titrations of the tryptophan fluorescence of HkB were performed with acrylamide, a polar, nonionic quencher, as titrant in the absence and in the presence of glucose and in the presence of Mg^{2+} , K⁺ and Na⁺ at pH 8.3 and 5.5 at 20° C. Acrylamide quenches 100% of the HkB fluorescence at 350 nm. The titrations were subjected to computer analysis to calculate the tryptophan fractional fluorescences and the Stern-Volmer constants. The four tryptophan residues of the monomer subunit in 0.05 M buffer pH 8.3 can be classified as two surface residues with nearly the same accessibility to acrylamide quenching, a glucose - quenchable cleft tryptophan and a 'partially buried' tryptophan. The earlier finding of Kramp and Feldman (Biochim. Biophys. Acta (178) 537, 406-416) that the two surface residues have widely differing Stern-Volmer constants toward quenching by iodide ion must be a result of a positively-charged microenvironment near one residue. Binding of the substrate glucose and the cofactor Mg^{2+} induces conformational changes which are accompanied by alteration of the exposure of the four tryptophans to the quenching action of acrylamide. Acrylamide titrations in the presence of 55% glycerol suggest that at pH 5.5 transient channels may allow quencher to diffuse to the interior protein matrix.

Norton, G. E. and Feldman, I.: Effects of free magnesium and alkali ions on the conformation and glucose-binding strength of yeast hexokinase isozymes. Biochim. Biophys. Acta, (in press) (UR-3490-1582)

Titrations of the tryptophan fluorescence of yeast hexokinase (ATP:D-hexose 6-phosphotransferase, EC 2.7.1.1) isozymes P-I (A) and P-II (B) were performed with Mg^{2+} , Li⁺, Na⁺ and K⁺ as titrant in absence and in presence of glucose, and vice versa, at pH 8.3 and 5.5 at 20° C. Mg^{2+} quenches the fluorescence of surface tryptophan primarily and does so by producing a conformational change which alters the microenvironment of the tryptophan. For both isozymes Mg^{2+} exerts a specific ion effect, i.e., significantly larger than the ionic strength (I) effect, which enhances the glucose quenching by causing a conformation change which increases the glucose-binding constant. For the P-I isozyme glucose binding exhibits positive cooperativity at both pH 8.3 and 5.5 when the ionic strength (I) is low, i.e., 0.04 or less, regardless of which of the above four cations is present. For P-II, however, glucose binding is noncooperative at pH 8.3 regardless of I or the cation species and at pH 5.5 and low I with K⁺ or Mg^{2+} as the predominant cation present, but there is apparent negative cooperativity at pH 5.5 and low I when Na⁺ or Li⁺ predominates. These results are discussed in terms of known structural characteristics of the isozymes.

Notter, R. H.; Tabak, S. A. and Mavis, R. D.: Surface properties of binary mixtures of some pulmonary surfactant components. J. Lipid Res., (in press) (UR-3490-1449)

The dynamic surface pressure-area properties of pure and binary mixed films of rac-1,2-dipalmitoylglycero-3-phosphocholine, 1,2-dioleoyl-sn-glycero-3-phosphocholine and cholesterol were invetigated at 23° C and 37° C. The pure films and binary mixtures of rac-1,2-dipalmitoyl-glycero-3-phosphocholine:1,2-dioleoyl-sn-glycero-3-phosphocholine and rac-1,2-dipalmitoyl-glycero-3-phosphocholine: cholesterol were characterized both for dilute surface initial concentrations of 150 Å²/molecule and for surface excess initial values of 15-50 Å²/molecule. The results show that the addition of 1,2-dioleoylsn-glycero-3-phosphocholine or cholesterol in a binary film with rac-1,2 dipalmitoyl-glycero-3-phosphosphocholine acts to improve the surface re-entry and respreading properties over those of pure rac-1,2dipalmitoyl-glycero-3-phosphocholine films upon dynamic compression past collapse. This effect is even more pronounced at 37° C than at 23° C, as demonstrated by the application of a collapse plateau

- 62 -

ratio criterion. The enhanced dynamic respreading correlates with the effect of 1,2-dioleoyl-snglycero-3-phosphocholine and cholesterol in decreasing the gel to liquid crystal transition temperature of rac-1,2-dipalmitoyl-glycero-3-phosphocholine water dispersions, as well as with their facilitation of postcollapse dynamic surface pressure relaxation in binary films with rac-1,2-dipalmitoylglycero-3-phosphocholine.

Notter, R. M.; Tabak, S. A.; Holcomb, S. and Mavis, R. D.: Postcollapse dynamic surface pressure relaxation in binary surface films containing dipalmitoyl phosphatidylcholine. J. Colloid Interface Sci., (in press)(UR-3490-1448)

The time dependent decay of dynamic surface pressure (π) is investigated for binary films of Dipalmitoyl Phosphatidylcholine: Dioleoyl Phosphatidylcholine (DPL:DOL) and of Diplamitoyl Phosphatidylcholine: Cholesterol (DPL:CHOL) after dynamic compression past monolayer collapse. The results show that the addition of either DOL or CHOL to DPL films acts to increase the degree of relaxation of postcollapse surface pressure. Thus, while pure DPL films exhibit a highly stable postcollapse dynamic surface pressure that is more than 20 dynes/cm in excess of the equilibrium value, films of 50:50 DPL:DOL show dynamic π relaxation to values within a few dynes/cm of equilibrium collapse pressure in times of the order of 100 seconds at 25° C. Films of 50:50 DPL: CHOL also relax to within a dyne/cm of the equilibrium value at 100 seconds, although the actual extent of relaxation is quite small for this specific binary because it is able to generate initial dynamic collapse pressures only a few dynes/cm above the equilibrium value. Films of both 90:10 DPL:DOL and 90:10 DPL:CHOL show postcollapse dynamic π values with a large extent of relaxation, but the relaxation process is relatively slow and these films show surface pressures still above the true equilibrium values after 1000 seconds. The increased relaxation imparted to DPL films by the addition of DOL or CHOL as a second monolayer component correlates with the effect of these other surfactants in increasing the dynamic respreading in DPL films compressed past collapse.

Ono, B-I.; Stewart, J. W. and Sherman, F.: Yeast UAA suppressors effective in ψ^+ strains: leucineinserting suppressors. J. Mol. Biol., 132: 507-520 (1979) (UR-3490-1527)

We have previously reported the isolation and characterization of UAA suppressors from a haploid strain of yeast Saccharomyces cerevisiae containing the ψ^+ non-Mendelian determinant which increases the efficiency of action of certain suppressors. Most of the suppressors caused the insertion of either tyrosine or serine. In contrast the pattern of suppression of nutritional markers suggested that the rare suppressor, SI/P26, inserted in an amino acid other than tyrosine or serine. In this investigation we report the characterization of additional suppressors, similar to SUP26, that

were isolated on a medium lacking uracil and containing canavanine; this medium is expected to exclude serine-inserting suppressors because they do not suppress the ura4-1 marker, and to exclude tyrosine-inserting suppressors because they suppress the can1-100 marker. The total of 155 revertants similar to the SUP26 suppressor were analyzed genetically and these could be assigned to one or another of the six distinct loci SUP26, SUP27, SUP28, SUP29, SUP32 and SUP33. The SUP26, SUP27 and SUP29 loci mapped on chromosomes XII, IV and X, respectively. The detailed map position of the SUP29 suppressor suggests that it may be allelic to the SUP30 suppressor reported by Hawthorne and Mortimer (1968). These six suppressors had the same pattern of suppression of UAA nutritional markers and all of them had a similar low efficiency of action on the iso-1-cytochrome c mutation cyc1-72. The efficiency of each of these suppressors was increased by a chromosomal allosuppressor, sal. Each of the six suppressors caused the insertion of leucine in iso-1-cytochrome c at the UAA site of the cyc1-72 mutation. It is suggested that the gene products of these suppressors are redundant forms of the same leucine transfer RNA.

Owens, M. R. and Miller, L. L.: Net biosynthesis of antithrombin III by the isolated rat liver perfused by 12–24 hours. Compared with rat fibrinogen and α -2 (acute-phase) globulin, antithrombin III is not an acute phase protein. Biochim. Biophys. Acta, (in press) (UR-3490-1578)

Antithrombin III-heparin cofactor has been isolated from normal rat plasma, purified to homogeneity on acrylamide gel electrophoresis and used to prepare a monospecific antiserum in rabbits. Measurements of rat antithrombin III were made by a single radial immunodiffusion assay.

Net synthesis of antithrombin III was investigated during 12- or 24-hour perfusions of the isolated rat liver. In perfusions performed under basal conditions cumulative synthesis of antithrombin-III was observed to occur at a rate sufficient to replace the total circulating plasma antithrombin III in about 6 hours. In perfusions performed under full supplementation conditions which greatly enhanced synthesis of fibrinogen and α -2 (acute-phase) globulin (known acute-phase reactant proteins) net synthesis of antithrombin III was not significantly greater than that observed in contron perfusions. Although these prolonged perfusions studies conclusively demonstrate net synthesis of antithrombin III by the isolated rat liver, they afford no evidence that this protein is an acute-phase reactant.

Prakash, L. and Prakash, S.: Genetic analysis of error prone repair systems in Saccharomyces cerevisiae. In <u>DNA Repair and Mutagenesis in Eucaryotes</u>, Ed. by F. deSerres, M. Shelby and W. Generoso. Plenum Press, New York, (in press) (UR-3490-1666)

The manner in which UV induced mutagenesis occurs in yeast is discussed and compared with UV mutagenesis in $E. \ coli$. In both excision proficient and excision deficient strains of $E. \ coli$, muta-

tions arise as the square of the UV dose whereas in yeast, mutations arise as the square of the dose only in excision proficient strains. In excision defective yeast strains, mutations induced by UV arise with linear kinetics. UV irradiation of excision proficient haploid or diploid yeast during G₁ results in fixation of mutation in both DNA strands prior to DNA replication, whereas in excision defective strains, the frequency of two strand mutations is very low and the frequency of one strand mutations and mutations appearing in the second postirradiation mitotic division is increased. All of these results in yeast can be explained by error prone excision repair of two closely spaced dimers in opposite DNA strands in excision proficient strains and occasional error prone filling in of postreplication gaps which are not usually overlapping daughter strand gaps in excision defective yeast. The dependence of UV mutagenesis on functional *RAD6*, *REV3*, *CDC8* and *MMS3* gene functions is discussed. The *MMS3* function appears to be required for UV mutagenesis in a/α diploids but is dispensible in a/a or α/α diploids and in haploids, suggesting that differences exist between error prone repair processes in haploids, a/a, α/α diploids vs a/α diploids.

Alkylating agent induced mutations in yeast depend on functional RAD6, RAD9, RAD51 and RAD52 genes. Different alleles of the RAD52 locus differ in their effects on EMS induced mutations of different sites within the same gene. Misreplication of O⁶-alkyl guanine probably does not account for most of the mutations induced by alkylating agents in yeast; instead, they probably result from RAD6-dependent error prone repair of gaps opposite O⁶-alkyl guanine. Error prone repair pathways for repair of radiation damage differ in some respects from error prone repair of damage induced by chemical agents.

Prakash, L. and Prakash, S.: Three additional genes involved in pyrimidine dimer removal in Saccharomyces cerevisiae: RAD7, RAD14 and MMS19. Mol. gen. Genet., 176: 351-359 (1979) (UR-3490-1671)

The ability to remove ultraviolet (UV)-induced pyrimidine dimers from the nuclear DNA of yeast was examined in two radiation-sensitive (rad) mutants and one methyl methanesulfonatesensitive (mms) mutant of the yeast Saccharomyces cerevisiae. The susceptibility of DNA from irradiated cells to nicking by an endonuclease activity prepared from crude extracts of Micrococcus luteus was used to measure the presence of dimers in DNA. The rad7, rad14 and mms19 mutants were found to be defective in their ability to remove UV-induced dimers from nuclear DNA. All three mutants belong to the same epistatic group as the other mutants involved in excision-repair. All three mutants show enhanced UV-induced mutations. The rad14 mutant also shows epistatic interactions with genes in the other two UV repair pathways. Prakash, L.; Hinkle, D. and Prakash, S.: Decreased UV mutagenesis in cdc8, a DNA replication mutant of Saccharomyces cerevisiae. Mol. gen. Genet., 172: 249-258 (1979) (UR-3490-1570)

A DNA replication mutant of yeast, cdc8, was found to decrease UV-induced reversion of lys2-1, arg4-17, tyr1 and ura1. This effect was observed with all three alleles of cdc8 tested. Survival curves obtained following UV irradiation in cdc8 rad double mutants show that cdc8 is epistatic to rad6, as well as to rad1; cdc8 rad51 double mutants seem to be more sensitive than the single mutants. Since UV-induced reversion in cdc8 rad1 and cdc8 rad51 double mutants is like that of the cdc8 single mutants, we conclude that CDC8 plays a direct role in error-prone repair. To test whether CDC8 codes for a DNA polymerase, we have purified both DNA polymerase I and DNA polymerase II from cdc8 and CDC+ cells. The purified DNA polymerases from cdc8 were no more heat labile than those from CDC+, suggesting that CDC8 is not a structural gene for either enzyme.

Prakash, S.; Prakash, L.; Burke, W. and Montelone, B. A.: Effects of the *RAD52* gene on recombination in *Saccharomyces cerevisiae*. Genetics, (in press) (UR-3490-1571)

Effects of the rad52 mutation in Saccharomyces cerevisiae on meiotic, γ -ray induced, UV induced and spontaneous mitotic recombination were studied. The rad52/rad52 diploids undergo premeiotic DNA synthesis; sporulation occurs but inviable spores are produced. Intra- and intergenic recombination during meiosis were examined in cells transferred from sporulation medium to vegetative medium at different time intervals. No intragenic recombination was observed at the his1-1/his1-315 and trp5-2/trp5-48 heteroalleles. Gene-centromere recombination was also not observed in rad52/rad52 diploids. No γ -ray induced intragenic mitotic recombination is seen in rad52/rad52 diploids and UV induced intragenic recombination is greatly reduced. However, spontaneous mitotic recombination is not similarly affected. The RAD52 gene thus functions in recombination in meiosis and in γ -ray and UV induced mitotic recombination but not in spontaneous mitotic recombination.

Puskin, J. S. and Coen, M. T.: Na⁺ and H⁺ dependent Mn^{2+} binding to phosphatidylserine vesicles as a test of the Gouy-Chapman-Stern theory. J. Memb. Biol., (in press) (UR-3490-1664)

 Mn^{2+} binding to phosphatidylserine (PS) vesicles was measured by EPR as a function of $[Na^+]$ and pH. At nearly physiological monovalent salt concentration the apparent Mn^{2+} affinity (K_a) increased monitonically over the pH range 5.7-8.35, with K_a roughly $\alpha[H^+]^{-1}$ above pH 7.3. It was found, moreover, that K_a fell off more rapidly with added NaCl at pH 6.1 than at pH 7.87. Qualitatively, these results are consistent with two types of Mn^{2+} -PS binding: (i) simple adsorption and (ii) adsorption with the release of an amino proton from PS. The existence of Mn^{2+} -induced H⁺ displacement from PS was verified through titration measurements, employing a pH electrode.

When H⁺ displacement is taken into account, the variation in K_a with [Na⁺] observed at pH 6.1 is found to be in reasonably good agreement with that expected from the Gouy-Chapman-Stern theory of ionic binding to charged surfaces.

Reddy, B. S.; Seshadri, T. P.; Sakore, T. D. and Sobell, H. M.: Visualization of drug—nucleic acid interactions at atomic resolution. V. Structure of two aminoacridine—dinucleoside monophosphate crystalline complexes, proflavine—5-iodocytidylyl (3'—5') guanosine and acridine orange—5-iodocytidylyl (3'—5') guanosine. J. Mol. Biol., 135: 787-812 (1979) (UR-3490-1574)

Acridine orange and proflavine form complexes with the dinucleoside monophosphate, 5-iodocytidylyl(3'-5')guanosine. The acridine orange—iodoCpG† crystals are monoclinic, space group $P2_1$, with unit cell dimensions a = 14.36 Å, b = 19.64 Å, c = 20.67 Å, $\beta = 102.5^{\circ}$. The proflavine—iodo-CpG crystals are monoclinic, space group C2, with unit cell dimensions a = 32.14 Å, b = 22.23 Å, c = 18.42 Å, $\beta = 123$ 3°. Both structures have been solved to atomic resolution by Patterson and Fourier methods, and refined by full matrix least-squares.

Acridine orange forms an intercalative structure with iodoCpG in much the same manner as ethidium, ellipticine and 3,5,6,8-tetramethyl-N-methyl phenanthrolinium except that the acridine nucleus lies asymmetrically in the intercalation site. This asymmetric intercalation is accompanied by a sliding of base pairs upon the acridine nucleus and is similar to that observed with the 9-aminoacridine—iodoCpG asymmetric intercalative binding mode described in previous papers. Base pairs above and below the drug are separated by about 6.8 Å and are twisted about 10° ; this reflects the mixed sugar puckering pattern observed in the sugar—phosphate chains: C3' endo (3'-5') C2' endo (i.e., each cytidine residue has a C3' endo sugar conformation, while each guanosine residue has a C2' endo sugar conformation), alterations in glycosidic torsional angles and other small but significant conformational changes in the sugar—phosphate backbone.

Proflavine, on the other hand, demonstrates symmetric intercalation with iodoCpG. Hydrogen bonds connect amino groups on proflavine with phosphate oxygen atoms on the dinucleotide. In contrast to the acridine orange structure, base pairs above and below the intercalative proflavine molecule are twisted about 36° . The altered magnitude of this angular twist reflects the sugar puckering pattern that is observed: C3' endo (3'-5') C3' endo. Since proflavine is known to unwind DNA in much the same manner as ethidium and acridine orange, one cannot use the information from this model system to understand how proflavine binds to DNA (it is possible, for example,

† Abbreviation used: iodoCpG, 5-iodocytidylyl(3'-5')guanosine.

that hydrogen bonding observed between proflavine and iodoCpG alters the intercalative geometry in this model system).

Instead, we propose a model for proflavine—DNA binding in which proflavine lies asymmetrically in the intercalation site (characterized by the C3' endo (3'—5') C2' endo mixed sugar puckering pattern) and forms only one hydrogen bond to a neighboring phosphate oxygen atom. Our model for proflavine—DNA binding, therefore, is very similar to our acridine orange—DNA binding model. We will describe these models in detail in this paper.

Rifkin, B. R.; Cushing, J. E. and Brand, J. S.: Fine structure of fetal rat calvaria, provisional identification of preosteoclasts. Calc. Tiss. Intern., (in press) (UR-3490-1403)

This is a study of the fine structure of cells of the twenty-day fetal rat calvarium. Special attention is given to identifying and characterizing preosteoclasts. These cells are relatively common and located largely, but not exclusively, at the endocranial bone surface. The preosteoclasts are characterized by abundant mitochondria, conspicuous Golgi zones, and variable-shaped dense granules. The dense granules are unique in appearance in that they contain an internal dense matrix surrounded by a clear halo. Most granules are circular in shape but some are elongate or tubular in form. Granules with identical appearance are observed in osteoclasts. The preosteoclasts are mononucleate, or occasionally binucleate. It is suggested that because preosteoclasts are morphologically distinctive and relatively abundant, it should be feasible to separate these cells from a heterogeneous cell isolate.

Rosler, R. N.: Calcium transport in vesicles energized by cytochrome oxidase. Ph.D. Thesis, University of Rochester School of Medicine and Dentistry (Supervised by Dr. T. E. Gunter) (1979) (UR-3490-1549)

Experiments on the reconstitution of cytochrome oxidase into phospholipid vesicles were carried out using techniques of selectively energizing the suspensions with ascorbate and cytochrome c or ascorbate, PMS, and internally trapped cytochrome c. It was found that the K⁺ selective ionophore valinomycin stimulated the rate of respiration of cytochrome oxidase vesicles regardless of the direction of the K⁺ flux across the vesicle membranes. The stimulation occurred in the presence of protonophoric uncouplers and in the complete absence of potassium or in detergent-lysed suspensions. Gramicidin had similar effects and it was determined that the ionophores acted by specific interaction with cytochrome oxidase rather than by the previously assumed collapse of membrane potentials.

When hydrophobic proteins and appropriate coupling factors were incorporated into the cytochrome oxidase vesicles phosphorylation of ADP could be coupled to the oxidation reaction of cytochrome oxidase. Relatively low P:O, representing poor coupling of the system, were problematical and precluded measurements of protonmotive force. However, the system was used to study ion translocation.

The primary problem in the study of ion transport in proteoliposomes is the difficulty of separating the small vesicles from the suspending medium by conventional techniques of filtration or centrifugation. A system of vesicle aggregation was developed which involved the addition of polylysine or protamine to vesicle suspensions to cause clumping so that conventional filtrations could readily be used to quantitate ion transport. The system was found to be applicable to a wide range of types of artificial and natural vesicles.

Using this separatory system, cation uptake in submitochondrial particles and cytochrome oxidase vesicles was studied. A number of tests of the sidedness of the vesicles demonstrated the cytochrome oxidase to be in bidirectional orientation in both types of vesicles, and techniques of selective energization were developed to allow generation of either internally positive or negative membrane potentials in the vesicles. Under these conditions of selective energization it was found that submitochondrial particles accumulated calcium when either internally negative or positive membrane potentials were generated. The characteristics of the transport were studied and uptake against the electrochemical gradient (in internally positive submitochondrial particles) of both calcium and manganese was found to be inhibited by levels of protonophoric uncoupler too low to dissipate the protonmotive force. Other experiments indicated that the mechanism of this type of transport was either an electrogenic pump coupled to oxidation or an antiport type of carrier, while the mechanism in the internally negative particles was consistent with a uniport.

Cytochrome oxidase vesicles were found to take up calcium and manganese when energized to generate inside negative membrane potentials. Uptake in inside positive vesicles or enhancement of uptake in inside negative vesicles could be obtained by co-reconstitution with complex V. This uptake was also sensitive to low levels of uncouplers and further experiments indicated similarity to the submitochondrial particle experiments, in that uptake in internally negative vesicles was mediated most likely by a uniport type of carrier while uptake against the electrochemical gradient in the internally positive vesicles was more consistent with an antiport or electrogenic pump coupled to oxidation. Uptake of divalent cation in both submitochondrial particles and the reconstituted system was sensitive to uncouplers or inhibitors of oxidation.

- 69 -

Rosier, R. N. and Gunter, T. E.: Calcium uptake by cytochrome oxidase vesicles. FEBS Letters, (in press) (UR-3490-1727)

Liposomes reconstituted with cytochrome oxidase are well known to be capable of energy dependent membrane potential and protein gradient formation. In the past, membrane potential generation in cytochrome oxidase vesicles (COV) has been shown to drive monovalent cation uptake in the presence of an appropriate ionophore, but energy dependent divalent cation transport in COV has not been reported. A protamine-aggregation filtration technique for quantitation of ion transport in vesicles was used to obtain the data presented which indicates that Ca⁺⁺ is accumulated in COV which are energized so as to form an internally negative membrane potential. This accumulation occurs without addition of specific known mediators of Ca^{++} permeability. The transport is dependent on substrait oxidation and is inhibited by KCN or uncouplers such as CCCP and the combination of nigericin, valinomycin and K^+ . Ca⁺⁺ uptake is inhibited by mild sonication or the presence of cytochrome c at the time of vesicle formation. Addition of a subfraction of cytochrome oxidase devoid of oxidative activity enhances the Ca⁺⁺ transport rate, as does a known electrogenic ionophore. The data suggest that cytochrome oxidase contains an inherent mediator of Ca⁺⁺ permeability which can allow electrogenic transport of Ca^{++} in an energy dependent manner. It is possible that this component may be involved in the coupling of mitochondrial ion transport to oxidation.

Rothstein, R. J. and Sherman, F.: Dependence of mating type for the overproduction of iso-2cytochrome c in the yeast mutant CYC7-H2. Genetics, (in press) (UR-3490-1608)

The CYC7-H2 mutation causes an approximately 20-fold overproduction of iso-2-cytochrome c in $\underline{\alpha}$ and α haploid strains of the yeast Saccharomyces cerevisiae due to an alteration in the nontranslated regulatory region which is presumably contiguous with the structural region. In this investigation it was demonstrated that heterozygosity at the mating type locus, \underline{a}/α or $\underline{a}/\underline{a}/\alpha$, prevents expression of the overproduction while homozygosity, \underline{a}/α and α/α , and hemizygosity, \underline{a}/α and α/α , allow full expression of the CYC7-H2 mutation, equivalent to the expression observed in \underline{a} and α haploid strains. There is no decrease in the overproduction of iso-2-cytochrome c in \underline{a}/α diploid strains containing either of the other two similar mutations, CYC7-H1 and CYC7-H3. It appears as if active expression of one or another of the mating type alleles is required for the overproduction of iso-2-cytochrome c in CYC7-H2 mutants. Rothstein, R. J. and Sherman, F.: Genes affecting the expression of cytochrome c in yeast: genetic mapping and genetic interactions. Genetics, (in press) (UR-3490-1651)

The four mutant genes cyc2, cyc3, cyc8 and cyc9 that affect the levels of the two iso-cytochromes c in the yeast Saccharomyces cerevisiae have been characterized and mapped. The two genes cyc2 and cyc3 lower the amount of both iso-1-cytochrome c and iso-2-cytochrome c, and the two genes cyc8 and cyc9 increase the amount of iso-2-cytochrome c. The cyc2, cyc3, cyc8 and cyc9 genes are located, respectively, on chromosomes XV, I, II, and III, and are therefore unlinked to each other and unlinked to CYCI, the structural gene of iso-1-cytochrome c and to CYC7, the structural gene of iso-2-cytochrome c. While some cyc3 mutants are completely or almost completely deficient in cytochromes c, none of the cyc2 mutants contained less than 10% of parental levels of cytochrome c even though over one-half of the mutants contain UAA or UAG nonsense mutations. Thus it appears as if a complete block of the cyc2 gene product still allows the formation of a residual fraction of cytochrome c. The cyc2 and cyc3 mutant genes cause deficiencies even in the presence of CYC7, cyc8 and cyc9 genes that normally cause overproduction of iso-2cytochrome c. It is suggested that the cyc2 and cyc3 genes may be involved with the regulation or maturation of the iso-cytochrome c. In addition to having high levels of iso-2-cytochromes c, the cyc8 and cyc9 mutants were associated flocculent cells and other abnormal phenotypes. The cyc9 mutant was shown to be allelic with the tup1 mutant and to share its properties that include the ability to utilize exogenous dTMP, a characteristic flocculent morphology, the lack of sporulation of homozygous diploids and low frequency of mating and abnormally shaped cells of α strains. The diversed abnormalities suggest that cyc8 and cyc9 are not simple regulatory mutants controlling iso-2-cytochrome c.

Sakore, T. D.; Reddy, B. S. and Sobell, H. M.: Visualization of drug—nucleic acid interactions at atomic resolution. IV. Structure of an aminoacridine—dinucleoside monophosphate crystalline complex, 9-aminoacridine—5-iodocytidylyl (3'—5') guanosine. J. Mol. Biol., 135: 763-785 (1979) (UR-3490-1573)

9-aminoacridine forms a crystalline complex with the dinucleoside monophosphate, 5-iodocytidylyl(3'-5')guanosine (iodoCpG). These crystals are monoclinic, space group $P2_1$, with a =13.98 Å, b = 30.58 Å, c = 22.47 Å and $\beta = 113.9^\circ$. The structure has been solved to atomic resolution by Patterson and Fourier methods and refined by a combination of Fourier and sum-function Fourier methods. The asymmetric unit contains *four* 9-aminoacridine, molecules, *four* iodoCpG molecules and 21 water molecules, a total of 245 atoms. 9-aminoacridine demonstrates *two* different intercalative binding modes and, along with these, two slightly different intercalative geometries in this model system.

The first of these is very nearly symmetric, the 9-amino group lying in the narrow groove of the intercalated base-paired nucleotide structures. The second shows grossly asymmetric binding to the dinucleotide, the 9-amino group lying in the wide groove of the structure. Associated with these two different intercalative binding modes is a difference in geometries in the structures. Although both structures demonstrate C3' endo (3'-5') C2' endo mixed sugar puckering patterns (i.e., both cytidine residues have C3' endo sugar conformations, while both guanosine residues have C2' endo sugar conformations), with corresponding twist angles between base pairs of about 10°, they differ in the magnitude of the helical screw axis dislocation accompanying intercalation. In the pseudosymmetric intercalative structure, this value is about +0.5 Å, whereas in the asymmetric intercalative structure this value is about +2.7 Å. These conformational differences can be best described as a "sliding" of base pairs on the intercalated acridine molecule.

Although the pseudosymmetric intercalative structure can be used in 9-aminoacridine—DNA binding, the asymmetric intercalative structure cannot since this poses stereochemical difficulties in connecting neighboring sugar-phosphate chains to the intercalated dinucleotide. It is possible, however, that the asymmetric binding mode is related to the mechanism of 9-aminoacridine-induced frameshift mutagenesis and we discuss this possibility here in further detail.

Schneider, N.; Teitelbaum, A. P. and Neuman, W. F.: Tissue deposition and metabolism of ¹²⁵Ilabeled synthetic amino-terminal parathyroid hormone bPTH(1-34). Calc. Tiss. Intern., (in press) (UR-3490-1621)

The tissue deposition and metabolism of 125I-labeled synthetic aminoterminal parathyroid hormone, bPTH(1-34) was studied in rats. In comparison with the intact hormone molecule bPTH(1-84), the synthetic fragment was: a) cleared more rapidly from serum; b) degraded more rapidly in peripheral tissues; c) deposited to a greater extent in kidney; d) deposited to a much smaller extent in liver. In bone, the accumulation of total radioactivity was approximately the same with both labeled hormones. The possibly physiological significance of these patterns of distribution and metabolism is discussed.

Scott, T. L.: Interaction between the catalytic and ion transport sites of the adenosine triphosphatase of sarcoplasmic reticulum. Ph.D. Thesis, University of Rochester School of Medicine and Dentistry (Supervised by Dr. A. E. Shamoo) (1979) (UR/3490/LCP-15)

The goal of this thesis is the elucidation of the mechanism of energy transduction between the ATP catalytic site and the ion transport sites of the $Ca^{2+}Mg^{2+}$ ATPase of skeletal muscle sarco-

plasmic reticulum (SR). Modification of the ATPase peptide by thiol group blockage with mercurial reagents and proteolytic fragmentation with trypsin is used to perturb the interactions between the hydrolytic and transport processes.

Inhibition of the functional activities of the calcium pump system by methylmercuric chloride and mercuric chloride is examined. Both calcium uptake and Ca^{2+} -dependent ATPase activities are inhibited by methylmercuric chloride with the same dose response. Total inhibition of both activities occurs at a dose of 2.8 to 3 mol CH₃Hg⁺ per 10⁵ g SR. Both activities are also inhibited by mercuric chloride, but calcium uptake is inhibited at a lower dose of Hg²⁺ than that required to abolish ATP hydrolysis activity. Direct determination indicates that Hg²⁺ blocks thiol groups of the ATPase enzyme, with complete inhibition of transport at a dose of 3.5 mol Hg²⁺/10⁵ g SR and of hydrolysis at 5 mol Hg²⁺/10⁵ g SR. The differential effect of Hg²⁺ on the two functions indicates that transport and hydrolysis can be uncoupled by the modification of an essential thiol of the ATPase enzyme. Thiol blockage of the SR ATPase by CH₃HgCl and HgCl₂ is compared with previous studies of thiol involvement in the functions of this system and discussed in terms of the mechanism of active ion transport by the SR Ca²⁺ pump.

Proteolytic fragmentation of SR vesicles with trypsin is used as a structural modification with which to examine the interaction between the ATP catalytic site and the Ca^{2+} transport sites of the SR Ca^{2+} -Mg²⁺ ATPase. The kinetics of trypsin fragmentation are examined and the time course of fragment production is compared with hydrolytic and Ca^{2+} uptake activities of the digested vesicles. The initial cleavage (TD1) of the native ATPase to A and B peptides has no effect on the functional integrity of the enzyme, hydrolytic and transport activities remaining at the levels of the undigested control. Concomitant with the second event of trypsin cleavage (TD2) of the A peptide to A₁ and A₂ fragments, Ca^{2+} transport is inhibited. Kinetic analysis demonstrates that the rate constant for inhibition of transport is correlated with the rate constant of A fragment disappearance. Both Ca^{2+} -dependent and total ATP hydrolysis rates are unaffected by this second cleavage. Passive loading of vesicles with Ca^{2+} and subsequent measurements of efflux rates show that TD2-induced transport inhibition is not the result of increased membrane permeability to Ca^{2+} even at considerable extents of the digestion reaction.

SR vesicles are shown to contain "tightly bound" nucleotides, 2.8 to 3.0 mol ATP and 2.6 mol ADP per 10^5 g SR, by methods similar to those employed for analysis of "tightly bound" nucleotides in mitochondria and chloroplasts. The ADP content of SR remains essentially unchanged with TD1 cleavage, but is removed by TD2 with a time course that parallels the disappearance of the A fragment and the inhibition of Ca²⁺ transport. The ATP content is essentially constant throughout

the course of digestion.

Steady-state levels of acid-stable phosphorylated intermediate are unaffected by either TD1 or TD2, indicating that uncoupling of the hydrolytic and transport processes does not increase the enzyme turnover rate or alter the essential structure of the hydrolysis site. The results demonstrate that cleavage of an essential bound in the ATPase peptide disrupts energy transduction and are discussed in terms of current models of the SR Ca^{2+} pump.

The effects of trypsin fragmentation on Ca^{2+} binding and Ca^{2+} activation of ATP hydrolysis by the high affinity binding-transport sites of the ATPase are examined. SR vesicles are shown to contain 0.7 to 1.1 mol Ca^{2+} binding sites per 10^5 g with association constant K = 0.2 to 1 X 10^6 M^{-1} , as well as sites of lower affinity. The first cleavage of the enzyme with trypsin, (TD1), has no effect on the binding parameters of the high affinity sites. TD2, which has been shown to disrupt energy coupling, decreases the affinity of these sites to K = 3 X 10^4 M⁻¹, with conservation of the total number of sites.

The purified ATPase contains 2 mol high affinity Ca^{2+} sites per mol at 22° (K = 0.2 to 2 X 10⁶) M^{-1}), while at 0 to 4° there is 1 high affinity site and 1 intermediate affinity site (K = 3 X 10⁴ M⁻¹). Trypsin digestion to TD1 has no effect on either the number or binding constant of the high affinity sites. The enzyme subjected to TD2 cleavage maintains 1 site in the high affinity state, but the second site is altered to the intermediate affinity state at 22°. This is similar to the behavior of one of the sites of the intact ATPase upon temperature reduction but TD2 modification has the unique property that both of the sites are altered to the intermediate affinity state when binding is assayed at 4°. This indicates that TD2 affects the site that is not temperature sensitive. On the basis of the binding results, several models for Ca^{2+} activation of ATP hydrolysis are derived in the Appendix. The derivations show that for the independent binding sites of the ATPase, the standard Hill plot analysis is insufficient to distinguish among various models for the roles of the binding sites in the stimulation of ATP hydrolysis. Comparison of the predictions of these models with the experimental Ca^{2+} activation profiles of the undigested enzyme indicates that Ca^{2+} binding to either of the high affinity sites can stimulate hydrolysis. The Ca^{2+} activation at 4° of the native enzyme has different properties than those at 22°, corresponding to stimulation by the one remaining high affinity site which is present at low temperature. The Ca^{2+} dependence of ATP hydrolysis by the TD2 enzyme indicates that stimulation results from Ca^{2+} binding to the single high affinity site present in the TD2 enzyme at 22°.

These results are summarized in a scheme in which the two high affinity binding-transport sites are depicted as A_{TEMPATD}, where the subscripts denote sensitivity to low temperature and TD2

modification, respectively. The important finding of these results is that while either site may stimulate ATP hydrolysis, one of the sites, A_{TD} , is essential for Ca^{2+} transport. These conclusions are presented in a proposed model for the coupling among the ATP hydrolytic site, the transport sites and the ion translocation process.

Segel, G. B. and Lichtman, M. A.: Lymphocyte sodium concentration regulates monovalent cation transport after PHA stimulation. Proc. 13th Intern. Leukocyte Culture Conf., May 1979, Ottawa, Canada, (in press) (UR-3490-1644)

In these studies it has been shown that an increase in lymphocyte sodium following phytohemagglutinin treatment is responsible for the increased sodium and potassium transport rates.

Segel, G. B.; Kovach, G. and Lichtman, M. A.: Sodium-potassium adenosine triphosphatase activity of human lymphocyte membrane vesicles: kinetic parameters, substrate specificity, and effects of phytohemagglutinin. J. Cell. Physiol., 100: 109-118 (1979) (UR-3490-1416)

We have prepared human blood lymphocyte membrane vesicles of high purity in sufficient quantity for detailed enzyme analysis. This was made possible by the use of plateletpheresis residues, which contain human lymphocytes in amounts equivalent to thousands of milliliters of blood.

The substrate specificity and the kinetics of the cofactor and substrate requirements of the human lymphocyte membrane Na⁺, K⁺-ATPase activity were characterized. The Na⁺, K⁺-ATPase did not hydrolyze ADP, AMP, ITP, UTP, GTP or TTP. The mean ATPase stimulated by optimal concentrations of Na⁺ and K⁺ (Na⁺, K⁺-ATPase) was 1.5 nmol of P_i hydrolyzed, μ g protein⁻¹, 30 min⁻¹ (range 0.9-2.1). This activity was completely inhibited by the cardiac glycoside, ouabain. The K_m for K⁺ was approximately 1.0 mM and the K_m for Na⁺ was approximately 15 mM.

Active Na⁺ and K⁺ transport and ouabain-sensitive ATP production increase when lymphocytes are stimulated by PHA. Na⁺, K⁺-ATPase activity must increase also to transduce energy for the transport of Na⁺ and K⁺. Some studies have reported that PHA stimulates the lymphocyte membrane ATPase directly. We did not observe stimulation of the membrane Na⁺, K⁺-ATPase when either lymphocytes or lymphocyte membranes were treated with mitogenic concentrations of PHA. Moreover, PHA did not enhance the reaction velocity of the Na⁺, K⁺-ATPase when studied at the K_m for ATP, Na⁺, K⁺ or Mg⁺, indicating that it does not alter the affinity of the enzyme for its substrate or cofactors. Thus, our data indicate that the increase in ATPase activity does not occur as a direct result of PHA action on the cell membrane. Segel, G. B.; Simon, W. and Lichtman, M. A.: Regulation of sodium and potassium transport in phytohemagglutinin-stimulated human blood lymphocytes. J. Clin. Invest., 64: 834-841 (1979) (UR-3490-1440)

Phytohemagglutinin (PHA) or concanavalin A treatment of lymphocytes causes an increase in membrane permeability so that the leak rates of Na and K increase 1.5- to 2-fold. Active Na and K transport increase proportionately in response to the increased membrane permeability. We have examined the role of lymphocyte Na concentration in sustaining the increased Na and K transport observed after PHA treatment. Cell Na concentration increases from 14.8 to 20.5 mmol/liter cell water in PHA-treated lymphocytes (P < 0.001). Four lines of evidence suggest that the 5–6 mmol/ liter cell water increase in lymphocyte Na accounts for the increase in active Na and K transport in mitogen-treated lymphocytes. First, PHA does not increase directly the maximal Na, K-ATPase activity of isolated lymphocyte membrane vesicles. Second, when the Na concentration is increased by 6 mmol/liter cell water in unstimulated lymphocytes, Na and K transport increase nearly twofold. Third, the cell Na concentration (15 mmol/liter cell water) is near the K_m for Na activation of the Na, K-ATPase in lymphocyte membranes. The ATPase activity thus is capable of increasing as the cell Na rises above normal. Fourth, if lymphocytes are incubated in a medium containing a low Na concentration, K transport does not maintain the internal K concentration and the fall in cell K is accentuated in PHA-treated lymphocytes. These studies indicate that the adaptive acceleration of Na and K transport in mitogen-treated lymphocytes is mediated by a small increase in cell Na.

Shamoo, A. E. and Tivol, W. F.: Criteria for the reconstitution of ion transport systems. In <u>Current</u> <u>Topics in Membrane Transport</u>. Academic Press, New York, (in press) (UR-3490-1596)

Biochemical studies in general consist of observations of a system of interest *in situ*, isolation and characterization of the components of the system, and reassembly of these components to recreate a working system *in vitro*. This review is concerned with the reassembly of ion transport systems. The term "reconstitution" refers to such reassembly and has been used broadly in the literature. In the most limited sense, reconstitution implies the rebuilding of a system from isolated, molecularly well-defined components such that the biological activities of the reconstituted system are identical to those of the same system *in vivo*. For example, if one combines $Ca^{2+} + Mg^{2+}$ -ATPase, phosphatidyl ethanolamine, and phosphatidyl choline, and if one sonicates these ingredients in an appropriate aqueous buffered salt solution, vesicles will form which will efficiently translocate calcium ions when magnesium ions and ATP are present, if the pH and ionic strength of the suspensions are maintained at physiological values.

Less successful reassembly which recreates only some of the biological activities is also referred

to as reconstitution. For example, Bradley et al. report a reconstitution of rabbit skeletal muscle acetylcholine receptor (AchR) in a planar bilayer which gives quantal conductance increases when stimulated by carbamyl choline and is antagonized by curare, α -bungarotoxin, DTT and ConA; however, quantitative properties such as agonist independent conductance, channel magnitude and lifetime are different from the values found in the intact receptor. Reconstitution using only some of the components of a system or using fragments of a system can also recreate only a part of the biological activities. In this case, of course, one expects to recover only a specific fraction of the activity, and such partial reconstitutions are useful in assigning particular biological activities to particular components of a system or in studying the interactions between components of a system.

Razin suggests that the term reconstitution be used to refer to cases when both membrane structure and normal enzymic activities have been restored, that reformation be used when membrane structure, but not necessarily function, is restored, and that reaggregation be used when no firm conclusions can be drawn regarding the structure or function of the end product. He also suggests reserving the term recombination for those cases where the proteins and lipids had been isolated prior to mixing. In spite of the many terms and their many uses in the literature, it would be valuable to distinguish among degrees of success in recreating membrane structure and function. We endorse Razin's suggestions and propose that "partial reconstitution" refer to the case where some but not all of the biological activities are restored.

If phospholipids are suspended in an aqueous phase, the lipid molecules spontaneously aggregate into structures in which all the polar head groups are in contact with the aqueous phase, and the nonpolar fatty acid chains are not. Considerations of optimal areas for both head groups and acyl chains lead to the conclusion that two related structures have the lowest chemical potential: extended bilayer sheets and bilayer surfaces enclosing an aqueous cavity, which are called vesicles or liposomes. By varying the conditions of formation either open bilayer membrane (bounded by suitable hydrophobic supports, usually a polyethylene or teflon frame) or vesicles can be formed. Under appropriate conditions, the vesicles will be single-walled, as opposed to multilammelar, onionlike structures.

Both open lipid bilayer membranes and closed vesicles have been used in reconstitution and each structure has its own advantages and disadvantages. Open bilayers have the advantage that both sides of the bilayer are accessible to measurement or modification. This allows the measurement of transmembrane differences, for example voltage or osmotic pressure. Openness has the disadvantage that there is no enclosed volume so that any transported ions are diluted instead of being collected in a small space. This renders the measurement of transmembrane ion currents

- 77 -

very difficult even with radioactive isotopes. Other disadvantages of the open bilayer come from the usual method of formation. An unknown amount of organic solvent is usually present which vastly complicates the interpretation of any measurements — especially when the reconstituted system differs from the *in vivo* one. Little is known about the properties of the lipid torus, called the Plateau-Gibbs border (P-G border), which is found at the edge of the frame used to support the bilayer. This thick lipid structure can affect membrane area measurements and may contribute errors to current measurements.

The advantages of vesicles are that there is generally no organic solvent present and that they enclose a volume which is smaller relative to surface area than in any practical open bilayer system. Electrical measurements are notoriously difficult, however, due both to the problem associated with implanting a sufficiently small electrode inside the vesicle and to uncertainties about the region where the lipid joins the electrode wall. Another disadvantage in vesicles is that some parameters are very poorly defined in the inside of a vesicle. Typical methods of preparation give vesicles smaller than 1 μ m diameter. A 1 μ m diameter vesicle at pH = 7 contains about thirty H⁺ ions and since many ion concentration ranges of physiological interest are in the 1 to 10 μ M range this means that there are at most only a few hundred or perhaps a few thousand ions inside a vesicle when a measurement is of interest. Application of a theoretical equation describing a macroscopic solution to such a situation is either dubious or completely inappropriate.

Recent developments have led to the production of much larger vesicles, typically having a diameter of about $100 \,\mu$ m. In these "giant" vesicles such quantities as pH are probably well defined. Kecent measurements in this laboratory have shown that whereas membrane capacitance can be readily measured in giant vesicles, membrane resistance measurements are inconsistent with the values reported in the literature and have a large scatter. There is no organic solvent in giant vesicles and the geometric uncertainties are absent (except in electrical resistance measurements, etc.). There are, no doubt, limitations on the use of giant vesicles which will become apparent with sufficient experience in their use. At this time, though, they seem to offer great promise for reconstitution studies.

Shamoo, A. E.; Hermann, T.; Abramson, J. J. and Murphy, T.: Energy transduction between the catalytic and ionophoric sites of $Ca^{2+} + Mg^{2+}$ -ATPase molecule. In <u>Function and Molecular Aspects of Biomembrane Transport</u>, Ed. by E. Quagliariello et al., (Proc. Intern. Symp., April 1979, Bari, Italy). Elsevier/North-Holland Biomedical Press, Amsterdam, pp. 91-99 (1979) (UR-3490-1580)

Our data have shown that the intact sarcoplasmic reticulum (SR) $Ca^{2+} + Mg^{2+}$ -ATPase molecule contains the Ca²⁺-conducting pathway (Ca²⁺-ionophorous property) as an integral part of the enzyme molecule. Furthermore, we have shown that controlled tryptic digestion of the enzyme results first in the production of 55,000 (A) and 45,000 (B) dalton fragments followed by a further cleavage of the 55K fragment into 30,000 (A₁) and 20,000 (A₂) dalton fragments. Digestion of the 55K dalton fragment into 20K and 30K dalton fragments results in inhibition of calcium transport in SR vesicles, but does not affect ATPase activity. This is consistent with disruption of energy transduction between the hydrolytic site (30K) and the ionophoric site (20K). It was also shown that the 55K (A₁) and 20K (A₂) have ionophorous activity similar to that of the intact enzyme, and that the 45K dalton fragment has nonselective "channel-like" activity. The 20K (A₂) fragment possesses Ca²⁺ ionophorous properties in phosphatidylcholine vesicles similar to those observed in black lipid membranes. Also, it is shown that a cyanogen bromide cleavage fragment (13,000 daltons) of the 20K fragment contains the viable Ca²⁺-ionophore. A model relating the structure-function relationship of the various sites of action in Ca²⁺ + Mg²⁺-ATPase molecule is presented.

Smith, F. A. and Hodge, H. C.: Airborne fluorides and man: Part II. Crit. Rev. Environ. Control, 9: 1-25 (1979) (UR-3490-1593)

It has long been recognized that some species of vegetation, as well as some animals, e.g., cattle, are especially sensitive to fluoride. As a result, standards governing the emission of fluorides from industrial sources, fluoride concentrations in the ambient air downwind from such sources, and fluoride concentrations in vegetation have been established. These standards, as well as occupational standards in various nations, are reviewed here.

Sobell, H. M.: DNA dynamics and drug intercalation. In <u>Molecular Actions and Targets for Cancer</u> <u>Chemotherapeutic Agents</u>. (Proc. Second Annual Bristol-Myers Symp. in Cancer Research, November 1979, New Haven, Conn.), Ed. by A. C. Sartorelli. Academic Press, New York, (in press) (UR-3490-1819)

This paper describes unifying structural concepts that have emerged in understanding a broad range of drug-DNA interactions. It begins by first describing a detailed molecular model for ethidium-DNA binding based on the geometry determined in the ethidium-dinucleoside monophosphate crystalline complexes. The model explains a large mass of physical and biochemical data concerning the interaction of ethidium and DNA and contains the more general stereochemical postulate that drug intercalation gives rise to a helical screw axis dislocation in DNA, a variable whose magnitude determines the relative ring overlap between an intercalative drug molecule and adjacent base pairs. This concept allows us to understand how other drugs (such as ellipticine, 9-aminoacridine, acridine orange, etc.) bind to DNA. In addition, conformational changes in the sugar-phosphate backbone that accomapny intercalation have led us to ask if DNA first bends or "kinks" to accept an intercalative drug or dye. This is made possible by altering the normal C2' endo deoxyribose sugar ring puckering in B DNA to a mixed puckering pattern of the type: C3' endo (3'-5') C2' endo and partially unstacking base pairs. This concept allows us to understand many of the kinetic features of drug intercalation. Moreover, it leads us to propose detailed models for actinomycin-DNA and irehdiamine-DNA binding, two interactions that utilize intercalative-and kinked-type geometries.

It appears that the stereochemical principles that have emerged from these studies may be intimately related to understanding the nature of protein-DNA interactions and could, therefore, be of still broader interest in molecular biology. We describe this in detail in this paper.

Sobell, H. M.: Importance of symmetry and conformational flexibility in DNA structure for understanding protein-DNA interactions. Chapt. 5 in <u>Biological Regulation and Development</u>, <u>Volume 1</u>, Ed. by R. F. Goldberger. Plenum Publishing Corp., New York, pp. 171-199 (1979) (UR-3490-1301)

During the past few years there has been a growing realization that two aspects of DNA structure, namely, its symmetry and its conformational flexibility, play important roles in protein—DNA interactions involved in genetic regulation. This chapter reviews evidence along these lines, beginning with our structural studies of drug intercalation (these studies have given direct structural information concerning the roles of symmetry and conformational flexibility in DNA structure in a variety of drug—DNA interactions), enlarging on this theme with a discussion of the nature of DNA breathing and DNA denaturation, and ending with discussions of specific protein—DNA interactions that involve various aspects of DNA symmetry and flexibility — that is, histone-DNA interactions in chromatin, RNA polymerase-promoter recognition, operator-repressor recognition, and so on. No attempt is made to review the wealth of nucleotide sequence information currently available; rather, specific examples of protein—DNA interactions are discussed in detail and these will serve to illustrate the general principles involved.

Stern, S.: Behavioral effects of microwaves. Neurobehav. Tox., (in press) (UR-3490-1764)

Microwaves can produce sensations of warmth and sound in humans. In other species, they also can serve as cues, they may be avoided, and they can disrupt ongoing behavior. These actions appear to be due to heat produced by energy absorption. The rate of absorption depends on the microwave parameters and the electrical and geometric properties of the subject. We, therefore, cannot predict the human response to microwaves based on data from other animals without appropriate scaling considerations. At low levels of exposure, microwaves can produce changes in behavior without large, or even measurable, changes in body temperature. Thermoregulatory behavior may respond to those low levels of heat and thereby affect other behavior occurring concurrently. There are no data that demonstrate that behavioral effects of microwaves depend on any mechanism other than reactions to heat. Our interpretation of whether a reported behavioral effect indicates that microwaves may be hazardous depends on our having a complete description of the experiment and on our criteria of behavioral toxicity.

Stern, S.; Margolin, L.; Weiss, B.; Lu, S-T. and Michaelson, S. M.: Microwaves: effect on thermoregulatory behavior in rats. Science, 206: 1198-1201 (1979) (UR-3490-1537)

Rats, with their fur clipped, pressed a lever to turn on an infrared lamp while in a cold chamber. When they were exposed to continuous-wave microwaves at 2450 megahertz for 15-minute periods, the rate at which they turned on the infrared lamp decreased as a function of the microwave power density, which ranged between 5 and 20 milliwatts per square centimeter. This result indicates that behaviorally significant levels of heating may occur at an exposure duration and intensities that do not produce measurable changes in many other behavioral measures or in colonic temperature. Further study of how microwaves affect thermoregulatory behavior may help us understand such phenomena as the reported "nonthermal" behavioral effects of microwaves.

Sugata, Y. and Clarkson, T. W.: Exhalation of mercury – further evidence for an oxidation-reduction cycle in mammalian tissues. Biochem. Pharmacol., 28: 3474-3476 (1979) Short Communication (UR-3490-1548)

The time course of the exhalation of mercury vapor was studied after the exposure of acatalasemic mice or 3-amino-1,2,4-triazole (AT) treated mice to metallic mercury vapor. In both cases, the accelerated exhalation of mercury was observed over periods of several hours compared with the corresponding control in catalase activity. AT caused an increased exhalation of mercury even after the dosing of mercuric chloride. These observations indicate that mercury is in a dynamic equilibrium between metallic and mercuric mercury in the body.

Szostak, J. W.; Stiles, J. I.; Tye, B.-K.; Chiu, P.; Sherman, F. and Wu, R.: Hybridization with synthetic oligonucleotides. Methods Enzymol., 68: 419-428 (1979) (UR-3490-1581)

In this paper we describe procedures for the use of synthetic oligonucleotides for Southern blot experiments and gene bank screening and demonstrate the effect of various mismatches on the efficiency of hybridization. In general, the temperature of hybridization should be 15° to 20° below the Tm of the hybrid; but in practice the conditions of the hybridization reaction must be carefully optimized in order to achieve both high sensitivity and specificity. We have tested the effects of several different mismatches and find that errors near the middle of the sequence are less critical than errors near the end. We have found that a synthetic deoxyribonucleotide of 15 bases is sufficient to detect a unique sequence, the iso-1-cytochrome c gene, in the yeast Saccharomyces cerevisiae using the Southern blotting procedure. One additional minor sequence that cross hybridized was detected in the yeast DNA. This 15-mer was also found sufficient to isolate these fragments from a phage λ bank of cloned total yeast DNA using a modification of the Benton and Davis plaque transfer technique. Methods are discussed to limit the background associated with these techniques. It was estimated that synthetic oligonucleotides 13 to 15 nucleotides long could be used as probes for isolating genes from prokaryotes and lower eukaryotes, while 18 to 20 nucleotides probes are required for isolating genes from higher eukaryotes.

Teitelbaum, A. P.; Schneider, N. and Neuman, W. F.: On the relation between peripheral cleavage of parathyroid hormone and its biological activity in kidney. Metab. Bone Disease Related Res., (in press) (UR-3490-1554)

The time course of the renal metabolism of electrolytically iodinated ¹²⁵I-bPTH(1-84) (E-PTH), previously shown to retain biological activity, was compared with that of Chloramine-T labeled, biologically inactive ¹²⁵I-bPTH(1-84) (CT-PTH), the assumption being that observed differences would reflect biological specificities of metabolism. Denaturant gel filtration of kidney extracts indicated that the initial rate of cleavage of E-PTH was more rapid than that of CT-PTH. This difference was maximal at 5 minutes when the amount of unmetabolized hormone, expressed as a percentage of total kidney radioactivity was 40% for E-PTH and 68% for CT-PTH. The time course of disappearance of intact E-PTH and CT-PTH from serum were similar.

The metabolism of PTH labeled by the two methods was studied in vitro in rat renal cortical membranes (RCPM). As was the case in vivo, E-PTH was cleaved 2 to 3 times more rapidly than CT-PTH by RCPM. Basal lateral membranes, containing PTH responsive adenylate cyclase activity, and brush border membrane fractions separated by free flow electrophoresis of RCPM also metabolized E-PTH 2 to 3 times more rapidly than CT-PTH. E-PTH metabolism in RCPM was not inhibited by 10^{-6} M unlabeled bPTH(1-84). However, histone f₃ (1 mg/ml) completely blocked metabolism of E-PTH in RCPM, and enhanced PTH-stimulated adenylate cyclase activity fivefold.

Thompson, T. R.: Biomembrane modeling: molecular dynamics simulation of phospholipid monolayers. Ph.D. Thesis, University of Rochester School of Medicine and Dentistry (Supervised by Dr. D. A. Goldstein) (1979) (UR-3490-1770)

As a first step toward a computer model of a biomembrane-like bilayer, a dynamic deterministic model of a phospholipid monolayer has been constructed. The model moves phospholipid-like centers of force according to an integrated low of motion in finite difference form. Forces on each phospholipid analogue are derived from the gradient of the local potential, itself the sum of Coulombic and short-range terms. The Coulombic term is approximately by use of a finite-difference form of Poisson's equation, while the short-range term results from finite-radius, pairwise summation of a Lennard-Jones potential. Boundary potentials are treated in such a way that the model is effectively infinite in extent in the plane of the monolayer. The two-dimensional virial theorem is used to find the surface pressure of the monolayer as a function of molecular area. Pressure-versus-area curves for simulated monolayers are compared to those of real monolayers. Dependence of the simulator's behavior on Lennard-Jones parameters and the specific geometry of the molecular analogue is discussed. Implications for the physical theory of phospholipid monolayers and bilayers are developed.

Toribara, T. Y.: Book review of "A Handbook of Decomposition Methods in Analytical Chemistry" by R. Bock, Translated and Revised by I. L. Marr. John Wiley & Sons, New York, xii + 444 pp., 1979. J. Am. Chem. Soc., (in press) (UR-3490-1763)

This book covers a variety of methods for the preparation of samples for analyses. As indicated in the title, the method of choice is that of decomposition. Included are techniques such as simple solution, oxidation and reduction reactions, as well as the use of elevated temperatures. Of especial value to those relatively new to the analytical field is the inclusion of a section on common but possibly unsuspected sources of error such as losses by volatilization or by adsorption to containing vessels.

Toribara, T. Y.: Book review of "Handbook of Environmental Engineering. Vol. 1, Air and Noise Pollution Control", Ed. by L. K. Wang and N. C. Pereira. The Humana Press, Clifton, N. J., 1979. J. Am. Chem. Soc., (in press) (UR-3490-1739)

This volume covers in detail a number of specific techniques for cleaning the air. The details cover the mathematical treatment of the theory or theories involved in the technique as well as the various applications. The two chapters on noise pollution occupy a minor portion of the book because of the paucity of material available. Toribara, T. Y.: Book review of "Zinc", by Subcommittee on Zinc, Committee on Medical and Biological Effects of Environmental Pollutants, Division of Medical Sciences, Assembly of Life Sciences, National Research Council. University Park Press, Baltimore, Md., 471 pp., 1979. J. Am. Chem. Soc., (in press) (UR-3490-1731)

This book consists of a very broad coverage of the subject of zinc. It starts with the properties and uses, the availability and the biological effects of both the lack and excess of the element.

Toribara, T. Y.; Miller, M. W. and Morrow, P. E., Editors: <u>Polluted Rain</u>. (Proc. 12th Rochester Intern. Conf. on Environmental Toxicity, May 1979, Rochester, N. Y.). Plenum Press, New York, (in press)

The object of this international conference was to give as complete as possible an overall picture of the problems of the polluted rain. The 24 papers covered: (1) the causes of pollution, (2) the nature of the pollutants, (3) the damage to flora and fauna, established and anticipated, (4) the monitoring of the pollution, and finally (5) the status of the legal efforts, international and interstate, to control the problems.

Utell, M. J.; Aquilina, A. T.; Hall, W. J.; Speers, D. M.; Douglas, R. G., Jr.; Gibb, F. R.; Morrow, P. E. and Hyde, R. W.: Development of airway reactivity to nitrates in subjects with influenza. Am. Rev. Resp. Diseases, (in press) (UR-3490-1617)

Although epidemiologic studies have found a correlation between increased symptoms in asthmatics and increased concentrations of atmospheric nitrates, acute short-term exposure to nitrates does not alter airway function in normal subjects or asymptomatic asthmatics. To examine the potential synergy between acute exposure to pollutant and acute respiratory infections, we studied the effects on the airways of acute exposure to nitrate during uncomplicated influenza A (H_1N_1) infections in 11 previously healthy adults. Subjects were studied at the time of acute illness and 1, 3, and 6 weeks thereafter. By double blind randomization, each subject breathed an aerosol of either sodium chloride or sodium nitrate for an initial 16-minute period and then breathed the other aerosol for 16 minutes 3 hours later. The mass median aerodynamic diameter of the NaNO₃ aerosol was 0.49 μ m; the concentration, 7,000 μ g/m³. Deposition studies showed a mean retention of 45 to 50% for both inhaled aerosols. Compared to inhalation of sodium chloride, at initial examination and 1 week later, exposure to sodium nitrate produced significant decreases in specific airway conductance (p < 0.005) and partial expiratory flows at 40% of total lung capacity (p < 0.05). By 3 weeks, inhalation of sodium nitrate no longer produced changes in airway function. Unlike normal or asymptomatic asthmatic subjects, subjects with acute respiratory disease have airway constriction after acute exposure to nitrate. Because no significant constriction developed

with exposure to sodium chloride at these times, the constriction is a specific effect of the sodium nitrate rather than a nonspecific response to the particles. Therefore, subjects with acute respiratory disease are susceptible to bronchoconstriction from specific air pollutants that normally do not influence airway function.

Von Burg, R.; Northington, F. J. and Shamoo, A. E.: Methylmercury inhibition of rat brain muscarinic receptors. Toxicol. Appl. Pharmacol., (in press) (UR-3490-1649)

The distribution of MeHg in subcellular organelles of the rat brain varied slightly in relation to the *in vivo* or the *in vitro* mode of labelling with Me²⁰³HgCl. The differences may be explained by disruption of the normal diffusion path into the brain cells and the amount of MeHg that is bound along this diffusion path. When Me²⁰³Hg and ³H-QNB were added directly to brain homogenates, the subcellular fractions demonstrated a molar QNB/MeHg binding ratio greater than 1:100. This suggests that MeHg binding sites are in considerable excess over QNB binding sites and represents a relatively large sink for decreasing effective MeHg concentrations. HgCl₂ was 100 times as potent as MeHg for blocking specific QNB binding sites. (MeHg ID₅₀ = 10⁻⁵ M; HgCl₂ ID₅₀ = 10⁻⁷ M.) On the basis of the respective ID₅₀ points, a 1% conversion of MeHg to the inorganic form would produce a separate but equivalent block of muscarinic binding sites. Therefore, it is suggested that the early theory involving organic to inorganic Hg conversion be re-examined as a possibility for producing the selective toxicity to the CNS observed in cases of MeHg poisoning.

Waugh, R. E. and La Celle, P. L.: Abnormalities in the membrane material properties of hereditary spherocytes. J. Biomech. Engineering, (in press) (UR-3490-1768)

Mechanical measurements of intrinsic membrane material properties are used to characterize the defect in hereditary spherocyte membrane at a continuum level. The value of the surface elastic shear modulus is two-thirds as large as normal values and the value of the yield shear resultant is one-third as large as normal values. The viscosity of the surface above the elastic-plastic transition appears normal. Under similar geometric conditions, the force required to fragment a hereditary spherocyte is about one-third as large as the force required to fragment a normal cell.

Weiss, B.: Behavioral assays in environmental toxicology. Proc. NATO Advanced Research Institute Symp., September 1979, Monte Carlo, Monaco, (in press) (UR-3490-1742)

Behavioral toxicology treats the whole organism as an assay system. Certain features of such an approach are exceedingly resistant to simplification and it is doubtful that we will ever have the luxury of something approaching *in vitro* testing in convenience and clarity. Three aspects of behavioral assessment are especially difficult to simplify in reasonable ways. *Psychophysics* is the discipline that allows us to determine sensory capacity. With animals, complex, lengthy procedures are often the only alternative to subtle questions of sensory dysfunction. Measures of *aversiveness* and *attractiveness* are also definable only by behavioral techniques, yet constitute critical data for environmental standards. *Behavioral epidemiology* is the most obvious enemy of simplification since it deals with how people feel and function.

Weiss, B.: Dietary intake contributions to hyperkinesis. Proc. Workshop on Hyperkinetic Behavior Syndrome, June 1978, Washington, D. C., (in press) (UR-3490-1618)

Recent assortions about an etiologic role for food additives in hyperkinesis stem from earlier clinical observations of hypersensitivity reactions involving more typical symptoms such as urticaria. Behavioral reactivity to food colors, particularly, seems to be a pharmacologic phenomenon, however. That is, incidence is a function of dose. Behavior disorders in children should be examined more carefully for possible contributions from diet.

Weiss, B.: First U.S.-U.S.S.R. workshop on behavioral toxicology. Neurotoxicol., (in press) (UR-3490-1598)

Since 1973, behavioral toxicology has been a component of the U.S.-U.S.S.R. Environmental Health Exchange Agreement. To help resolve the sources of discrepencies in exposure standards between the two countries, a joint workshop was held in the U.S.S.R. in November 1978. The workshop highlighted differences in practice that ranged from scientific communication to reliance on biological indicators of exposure. Further workshops are planned.

Weiss, B.: Food additives. Chapt. 38 in <u>Pediatric Nutrition Handhook</u>, Committee on Nutrition, American Academy of Pediatrics, Evanston, Ill., pp. 454-464 (1979) (UR-3490-1824)

About 3,000 substances are deliberately added to foods to preserve them, to modify their texture, to alter their color, to change their taste, and for many other reasons. Safety evaluation of these substances has been required since the Food Additive Amendment of 1958, but previously used substances were incorporated into a GRAS (Generally Regarded as Safe) list. Typically, such evaluations omit testing for allergenicity and behavior. Behavioral testing has assumed new importance with the alleged connection between food additives and behavioral disorders such as hyperkinesis in children. Weiss, B. and Laties, V. G.: Assays for behavioral toxicity: a strategy for the Environmental Protection Agency. Neurobehav. Toxicol., 1: Suppl. 1, 213-215 (1979) (UR-3490-1615)

Broad agreement on specific approaches or standardized test batteries for assessing behavioral toxicity is unlikely to emerge in the foreseeable future. EPA should reject test standardization in any case, however; standardization stifles progress and, in addition, may bypass unique properties of new types of substances. The optimal strategy is to prescribe a set of functions, such as sensory, motor, and complex performance processes, leaving it to the manufacturer to select adequate tests. Adequacy would be judged by EPA staff, in consultation with advisory panels, and resolved, in most cases, by a dialogue with the manufacturer.

Weiss, B.; Cox, C.; Young, M.; Margen, S. and Williams, J. H.: Behavioral epidemiology of food additives. Neurobehav. Toxicol., 1: Suppl. 1, 149-155 (1979) (UR-3490-1605)

Behavioral toxicology in the natural environment can be considered a special branch of epidemiology. Behavioral epidemiology, because it typically relies on complex functional criteria, faces all of the problems of behavior measurement posed by uncontrollable variation, and amplified even further by chemical exposure. Many such issues arose in a study of behavioral responses to artificial food colors in children. Difficulties in employing Applied Behavioral Analysis in such a context run the gamut from selection of retrospective criteria to appropriate statistical models.

Weiss, B.; Williams, J. H.; Schultz, S.; Margen, S.; Abrams, B.; Citron, L. J.; Cox, C.; McKibben, J. and Ogar, D.: Behavioral responses to artificial food colors. Science, (in press) (UR-3490-1670)

Twenty-two young children, maintained on an elimination diet, were challenged intermittently with a blend of seven artificial colors in a double-blind trial. Parents' observations provided the criteria of response. One mild responder and one dramatic responder were detected. The latter, a 34-month old female, demonstrated significant elevations of aversive behaviors. These results further confirm previous controlled studies.

Wheeler, K. T. and Wallen, C. A.: Is cell survival a determinant of the *in situ* response of 9L tumors? Proc. 9th L. H. Gray Memorial Conf., September 1979, Cambridge, England, Brit, J. Cancer, (in press) (UR-3490-1725)

The influence of growth rate, location, size, and cellular recovery on either the apparent cellular radiosensitivity, the apparent tumor response (increase in life span), or the relationship between measured cell survival and tumor response was studied using two sublines of the 9L rat brain tumor, designated 9L/Ro and 9L/SF. The median day of death of rats bearing the intracerebral (i.c.) 9L/Ro

tumors was 16 to 18 days; for i.c. 9L/SF tumors it was 23 to 25 days. The doubling time of 9L/Ro cells was slightly faster than that for 9L/SF cells both in culture and in the brain. The cellular radiosensitivity of both i.c. tumor cells was identical when measured immediately after irradition by an *in vivo* to *in vitro* colony formation assay. However, the D_O of subcutaneous (s.c.) 9L/Ro tumor cells was considerably higher (332 rad) than the D_O determined for the i.c. 9L/Ro tumor cells (180 rad). There was no evidence of a substantial hypoxic fraction in either the i.c. or s.c. tumors. When i.c. 9L/Ro and 9L/SF tumors of similar size were treated with fractionated doses of BCNU, X-rays, or combinations of BCNU and X-rays, the responses of the tumors as measured by an increase in life span or the number of intracerebral tumor-free survivors were essentially identical. The rate and extent of recovery from radiation-induced potentially lethal damage (PLD) of i.c. 9L/Ro and 9L/SF tumor cells were identical. Although the PLD recovery rate of s.c. 9L/Ro tumor cells was similar to that of i.c. 9L/Ro cells, the extent of the PLD recovery was apparently greater in s.c. tumors. Increases in life span of rats bearing i.c. 9L/Ro tumors appeared to be correlated with the tumor cell kill measured after completion of PLD recovery rather than with the tumor cell kill determined immediately after irradiation.

Wood, R. W.: Behavioral evaluation of sensory irritation evoked by ammonia. Toxicol. Appl. Pharmacol., 50: 157-162 (1979) (UR-3490-1366)

Mice will respond to escape from ammonia vapor, a prototypical airborne chemical irritant. Nose poking at a conical sensor is maintained if it terminates the delivery of ammonia to a small exposure chamber and produces a facial shower of clean, humidified air from the sensor. The duration of exposure to ammonia tolerated decreased as ammonia concentration increased (0.0 to 0.2%). The percentage of ammonia deliveries terminated by a response also increased as concentration increased. The behavior did not result from a general increase in activity. Thus, ammonia vapor delivery is an effective negative reinforcer for the mouse. This technique can help evaluate the aversive properties of atmospheric contaminants.

Wood, R. W.: Reinforcing properties of inhaled substances. Neurobehav. Toxicol., 1: Suppl. 1, 67-72 (1979) (UR-3490-1604)

Inhaled substances can support behavior by acting as reinforcing stimulus events. The deliberate inhalation of volatile materials is attributable to the positively reinforcing properties of these substances and can induce profound toxicity. On the other hand, inhaled substances can also be aversive, e.g., corrosives, certain solvents, and combustion products. Both positive and negative reinforcing properties of inhaled materials can be used to support the behavior of laboratory animals. Several rules of evidence should be met, however, to demonstrate conclusively that an inhalant has such properties. Such properties should be considered in industrial hygiene and environmental quality decisions.

Wood, R. W.; Warren, P. H. and Weiss, B.: Attenuated aversiveness of electric shock during nitrous oxide exposure. J. Pharmacol. Exptl. Therap., (in press) (UR-3490-1720)

The analgesic properties of nitrous oxide (N_2O) were evaluated with a fractional escape procedure ("shock titration" schedule). Shock intensity rose by a small step every few seconds. Each designated response by a rat or squirrel monkey subject reduced the amplitude of the shock by one step. Both species maintained stable tolerated levels of shock when exposed to pure oxygen or to air. Exposure to N₂O yielded an elevation in maintained shock level whose magnitude depended on concentration. Statistically significant rises generally were apparent at N₂O concentrations of 30 to 70%, which also tended to reduce shock level fluctuations. Since the raised shock levels were not accompanied by changes in overall response rate, they can be attributed to the analgesic properties of N₂O.

Zook, B. C.; Bradley, E. W.; Casarett, G. W.; Hitzelberg, R. A. and Rogers, C. C.: The pathologic effects of fractionated fast neutrons or photons on canine liver. Cancer Clinical Trials, (in press) (UR-3490-1803)

Thirty-nine adult male purebred beagles received either fast neutron or photon irradiation to the right thorax to determine the effects on pulmonary tissue. The right half of the liver was included in the field of radiation. Twenty-four dogs (six/group) received fast neutrons with a mean energy of 15 MeV to total doses of 1000, 1500, 2250, or 3375 rad in four fractions per week for six weeks. Fifteen dogs received 3000, 4500, or 6750 total rad of photons (five dogs/group) in an identical fractionation pattern. All neutron-irradiated dogs receiving 3375 or 2250 rad and one receiving 1500 rad developed clinical signs, hepatic enzyme, and bilirubin elevations, and the dogs died or were euthanized *in extremis* on postirradiation day 47 to 291. Signs of liver injury, other than enzyme changes, have not developed to date (1200 to 1300 days) in the remaining dogs, except in one 6750-rad photon dog that died of hepatic failure on postirradiation day 708. At necropsy, the irradiated right lobes of the liver were atrophic and the nonirradiated left lobes underwent compensatory hypertrophy. Hepatic arterioles and bile ducts were injured in every dog, but no obstructive lesions were observed in hepatic veins. Portal fibroplasia, bile retention, and proliferation of bile ductules was common; the latter two changes also occurred in the nonirradiated lobes. No qualitative differences were observed between hepatic lesions in neutron-versus photonirradiated dogs. The relative biological effectiveness of fast neutrons for liver damage appears to be no less than 4.5.

- 91 -

INDEX*

Henry E. Auer – Biophysical Studies of Proteins and Polypeptides – p. 47

George G. Berg — Toxicity of Heavy Metals — p. 3

William A. Bernhard – Effects of Ionizing Radiation on DNA Model Systems – pp. 44, 45, 45

John S. Brand – Hormonal Control of Bone Metabolism – pp. 5, 15, 16, 17, 24, 68

George W. Casarett – Mechanisms of Permanent and Delayed Pathologic Effects of Radiation – pp. 11, 11, 33, 34, 45, 89

Thomas W. Clarkson – Biophysical Aspects of Heavy Metal Poisoning – pp. 7, 13, 18, 81

Giles R. Cokelet – Microcirculatory Blood Flow – pp. 13, 14

James R. Coleman – Localization of Cell Calcium with the Electron Probe -p. 14

Richard A. Doherty — Genetic, Reproductive, and Developmental Mammalian Toxicology — pp. 29, 29, 30, 30

Helen I. Eberle – Regulatory Mechanisms and Proteins Involved in DNA Synthesis and Division – p. 18

Isaac Feldman – Metal Ion Effects on Hexokinase Reaction – pp. 61, 62

Juraj Ferin – Mechanisms of Pulmonary Clearance of Particles from Alveoli - p. 19

Gilbert B. Forbes – Metabolism, Growth, and Development – p. 20

David A. Goldstein – Models for Membrane Transport – pp. 2, 22, 83

T. Daniel Griffiths – The Effects of Physical and Chemical Mutagens on DNA Synthesis – pp. 15, 20, 20, 21, 21

Thomas E. Gunter – Paramagnetic Probe Studies of Membrane – pp. 68, 70

Richard W. Hyde – Pulmonary Pathophysiology – pp. 57, 84

Mary Jane Izzo – Studies of 125I-Labelled Insulin in Rat Liver – p. 24

George A. Kimmich – Mechanisms of Na⁺-Metabolite Transport – pp. 9, 10, 31, 32, 33, 33

Francis H. Kirkpatrick – Red Cell Membrane Cytoskeleton – pp. 23, 34, 39

Paul L. La Celle – Pollutant Effects on Blood Cell Rheology – p. 85

Christopher S. Lange – The Cellular and Molecular Basis for Recovery from Radiation Injury – pp. 20, 20

This index is set up according to each investigator and his project title. The page numbers indicate where abstracts of papers which were supported by a given project appear. Not all papers are necessarily authored by the investigator himself.

INDEX (Cont.)

- Victor G. Laties Behavioral Pharmacology and Toxicology pp. 21, 39, 40, 80, 81, 87
- Christopher W. Lawrence Genetic and Molecular Analysis of Radiation Mutagenesis pp. 17, 40, 40
- Marshall A. Lichtman Membrane Structure and Function of Blood Cells pp. 1, 5, 6, 41, 41, 42, 75, 75, 76
- Jack Maniloff Biophysics of the Smallest Cells and Their Viruses p. 47
- Richard D. Mavis Lung Biochemistry pp. 19, 35, 37, 38, 38, 62, 63
- Thomas T. Mercer Respirable Aerosols: Their Characterization and Properties pp. 19, 50, 58
- Solomon M. Michaelson Mcchanisms of Neuroendocrine Responses to Electromagnetic Radiant Energy – pp. 23, 43, 48, 51, 52, 53, 81, 87
- Leon L. Miller Plasma and Tissue Protein Metabolism p. 64
- Morton W. Miller Physical and Environmental Radiation Cytology ELF: Power Frequency Electric Fields – pp. 9, 20, 20, 29, 54, 54, 84

Donald A. Morken – Radiobiology of Radon and its Decay Products – p. 55

- Paul E. Morrow Dust Deposition and Retention Studies of UF₆, UO₂F₂ in Experimental Animals – pp. 57, 57, 57, 58, 84, 84
- Margaret W. and William F. Neuman Chemical Dynamics of Bone Metabolism pp. 6, 59, 59, 60, 60, 72, 82
- Louise Prakash Repair of Damaged DNA and Mutagenesis in Yeast pp. 47, 64, 65, 66, 66
- Jerome S. Puskin Membrane Structure and Ion Transport p. 66
- Adil E. Shamoo Effects of Heavy Metals on Ion Transport Processes pp. 1, 3, 7, 26, 28, 28, 76, 78, 85
- Fred Sherman Genetic and Biochemical Studies of the Cytochrome and Related Systems in Yeast pp. 11, 12, 41, 42, 54, 54, 63, 70, 81
- Frank A. Smith Inhalation Toxicology of Mixed Airborne Contamination In Vivo. In Vivo Stabilization of the C-F Bond – pp. 55, 58, 79
- Henry M. Sobell X-ray Crystallography of Drug-Nucleic Acid Crystalline Complexes pp. 25, 43, 67, 71, 72, 79, 80
- John W. Stewart Primary Structural Analysis of Cytochrome c in Yeast Mutants p. 63

Taft Y. Toribara – Binding to Serum Proteins Analytical Problems: The Nuclear Chemistry of 203pb – pp. 83, 83, 84, 84

- David A. Weber Radioactive Tracer Kinetics and Imaging Instrumentation pp. 33, 34
- Bernard Weiss Behavioral Pharmacology and Toxicology pp. 15, 48, 50, 50, 51, 80, 81, 85, 86, 86, 87, 87, 87, 89

INDEX (Cont.)

Kenneth T. Wheeler – Molecular and Cellular Basis of Tumor Therapy – pp. 31, 87

John S. Wiberg – Studies on Nucleic Acid Synthesis and Breakdown, and on Regulation of Protein Synthesis in Bacteria – pp. 8, 12

Ronald W. Wood – Behavioral Toxicology of Solvents and Irritants – pp. 88, 88, 89